uOttawa

L'Université canadienne
Canada's university

FACULTÉ DES ÉTUDES SUPÉRIEURES ET POSTOCTORALES

uOttawa

L'Université canadienne
Canada's university

FACULTY OF GRADUATE AND POSDOCTORAL STUDIES

Dillon Waterman
AUTEUR DE LA THÈSE / AUTHOR OF THESIS

M.A.Sc. (Environmental Engineering)
GRADE / DEGREE

Faculty of Engineering
FACULTÉ, ÉCOLE, DÉPARTEMENT / FACULTY, SCHOOL, DEPARTMENT

Bench-scale analysis of ultra filtration membranes for investigating fouling by natural organic matter in surface water

TITRE DE LA THÈSE / TITLE OF THESIS

Dr. R. Narbaitz
DIRECTEUR (DIRECTRICE) DE LA THÈSE / THESIS SUPERVISOR

CO-DIRECTEUR (CO-DIRECTRICE) DE LA THÈSE / THESIS CO-SUPERVISOR

EXAMINATEURS (EXAMINATRICES) DE LA THÈSE / THESIS EXAMINERS

Dr. O. Basu

Dr. T. Matsuura

Dr. L. Fernandes

Gary W. Slater
Le Doyen de la Faculté des études supérieures et postdoctorales / Dean of the Faculty of Graduate and Postdoctoral Studies

THE UNIVERSITY OF OTTAWA-FACULTY OF GRADUATE STUDIES

CERTIFICATE OF EXAMINATION

Examining Board

Dr. Onita Basu

Dr. Leta Fernandes

Dr. Takeshi Matsuura

Advisor

The thesis by
Dillon A. Waterman
entitled
Bench-scale analysis of ultrafiltration membranes for investigating fouling by natural organic matter in surface water

is accepted in partial fulfillment
of the requirements of the degree of
Master of Applied Science (Environmental Engineering)
in the
Department of Civil Engineering

Date: 13 June 2008

Chairperson of Examining Board

BENCH-SCALE ANALYSIS OF ULTRAFILTRATION MEMBRANES FOR INVESTIGATING FOULING BY NATURAL ORGANIC MATTER IN SURFACE WATER

by
Dillon A. Waterman

A thesis
presented to the University of Ottawa in partial fulfillment of the requirements for
Master of Applied Science in Environmental Engineering

Department of Civil Engineering
University of Ottawa
Ottawa, Canada
K1N 6N5

May 2008

The M.A.Sc. in Environmental Engineering is a joint program
with Carleton University administered by the
Ottawa-Carleton Institute for Environmental Engineering

Your file Votre référence
ISBN: 978-0-494-48519-4
Our file Notre référence
ISBN: 978-0-494-48519-4

ACKNOWLEDGEMENTS

I would like to express my sincere gratitude to Dr. Roberto M. Narbaitz, for giving me the opportunity to work on this project, and for his continued encouragement, support, and guidance. I am very grateful to Dr. A. Tremblay and Dr. Takeshi Matsuura, for their invaluable comments and suggestions throughout this research.

I am indebted to my professors in the Environmental Engineering Program, Dr. R. Droste, Dr. L. Fernandes, and Dr. K. Kennedy.

My sincere thanks to Frank in the Civil Engineering Department, for all his help and patience in the laboratory and to Louis, and Gérard from the Chemical Engineering Department, who assisted me tirelessly, making this project a success.

Sincere thanks to my fellow graduate students, Huyen Dang, Omar Al-Attas, and Muna Albanna who assisted me throughout my research. I am also very grateful to my fellow graduate students and friends for the time we shared together at the University of Ottawa.

I also would like to express my gratitude to Membrana GmbH, Germany and Hydranautics, California, USA for supplying the membranes.

Finally, I would like to thank my wife Charmaine Waterman for her love, understanding, encouragement, and tremendous support throughout my studies.

This project was possible due to funding by the Natural Sciences and Engineering Research Council of Canada (NSERC).

ABSTRACT

Bench-scale systems, if properly designed, can become a valuable tool to evaluate fouling in dead-end ultrafiltration systems. The purpose of this study was to design and build a bench-scale hollow fiber ultrafiltration system to examine the effect of operational parameters and chemical pretreatment on membrane performance.

For this research, a bench-scale hollow fiber ultrafiltration system that operates at constant flux and includes a backwash cycle was designed and built. The system was also designed to be used as a tool in the evaluation of critical flux for source waters.

The study demonstrated that shorter operating time between backwash cycles resulted in reduced membrane fouling, improved backwash efficiency and natural organic matter rejection. The study also indicated that fouling rate increased with increase flux while backwash efficiency decreased with increasing operating flux. Chemically pretreated ORW showed superb reduction in normalized specific flux decline when compared with uncoagulated ORW.

TABLE OF CONTENTS

LIST OF TABLES

TABLE

LIST OF FIGURES

FIGURE

GLOSSARY/NOTATION

d	Fiber internal diameter
J	Flux (L/m^2/h)
J_{NSF}	Normalized specific flux
N	Number of fibers
L	Length of the fibers
R	Rejection
C_P	Permeate concentration (mg/L)
C_F	Feed concentration (mg/L)
ΔP	Axial pressure drop
P_0	Initial transmembrane pressure
γ_w	Wall shear
T_g	Glass transition temperature (^oC)
Q	Flowrate
P	Pressure at any time later in the operation
η	Backwash efficiency
μ	Viscosity [$ML^{-1}T^{-1}$]
α	Coefficient (128/Π)
P_i	Initial pressure at the start of the filtration cycle
P_f	Final pressure at the end of the filtration cycle)
P_n	Pressure following a backwash
R_m	Membrane resistances

Abbreviations

Al_2O_3	Alumina
AMWD	Apparent molecular weight distribution
AOC	Assimilable organic carbon
BDOC	Biodegradable Dissolve Organic Carbon
BWF	Backwash frequency

BWT	Backwash time
CA	Cellulose acetate
CTA	Cellulose triacetate
D/DBPs	Disinfectant/Disinfectant-by-products Rule
DBPs	Disinfection by-products DBPs
BDOC	Biodegradable dissolved organic carbon
DIA	Dialysis
DOC	Dissolved Organic Carbon
ED	Electrodialysis
EDR	Electrodialysis reversal
FA	Fulvic acid
GAC	Granular activated carbon
HA	Humic acid
HAAs	Haloacetic acids
IESWTR	Interim Enhanced Surface Water Treatment Rule
KHP	Ppotassium Persulphate
MCL	Maximum Contaminant Level
MD	Membrane distillation
MF	Microfiltration
MWCO	Molecular Weight Cut-off
NF	Nanofiltration
NSF	Normalized Specific Flux
NOM	Natural organic matter
NPSH	Net positive suction head

ORW	Ottawa River Water
PA	Polyamide
PAC	Powered activated carbon
PAN	Polyacrylonitrile
PC	Polycarbonate
PE	Polyethylene
PEEK	Polyetheretherketone
PEI	Polyether imide
PES	Polyethersulfone
PI	Polyimide
PP	Polypropylene
PS	Polysulfone
PTFE	Polytetrafluoroethylene
PV	Pervaporation
PVC	Polyvinyl chloride
PVDF	Polyvinylidene fluoroethylene
RO	Reverse osmosis
SDWA	Safe Drinking Water Act
SiC	Silicium carbide
SUVA	Specific ultraviolet absorbance
SWTR	Surface Water Treatment Rule
TiO_2	Titania
THMs	Trihalomethanes
TMP	Transmembrane pressure

TOC	Total organic carbon
TOX	Total organic halides
UF	Ultrafiltration
USEPA	United States Environmental Protection Agency
ZrO_2	Zirconia

CHAPTER 1

INTRODUCTION

1.1 Background

New regulations on filtration, disinfection, and disinfection by-products (DBPs) have resulted in extensive growth in the use of membrane processes for drinking water treatment. Membrane processes are used to remove bacteria, protozoa, particles, hardness, dissolved salts, and natural organic matter (NOM) that may be precursors to disinfection by-products. When compared to conventional water treatment processes, membrane treatment processes has many advantages. The main advantages are: superior quality of treated water, lower space requirement, easier control of operation, limited use of chemicals, and lower sludge production (Nakatsuka et al., 1996). However, in spite of the many advantages, the use of membrane processes for drinking water treatment is still restricted due to a number of concerns including permeate flux decline often referred to as membrane fouling. Membrane fouling is a phenomenon where substances in the source water, such as suspended particles, microorganisms, and organic molecules (e.g., humic substances) are deposited onto the surface of the membrane; adsorbed onto the wall of the pores; or plug the opening of the pores (Nakatsuka et al., 1996). Several studies have determined that one of the most important foulant in drinking water treatment is natural organic matter (Zularisam et al., 2006).

Current understanding of fouling is not sufficient for predicting fouling in dead-end ultrafiltration systems from measured water quality parameters and membrane properties since fouling rate depends on the nature of the foulants (Heijman et al., 2005a). Thus,

pilot testing is typically used to determine the treatability of a particular water source. Pilot-plant studies simulate very closely full-operation but are not very suitable for systematic investigations (Kim and DiGiano, 2006). Bench-scale systems, if properly designed, can become a valuable tool to evaluate fouling in dead-end ultrafiltration systems and thus predict fouling behavior in large-scale ultrafiltration plants (Heijman et al., 2005a).

Most bench-scale systems are designed to operate at constant pressure rather than constant flux and usually do not include a backwash cycle. For a constant pressure bench-scale system, fouling rate is measured by flux decline rather than by the increase in transmembrane pressure over time. However, constant flux operation is more common in pilot-plant and full-scale hollow fiber systems. Also, there are differences in fouling behavior between constant pressure and constant flux operations (Tarabara et al., 2002). In constant flux operations cake resistance increase due to compression as transmembrane pressure increase during the filtration cycle (Chellam et al., 1998).

1.2 Objectives

The purpose of this study is to design and build a bench-scale hollow fiber ultrafiltration (UF) system to examine the effect of operational parameters and chemical pretreatment on membrane performance such as fouling rate and backwash efficiency. Such a system will not only help conduct treatability studies using commercial hollow fiber membranes but will also aid the development of experimental hollow fiber membranes by our research group.

The specific objectives of this thesis are:

1. Design and test a bench-scale, ultrafiltration (UF) system that operates at constant flux and includes a backwash cycle.
2. Conduct bench-scale evaluation of critical flux.
3. Explore the effect of operating parameters such as backwash frequency and backwash time on membrane performance.
4. Examine the effect of different operating fluxes on membrane performance.
5. Investigate the impact of chemical pretreatment on membrane performance.

CHAPTER 2

LITERATURE REVIEW

2.1 Water quality challenges in drinking water treatment

Despite tremendous success in drinking water treatment in providing safe water over the past eighty years, drinking water systems continue to face challenges in delivering safe drinking water to its customers. One such challenge is the emergence of protozoan pathogens, such as Giardia and Cryptosporidium, which can be found even in high quality water sources. Even for water receiving conventional treatment, which includes coagulation, flocculation, sedimentation and filtration followed by chemical disinfection, there have been a significant number of waterborne disease cases. From 1991 to 2000, there were 2,073 cases of giardiasis and 407,642 cases of cryptosporidiosis in public water systems in the United States of America (American Chemistry Council, 2003). The 1993 Milwaukee Cryptosporidium outbreak was the largest waterborne disease outbreak documented in the United States history in which an estimated 403,000 people became ill and as many 112 deaths may have been caused by the disease (MacKenzie, et al., 1994). The outbreak resulted from a deteriorated raw water quality compounded with a simultaneous decrease in the effectiveness of the coagulation-filtration process (Kramer et al., 1996; MacKenzie et al., 1994).

The use of chemical disinfectants to control microorganisms gives rise to another major challenge to drinking water treatment: the formation of disinfection by-products (DBPs). Many of these DBPs have been shown to cause cancer and adverse reproductive and

developmental effects in laboratory animals. Hence drinking water producers are also faced with the challenge of controlling DBPs formation.

2.1.1 Microbiological threats

From the earliest of times, the practice of drinking water treatment has been entrenched in the need for pathogen removal which remains the highest priory today. It is well documented that waterborne contamination can bring with it disease of epidemic proportions as was seen in the Milwaukee cryptosporidium outbreak in 1993 (MWH, 2005).

The U.S. Centers for Disease Control and Prevention indicated that, between 1991 and 2000, 155 waterborne disease outbreaks were reported, with 431,846 associated cases of illness in public and individual United States water systems. It is believed that these reports may considerably understate the actual number of waterborne disease cases because many people who fall ill from such diseases do not consult medical professionals (American Chemistry Council, 2003). The center also revealed that, between 2001 and 2004, 61 waterborne disease outbreaks were reported and caused illness among an estimated 3,780 persons and were linked to seven deaths (Liang et al., 2006; Blackburn et al., 2004).

In Canada, in the spring of 2001, 1907 cases of cryptosporidiosis were identified in North Battleford, Saskatchewan (Stirling et al., 2001). Another well known waterborne disease outbreaks in Canada is the Walkerton tragedy in May 2000, where more than 2,300 individuals experience gastroenteritis and 7 people died as a result of the Escherichia coli

0157:H7 and Campylobacter jejuni contamination of the drinking water system (Hrudey et al., 2003).

In general, chemical disinfection is able to inactivate most microorganisms. However, a number of cyst forming bacteria and protozoa (Giardia lamblia and cryptosporidium parvum among them) are quite resistant to chlorine (MWH, 2005). To control many of the latter, it is necessary to use other disinfectants such as ozone and ultraviolet light as primary disinfects followed by chlorine as the secondary disinfectant, or use of a physical barrier like membranes.

Inactivation of cyst forming bacteria and protozoa requires higher disinfectant doses and longer contact time, which has also led to an increased formation of disinfection by-products.

2.1.2 Disinfection by-products formation

Disinfection by-products (DBPs) are formed when chemical disinfectants react with natural organic and inorganic matter in source water and distribution systems to form potentially harmful chemical compounds (USEPA, 1998).

Natural organic matter (NOM) is comprised of an extremely complex mixture of macro-organic molecules including humic substances, polysaccharides, proteins, and other classes of biopolymer formed by biological degradation of plant and animal matter in the watershed surrounding a water source (allochthonous NOM) and within the water source itself (autochthonous NOM) (Croue et al., 2000; Farahbakhsh et al., 2004).

It is now well established that all chemical disinfectants and oxidants currently used in water treatment form chemical by-products (MWH, 2005). As mentioned earlier, several DBPs have been shown to cause cancer and adverse reproductive and developmental effects in laboratory animals. However, even among those DBPs identified, the health effects are still uncertain (MWH, 2005).

Halogenated organic by-products are formed when natural organic matter (NOM) reacts with free chlorine or free bromine (USEPA, 1999). Chlorine is the most widely used disinfectant in potable water treatment and forms the greatest variety of known chlorinated by-products, for example trihalomethanes (THMs) and haloacetic acids (HAAs) (MWH, 2005). Free chlorine is usually introduced to water in the water treatment plant as a primary or secondary disinfectant through the use of chlorine, chlorine dioxide, or in the generation of chloramines.

Bromide ion also plays an important role in DBP formation (USEPA, 1999; MWH, 2005). Free chlorine or ozone oxidizes bromide ion to hypobromate ion/hypobromous acid, which subsequently forms brominated DBPs (USEPA, 1999). Brominated organic by-products include compounds such as bromoform, brominated acetic acids and acetonitriles, bromopicrin, and cyanogen bromide (USEPA, 1999). Bromide ions (Br^-) also participate in the reaction between NOM and chlorine to form various by-products that have a mix of chlorine and bromine substitutions (e.g., bromodichloromethane and bromochloroacetic acid) (MWH, 2005).

Factors affecting the formation of halogenated DBPs include the type and concentration of natural organic matter, oxidant type and dose, contact time, bromide ion concentration, pH, organic nitrogen concentration, and temperature (USEPA, 1999).

The type of NOM present in source waters also influences the amount of DBP formation (MWH, 2005). Numerous researchers have been able to fractionate NOM in different waters according to its molecular size and/ or chemical characteristics (Croue et al., 2000; Chen et al., 2007; Cho et al., 2000a; Gray et al., 2004; Kennedy et al., 2005; Storrar, 2005; Kim and Yu, 2005). In natural waters, NOM consists of a hydrophobic fraction composed of primarily humic material, and a hydrophilic fraction composed of primarily fulvic material (USEPA, 1999). According to Croue et al. (2000), hydrophobic NOM contribute more to THM and HAA formation than hydrophilic NOM on a mass/ mass basis in most natural waters.

Organic nitrogen also significantly influences the formation of nitrogen containing DBPs such as the haloacetonitriles, halopicrins, and cyanogen halides (USEPA, 1999). The concentration of total organic halides in a water sample (calculated as chloride) is represented by the parameter TOX of which less than 50 percent is identified in spite of their potential harm to humans(USEPA, 1999).

Non-halogenated DBPs are also formed when strong oxidants react with organic compounds found in water (USEPA, 1999). Ozone and peroxone oxidation of organics leads to the production of aldehydes, aldo- and keto-acids, organic acids, and, when bromide ion is present, brominated organics (USEPA, 1999). Many of the oxidation by-

products are biodegradable and appear as biodegradable dissolved organic carbon (BDOC) and assimilable organic carbon (AOC) in treated water (USEPA, 1999).

Owing to the potential health risk of DBPs, in December 1998, USEPA developed the Disinfectant/Disinfectant-by-products (D/DBPs) rules. The D/DBPs rule was promulgated into two stages; Stage 1 Disinfectants and Disinfection Byproducts Rule (Stage 1 DBPR) and Stage 2 Disinfectants and Disinfection Byproducts Rule (Stage 2 DBPR). Stage 1 DBPR is aimed at improving public health protection by limiting the amount of disinfection residual and DBPs in the distribution system (USEPA, 2001a). The rule required all water treatment plants to comply with a Maximum Contaminant Level (MCLs) local running annual averages of 120 and 100 μg/l for THMs and HAAs respectively at each monitoring site (USEPA, 1999).

The Stage 2 Disinfectants and Disinfection Byproducts Rule (Stage 2 DBPR) builds upon the Stage 1 DBPR to address public water systems with the greatest risk (USEPA, 2006). The rule strengthens public health protection for customers by tightening compliance monitoring requirements for two groups of DBPs, trihalomethanes (TTHM) and haloacetic acids (HAA5). The Maximum Contaminant Level (MCLs) local running annual averages for TTHMs and HAA5 were reduced to 80 μg/l and 60 μg/l, respectively (USEPA, 2006).

2.1.3 Balancing competing drinking water risks

The primary challenge for potable water suppliers is balancing the competing risks from microbial pathogens and disinfection byproducts.

The higher disinfectant doses and longer contact times necessary for the inactivation of cyst forming bacteria and protozoa often led to an increased formation of disinfection by-products (DBPs) in the water treatment plant and within the distribution systems. As a result, amendments to the Safe Drinking Water Act (SDWA in 1996 require EPA to develop rules to balance the risks between microbial pathogens and disinfection byproducts (DBPs). Thus, the effect of the SDWA Amendments has been to force water treatment professionals to consider the non-conventional treatment process such as membrane technologies that alone, or in conjunction with liquid-solid separation, will be capable of meeting the anticipated standards (Mallevialle et al., 1996).

2.2 Membrane processes

Mallevialle et al. (1996) defined membranes as a thin layer of material capable of separating materials as a function of their physical and chemical properties when a driving force is applied across the membrane.

Membrane processes in the drinking water industry are used for particle removal, microbial removal, softening, dissolved organics and colour removal, desalting, and many other purposes (Bergman, 2005). Membrane technologies, although becoming commercially available more than 30 years ago, are experiencing rapid development and improvements and are becoming increasingly cost-effective with better performance characteristics and as a result, their application continues to escalate (Bergman, 2005).

Membrane separation processes include microfiltration (MF), ultrafiltration (UF), nanofiltration (NF), reverse osmosis (RO), pervaporation (PV), membrane distillation

(MD), dialysis (DIA) and electrodialysis (ED). Membrane processes can be classified in a number of different ways including the type of material from which the membrane is made, the nature of the driving force, the separation mechanism, and the nominal size of the separation achieved (Metcalf and Eddy, 2003). The driving force used to promote separation can be gradients in pressure, electrical voltage, temperature, and concentration (Mulder, 1996).

The following subsection discusses in more details the membrane processes employed in drinking water treatment.

2.2.1 Membrane separation processes in drinking water treatment

Membrane processes that are pressure driven or electrically driven are the only commonly used membrane processes for water treatment (Bergman, 2005). Pressure driven membranes process commonly used in water treatment are reverse osmosis (RO), nanofiltration (NF), ultrafiltration (UF) and microfiltration (MF) and electrically driven membrane processes commonly used are electrodialysis (ED), and electrodialysis reversal (EDR) (Bergman, 2005). Table 2.1 summarizes the general characteristics of membrane processes used in water treatment including typical operating ranges, separation mechanisms, membrane driving forces, pore sizes, and typical constituents removed. Figure 2.1 showed some selected separation processes used in water treatment and size ranges of various materials found in raw waters.

Table 2.1 General characteristics of membrane processes (Metcalf and Eddy, 2003)

Membrane process	Membrane driving force	Typical separation mechanism	Operating structure (pore size)	Typical operating range, μm	Permeate description	Typical constituents removed
Microfiltration	**Hydrostatic pressure difference or vacuum in open vessels**	**Sieve**	**Macropores (>50 nm)**	**0.08-2.0**	**Water + dissolved solutes**	**Turbidity, protozoan oocysts and cyst, some bacteria and viruses**
Ultrafiltration	**Hydrostatic pressure difference**	**Sieve**	**Mesopores (2-50 nm)**	**0.005-0.2**	**Water + small molecules**	**Macromolecules, colloids, most bacteria, some viruses, proteins**
Nanofiltration	**Hydrostatic pressure difference**	**Sieve + solution/ diffusion + exclusion**	**Micropores (<2 nm)**	**0.001-0.01**	**Water + very small molecules, ionic solutes**	**Small molecules, some hardness, virus**
Reverse osmosis	**Hydrostatic pressure difference**	**solution/diffusion + exclusion**	**Dense (<2 nm)**	**0.0001-0.001**	**Water, very small molecules, ionic solutes**	**Very small molecules, colour, hardness, sulfates, nitrates, sodium, other ions**
Dialysis	**Concentration difference**	**Diffusion**	**Mesopores (2-50 nm)**	—	**Water + small molecules**	**Macromolecules, colloids, most bacteria, some viruses, proteins**
Electrodialysis	**Electromotive**	**Ion exchange with selective membranes**	**Micropores (<2 nm)**	—	**Water + ionic solutes**	**Ionized salt ions**

Microfiltration (MF) membranes have the largest pore size of the membrane processes, ranging from 0.1 μm to several μm. As a consequence of its large pore size, MF membranes can operate under ultra-low pressure conditions. MF can be used to remove large particulates matter including turbidity, and microorganisms including bacteria, Giardia and Cryptosporidium. MF has operating pressure ranging from 21 to 340 kPa (3 to 50 psig) for pressure type processes and -1 to -12 (-7 to -83 kPa) for vacuum type processes (Bergman, 2005).

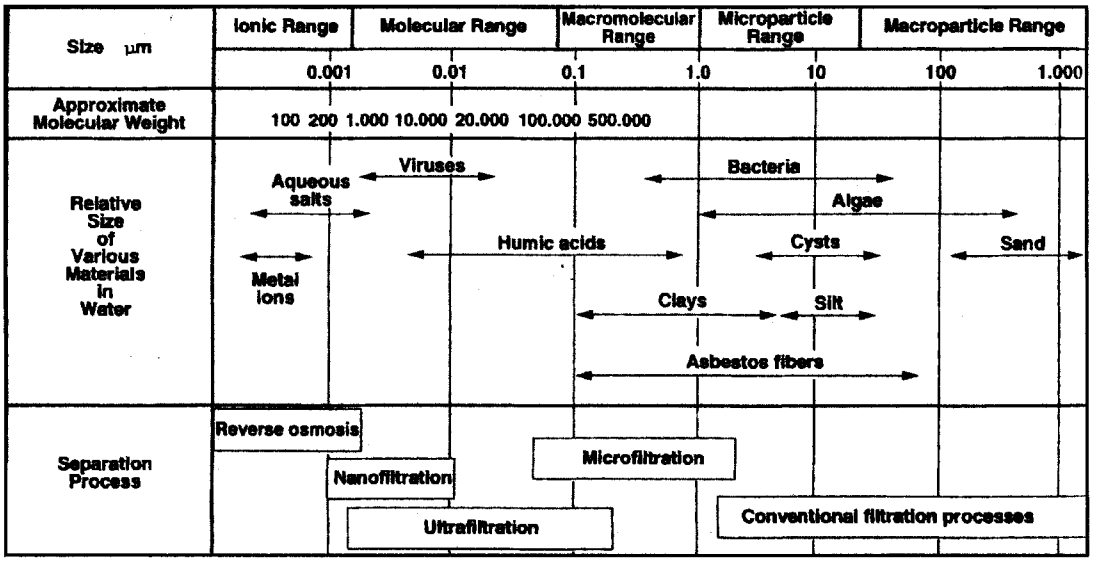

Fig 2.1 Application range of selected separation processes (Anselme and Jacobs, 1996)

Ultrafiltration (UF) membranes are also porous but have smaller pore sizes than those of MF, ranging from 0.005 to 0.2 μm (Aptel and Buckley, 1996). In addition to removing particulate matter and microorganisms including bacteria and protozoa (Giardia and Cryptosporidium) as MF, UF membranes are used for removing all types of microorganisms including viruses. Because the membrane is porous, only the coarsest solutes (macromolecules) are rejected. UF has operating pressures ranging from 50 to

500 kPa (7.25 to 72 psig) (Aptel and Buckley, 1996). Virus removal is currently not regulated, and for that reason, many water treatment UF membranes are made in the 0.1μm pore size range to compete with MF systems. Note that MF and UF membranes may have similar size pores and hence are also differentiated by the material and processes used to manufacture them.

Nanofiltration (NF), which is also called low-pressure reverse osmosis or membrane softening, lies between RO and UF in terms of the selectivity of the membrane and have pore sizes ranging between the two types of membranes (Aptel and Buckley, 1996). NF is used for the removal of multivalent ions (calcium and magnesium) in softening operations and also in the removal of organic matter including NOM. NF systems have operating pressures ranging from 340 to 1,030 kPa (50 to 150 psig) (Bergman, 2005).

Reverse Osmosis (RO) membranes are the tightest of the pressure driven membranes with pore size less than 1 nm in radius (Matsuura, 1994). In RO operations, the solvent of the solution is transferred through a dense membrane tailored to retain salts and low-molecular-weight solutes (Aptel and Buckley, 1996). While water molecules which have a radius of about one tenth of 1 nm can pass through RO membranes freely, electrolyte solutes for example sodium chloride and organics solutes that contain more than one hydrophilic functional group in the molecule cannot pass through the membrane due to the preferential sorption of water molecules at the solvent-membrane interface (Matsuura, 1994). RO are mostly used in desalination processes (e.g., brackish and seawater desalination) and the removal of small organic molecules from water (Matsuura, 1994). The operating pressure in RO operations ranges from 860 to 4140 kPa (125 to 600 psi)

when treating brackish water and from 5520 to 8270 kPa (800 to 1,200 psi) for seawater applications (Bergman, 2005).

In addition to pressure driven membrane operations, other membrane operations such as permeation is also used in water treatment. In these operations the driving force is the activity difference across the membrane (Aptel and Buckley, 1996). A permeation operation is pervaporation, which is a liquid/vapour separation process in which a liquid is partially vaporized through a dense membrane. In this operation, the activity difference is maintained by creating a partial vacuum on the permeate side of the membrane so that the pressure is kept below the vapour pressure of at least one component of the liquid in contact with the feed-side of the membrane (Aptel and Buckley, 1996). Pervaporation is often targeted for the removal of VOC from drinking water and wastewater (Aptel and Buckley, 1996).

Dialysis operations are membrane processes in which the solute is transported through the membrane. Electrodialysis (ED) is an operation by which ions are driven through ion-selective membranes under the influence of an electrical potential. ED is used in the production of potable water from brackish water (Aptel and Buckley, 1996).

The following section will discuss membrane materials and preparation in detail.

2.2.2 Membrane materials and preparation

In the early 1960s, the development of asymmetric membranes signifies a major breakthrough in industrial membrane applications. These membranes consisting of a very thin dense toplayer with thickness of 0.1 to 0.5 μm supported by a porous sublayer with

thickness of 50 to 200 μm) (Mulder, 1996). Asymmetric membranes combine the high selectivity of a dense membrane with the high permeation rate of a very thin membrane (Mulder, 1996). The dense top layer determined the resistance to mass transfer while the supporting sublayer layer provides mechanical support for the toplayer and has negligible resistance to mass transfer (Mulder, 1996).

Composite membranes, another type of asymmetric membranes with the top layer and sublayer originating from different polymeric materials were also later developed in the late 1970s (Cheryan, 1998). These membranes have the advantage of optimizing each layer independently (Mulder, 1996). Figure 2.2 represents schematic drawings of asymmetric and composite membranes. Composite membranes are widely used for nanofiltration and reverse osmosis applications.

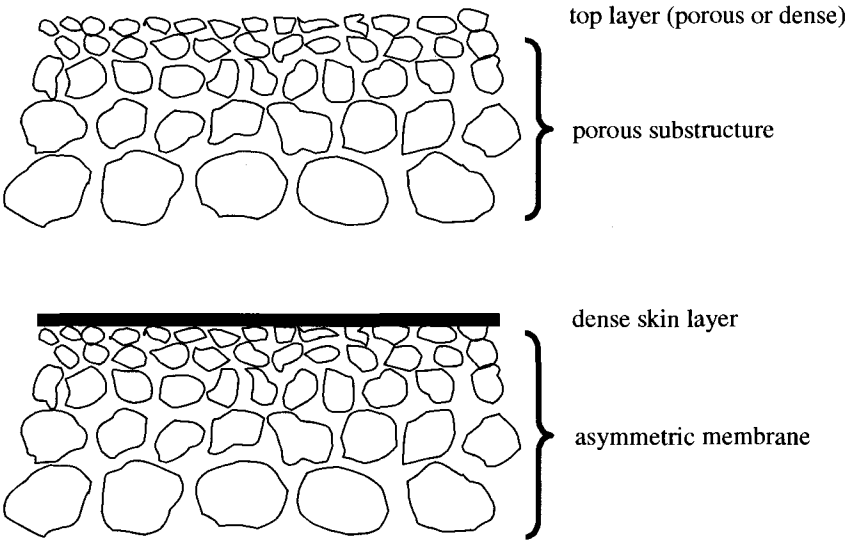

Figure 2.2 Schematic representations of an asymmetric membrane and a composite membrane (Aptel and Buckley, 1996)

Synthetic membranes can be made from a vast number of materials and can be divided into organic and inorganic membranes. Inorganic membranes include ceramic membranes, metallic membranes, glass membranes and zeolitic membranes. Ceramic membranes, the most common inorganic membrane, are formed by the combination of a metal (e.g. aluminum, titanium, or zirconium) with a non-metal oxide (nitrate or carbide) (Mulder, 1996). Metallic membranes are obtained by the sintering of metal powders such as stainless steel, tungsten or molybdenum and glass membranes (e.g., silicon oxide) are prepared by techniques involving leaching on demixed glasses (Mulder, 1996). Zeolite membranes were developed recently and have very narrow pore sizes and are applied in gas and pervaporation membrane operations (Mulder, 1996). Inorganic membranes usually possess superior thermal, and chemical, stability when compared to polymeric membranes, but generally brittle and expensive (Mulder, 1996).

Organic polymers are the most important class of membranes material. The choice of organic polymer for membrane material is based on very specific properties, originating from structural factors (Mulder, 1996). For a polymer to be successful in membrane manufacturing it must be suitable for the targeted application; be compatible with the selected preparation technique; be available and affordable; and be a good membrane former (Zeman and Zedney, 1996).

Several techniques can be employed in the preparation of membranes from synthetic materials. The objective is to modify the material by means of an appropriate technique to obtain a membrane with morphology suitable for the intended operation (Mulder, 1996). These techniques include sintering, stretching, track-etching, phase inversion and coating.

Sintering allows the production of porous membranes from organic as well as inorganic materials. The method entails compressing a powder with particles of a given size and sintering at elevated temperatures thus removing the interfaces between the contacting particles) (Mulder, 1996). The pore size of the resulting membrane is determined by the particle size and particle size distribution of the powder (Mulder, 1996). Hence, the narrower the particle size distribution of the powder the narrower the pore size distribution in the resulting membrane. Sintering is used to produce MF membranes.

Stretching involves stretching an extruded film or foil made from a partially crystalline polymeric material perpendicular to the direction of extrusion, so that the crystalline regions are located parallel to the extrusion direction (Mulder, 1996). When a mechanical stress is applied small ruptures occur and a porous structure is obtained with pore sizes of about 0.1 - 3 μm (Mulder, 1996). Stretching is used to produce MF membranes.

In the track-etching method high energy particle radiation is applied perpendicular to a foil or film which damages the polymer matrix and create tracks. The material is then immersed in an acid or alkaline bath and the polymer material is etched away along the tracks to form uniform cylindrical pores with narrow pore size distribution (Mulder, 1996). The porosity is mainly determined by the radiation time whereas the pore diameter is determined by the etching time (Mulder, 1996). Track-etching is used in the production of MF membranes.

Most commercially available membranes are produced by the phase inversion process. This technique is very versatile allowing the development of various kinds of morphologies. Phase inversion is a process whereby a polymer is transformed in a

controlled manner from a liquid to a solid state (Mulder, 1996). The process of solidification is initiated by the transition from one liquid state into two liquids (liquid-liquid demixing). At a certain stage, during demixing, one of the liquid phases (the high polymer concentration phase) solidifies and forms a solid matrix. By controlling the initial stage of the phase transition, the membrane morphology can be controlled (Mulder, 1996). The concept of phase inversion covers a range of different variations including solvent evaporation, precipitation by controlled evaporation, thermal precipitation, precipitation by vapour phase, and immersion precipitation (Mulder, 1996). Immersion precipitation is the most common method used to produce commercial membranes. The technique involves casting a polymer solution (polymer plus solvent) on a suitable support and immersing in a coagulation bath containing a nonsolvent. The nonsolvent replaces the solvent in the casting solution and the membrane is precipitated (Mulder, 1996). The membrane structure ultimately obtained results from a combination of mass transfer and phase separation (Mulder, 1996).

Unlike asymmetric membranes which are made from one material, composite membranes are made from more than one material. The basic notion for a composite membrane is to deposit a very thin selective layer on top of a highly permeable substrate that provides support and mechanical strength (Zeman and Zydney, 1996). Several coating procedures can be used such as dip coating, plasma polymerisation, interfacial polymerization, and in-situ polymerisation for forming these thin-film composite membranes.

Membranes are available in a number of different geometries: flat sheet membranes, tubular membranes and hollow fiber membranes. Flat-sheet membranes are used in plate and frame as well as spiral-wound systems. Mulder (1996) conveyed that these

membranes can be produced by casting the polymer solution upon a metal, or polymer belt. The flat-sheet is collected after the coagulation process.

An alternate geometry to flat-sheet membranes are hollow fiber membranes. In the formation of hollow fiber membranes, a viscous polymer solution containing a polymer, solvent and sometimes additives, is pumped through a spinneret, the polymer solution being filtered just before entering the spinneret. The bore injection fluid is pumped through the inner tube of the spinneret and after a short retention time in air or a controlled atmosphere the fiber is immersed in a nonsolvent bath where coagulation occurs. The outside diameters of the hollow fibers range from 0.5 to 2 mm (MWH, 2005). The fiber is then passed over rollers in a bath and is collected on a roll (Matsuura, 1994; Mulder, 1996).

Polymeric tubular membranes are not self-supporting and the polymer solutions are often cast on supporting tubular material, for instance non-woven polyester.

Several researchers (Cheryan, 1998; Mulder, 1996; and Zeman & Zydney, 1996) present various listings of the polymeric materials used in the manufacture of MF and UF and RO membranes.

Synthetic membranes may be prepared from a large number of different materials (see Table 2.2) of which polymers and ceramics are the most important.

A vast number of polymers can be used in the manufacture of MF membranes as depicted in Table 2.2. These polymers are generally crystalline in nature and exhibit high chemical resistance and thermal stability, owing to the cross-linking effect between amorphous

domains. (Anselme and Jacobs, 1996). The crystalline domains also hinder free rotation of polymers segments and inhibit compaction of the polymeric membranes by acting as cross-links (Anselme and Jacobs, 1996).

MF membranes can be prepared from various techniques such as sintering, stretching, track-etching and phase inversion.

Table 2.2 Common polymers used in commercial MF, UF and RO applications Mulder (1996), Cheryan (1998)

Membrane Material	MF	UF	RO
Cellulose esters	X		
Cellulose nitrate	X		
Polyamide , aliphatic	X		
Polytetrafluoroethylene (PTFE)	X		
Polyvinylidene fluoroethylene (PVDF)	X		
Polypropylene (PP)	X		
Polyethylene (PE)	X		
Polyester	X		
Polycarbonate (PC)	X		
Polyvinyl chloride (PVC)	X		
Polyacrylonitrile (PAN)	X	X	
Cellulose acetate (CA)	X	X	X
Cellulose triacetate (CTA)	X	X	X
Polysulfone (PS)	X	X	X
Polyethersulfone (PES)	X	X	X
Polyether imide (PEI)	X	X	X
Polyimide (PI)	X	X	X
Polyamide, aromatic (PA)	X	X	X
Polyetheretherketone (PEEK)	X	X	
Ceramic composites (zirconia on alumina)	X	X	
Alumina (Al_2O_3)	X	X	
Zirconia (ZrO_2)	X	X	
Titania (TiO_2)	X		
Silicium carbide (SiC)	X		

Polymers used in the manufacturing of UF membranes are quite similar to those used in the manufacturing of MF membranes. However, due to the smaller pore size of UF membranes, most commercially available UF membranes are prepared by the phase inversion technique. UF membranes are generally prepared from amorphous (glassy) polymers because the small pore sizes associated with these materials can be generated, regulated and controlled with relative ease during the phase inversion process (Anselme and Jacobs, 1996).

Cellulose acetate (CA) is often used in MF membrane manufacture. CA is prepared from cellulose by acetylation (reaction with acetic anhydride, acetic acid, and sulfuric acid) (Cheryan, 1998). CA membranes are very hydrophilic, possessing a wide range of pore sizes (suitable for MF to RO membranes). The membranes are also easy to manufacture at very low cost. Despite these advantages, CA membranes have narrow temperature and pH range (maximum recommended temperature 30 ^{o}C; pH range 2-8), and offers poor resistance to chlorine (less than 1 mg/L for continuous exposure and 50 mg/L in a shock dose) (Cheryan, 1998). CA suffers from compaction to a greater extent than most other membrane materials and is also highly biodegradable and is susceptible to microbial attack (Cheryan, 1998).

Polyamides (PA) membranes are also commonly used in UF membrane manufacture. PA membranes are characterized by having an amide bond in their molecular structure (-CONH-). PA membranes overcame several of limitation experienced by CA membranes such as their wider pH tolerance, but are much worse with regard to their tolerance to chlorine (Cheryan, 1998).

The family of polysulfone membranes (polysulfone, polyphenylenesulfone, and polyethersulfone) are widely used in UF membrane manufacture (Cheryan, 1998). The sulphur dioxide group ($-SO_2$) in these membranes is quite stable because of the electronic attraction of resonating electrons between adjacent aromatic groups shown in Figure 2.3. The oxygen molecules projecting from each repeating unit in this group each have two pairs of unshared electrons which contribute to strong hydrogen bonding with solute or solvent molecule (Cheryan, 1998). The repeating phenylene rings which create both steric hindrance to rotation within the molecule and the electronic attraction of resonating electron systems between adjacent molecules both contribute to a high degree of molecular immobility, producing high rigidity, strength, creep resistance, dimensional stability, and heat deflection temperature (Cheryan, 1998). Polysulfone (PS) and polyethersulfone (PES) are widely used today and are considered as significant breakthroughs (especially PES) for MF and UF applications due to the following characteristics (Cheryan, 1998):

1. High temperature limits (typically 75 ^{o}C).
2. Wide pH tolerances (continues exposures to pHs from 1 to 13). Significant advantage for cleaning purposes.
3. Good resistance to oxidants such as chlorine (chlorine exposure: 50 mg/L for short-term storage of membranes and 200 ppm for cleaning).
4. Easy to fabricate membranes in a wide variety of configuration and modules.
5. Wide range of pore sizes (1 to 20 nm) with molecular weight cut-offs (MWCOs) that range from 1000 to 500,000 daltons in commercial size modules.

6. Good chemical resistance to aliphatic hydrocarbons, halogenated hydrocarbons, alcohols, and acids.

PS and PES possess very good chemical and thermal stability indicated by their glass transition temperature (PS: T_g = 190° C, PES: T_g = 230° C) (Mulder, 1996). PS polymers are more hydrophobic than PES polymers, and are more suitable when mechanical strength and thermal stability are required (Cheryan, 1998). However due to its hyrophobicity PS membranes, have greater fouling tendencies when compared with more hydrophilic membranes such as cellulose and regenerated cellulose (Cheryan, 1998). PES membranes are slightly more hydrophilic than PS membranes (Figure 2.2). In addition, the membranes have low pressure limits (typically 100 psig for flat-sheet membranes and 25 psig for polysulfone hollow fibers (Cheryan, 1998).

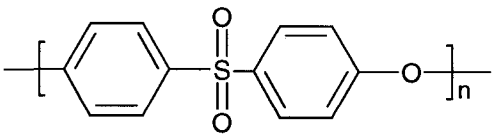

Figure 2.3 Molecular structure of PES (Anselme & Jacobs, 1996)

PES is an outstanding UF membrane material because of its membrane forming properties, excellent mechanical strength, and chemical stability. PES membranes have good resistance to inorganic chemicals, oils, greases, aliphatic hydrocarbons, alcohols, acids, halogenated hydrocarbon, and gasoline (Minnery, 2001; Cheryan, 1998). PES has high compatibility with other polymers allowing it to be used extensively in UF membrane manufacture and as a support material for composite membranes (Zeman and Zedney, 1996). PES is attacked by aromatic hydrocarbons, esters, ketones, ethers, and

methylene chloride (Minnery, 2001; Cheryan, 1998). The advantages of PES make it the most widely used polymer for manufacturing UF membranes (Hamza et al., 1997).

Other common UF polymeric membrane materials include Polyacrylonitrile (PAN), Polyether imide (PEI), and Polyimide (PI) (see Figure 2.2). The properties of these materials will not be discussed further since the focus of this thesis is on the application of UF PES membranes.

2.2.3 Ultrafiltration membrane configurations

UF is a low-pressure operation with operating pressures ranging from 50 to 500 kPa (7.25 to 72 psig) (Aptel and Buckley, 1996). UF membranes are usually fabricated in two main geometrical configurations: flat-sheet or tubular.

Flat-sheet membranes are used in plate-and-frame and spiral wound modules. Plate-and-frame modules use multiple flat-sheet membranes in a sandwich arrangement consisting of a support plate, a membrane and a channel spacer. The membranes are often sealed to the plates using gaskets and are held together by the pressure of the system. The permeate is separated from the feed stream by the use of manifolds. However, they can be combined within or outside of the module, depending upon the specific design of the plate-and-frame unit (Zeman & Zydney, 1996). The plate-and-frame units have packing density of about 100 to 400 m^2/m^3. The flat-sheet membranes in a plate-and-frame unit offer high versatility when compared with other module designs. When compared with other module design, the plate-and-frame units have one of the highest capital cost. Membrane replacement costs are usually low but, replacement labour costs are high.

Units can be easily dissembled to permit access for manual cleaning which aids in the detection of faulty membranes (Anselme and Jacobs, 1996).

Flat-sheet membranes are also used in spiral wound modules which were originally developed in the mid-1960s. Spiral wound modules were originally developed for RO operation, but have expanded into the UF field. The spiral wound configuration consist of a permeate spacer sandwiched between two membranes (facing outward) and separated by a highly porous support plate. Three edges of the membranes are sealed with an appropriate epoxy or polyurethane adhesive to form a membrane envelope, the open end being connected to a central perforated tube that collects the permeate. Feed spacers are placed in between the envelopes (connected to a single collecting tube) so that the feed liquid can reach the entire membrane surface and the envelopes and spacer are spirally wound around the collection tube. Multiple envelopes reduce the leaf length thus making the path length for permeate flow shorter thus lowering the overall manufacturing cost. The entire spiral is usually wrapped with fibreglass tape or shrink wrap for added mechanical strength and to prevent unwrapping of the spiral in operation. The spiral wound element is installed into the pressure vessel; several elements may be fitted into pressure vessels several meters in length. Each element is fitted with an antitelescoping device placed at both ends to prevent deformation of the spiral during operation. The pressurized feed is fed into one end of the pressure vessel so that it flows through the feed spacers parallel to the central tube whereas the permeate flows through the permeate spacers (inside the membrane envelopes) and spirals radially inward where it is collected through the central tube. The liquid that does pass through the membranes is then

collected at the other end of the module, and is called the retentate (Matsuura, 1994; Zeman and Zydney, 1996).

The spiral wound configuration has a relatively high membrane packing density and is currently one of the least expensive UF modules in terms of cost per unit of membrane area. However, the elements are more susceptible to particulate fouling and bacterial contamination. The modules cannot be backwashed which increase the risk of particulate fouling. Cleaning solution can also destroy the seals used to form the envelops thus compromising the integrity of the system (Zeman and Zydney, 1996; Anselme & Jacobs, 1996).

The hollow fiber modules were developed in the late 1960s for use in desalination and were subsequently developed in the early 1970s for MF and UF operations. The modules consist of a collection of hollow self supporting fibers with a dense skin layer that gives the membrane its permselectivity and a more porous structure that gives the membrane its structural integrity. The dense skin is on the lumen side for fibers that are used in an inside-out configuration and on the outside for outside-in configurations. Fiber diameters range from 0.2 mm to 2.5 mm, with wall thickness of around 0.2 mm (Matsuura, 1994; Zeman and Zydney, 1996).

Bundles of fibers are potted at the ends (held together) in an epoxy or polyurethane resin to secure and provide physical support to fibers, then the solidified resin ends (or bulheads) are machined to expose the lumens (fiber openings) of the fibers. O-rings are placed around the epoxy fiber bulkheads to form effective seal within the cylindrical housing, thereby insuring complete separation of the feed and permeate streams. The

modules can be operated with the feed flowing into the lumens of the fibers and the permeate flowing outward through the fiber walls (inside-out filtration) or with the feed on the outside of the fibers and collecting the permeate from the lumens of the fibers (outside-in filtration). The inside-out filtration mode enables the system to be operated at higher transmembrane pressures since several UF hollow fiber membranes have greater structural stability when the flow is directed radially outward from the lumen (Zeman and Zydney, 1996; Anselme and Jacobs, 1996).

The feed flow through the lumens in the hollow fiber modules is usually laminar, thus the axial pressure drop (ΔP) and wall shear (γ_w) are directly proportional to the volumetric flowrate (Q), [L^3T^{-1}], (Zeman and Zydney, 1996):

$$\frac{\Delta P}{L} = \alpha\mu \frac{Q}{Nd^4} \tag{2.1}$$

$$\gamma_w = \alpha\left(\frac{Q}{4Nd^3}\right) \tag{2.2}$$

Where N is the number of fibers, d is the fiber internal diameter, [L], L is the length of the fibers, [L], and μ the fluid viscosity [$ML^{-1}T^{-1}$]. The above equations are only approximations since they neglect the accumulation of retained solutes/particles in the boundary layer near the membrane surface. They were also derived using non-slip boundary condition at the tube wall which is not rigorously valid for porous membranes. The coefficient α can be evaluated parabolic (Poiseuille-type) flow as $\alpha = 128/\pi$ for nonporous hollow fibers and are found to be higher for porous hollow fibers by a factor of 2 for very low permeate flowrates to 10 for high flowrates (Zeman and Zydney, 1996).

One of the advantages of hollow fiber modules is the ability to obtain high mass transfer rates (i.e., due to high shear rates, γ_w) even at relatively low volumetric flowrate (Q) due to the very small value of the internal diameter (d) [Eq. (2.2]. The small diameter of the fibers used in these devices makes the hollow fiber module one of the most efficient designs with respect to pumping cost. Hollow fiber devices have a very high packing density due to the very small diameters of the fibers and the ability to pack the fiber bundles tightly in the cylindrical shell. The units also tend to have relatively low manufacturing cost since there is no need for any spacers as in the case of the spiral wound module. The hollow fibers can also be cleaned by simple backwashing of the device. One of the primary disadvantages of the hollow fiber modules is that they are highly susceptible to particulate plugging (Zeman and Zydney, 1996). Hollow fiber membranes also suffer from compaction. However, given that during the frequent backwashing steps hollow fiber systems release the pressure allowing the membrane material to rebound, hollow fiber membranes may perform better than flat sheet membranes.

Other ultrafiltration module configurations are tubular devices and rotating devices. Tubular devices are very similar in design to the hollow fiber module described but utilize much larger diameter tubes (typically 0.3-2.5 cm). The tubular modes are usually not self-supporting (with the exception of some inorganic membranes) and the membranes are generally cast in place within a porous support tube (Zeman and Zydney, 1996). Rotating devices which employ large flat-sheet discs are often used to increase the rate of bulk mass transfer. Tubular and rotating devices are not common in water treatment (Zeman and Zydney, 1996).

2.3 Ultrafiltration application in water treatment

This section discuss in detail the application of UF membranes in drinking water treatment and includes, system components; process design; turbidity and microbial removal; and integrated process applications.

The predominant removal mechanism in UF operations is straining, or size exclusion. In these operations the process can achieve perfect exclusion of particles regardless of the operating parameters such as influent concentration and operating pressure (MWH, 2005). However, contaminant-membrane chemistries also assist in particulate and microorganisms removal in UF operations but do so to a lesser extent (Wiesner and Buckley, 1996).

2.3.1 Critical flux concept

Critical flux has been traditionally defined either as the flux at which the transmembrane pressure starts to deviate from the pure water line or as the flux below which a decline of flux with time does not occur (Bacchin et al., 2006). In general, critical flux can be defined as the flux at which fouling become noticeable (Bacchin et al., 2006).

Critical flux also can be defined theoretically by transport phenomena and is considered as the flux at which the hydrodynamic force transporting the particles towards the membrane is exactly balanced by the opposing back-transport forces. These forces includes Brownian backtransport from the membrane, shear-induced diffusion which considers orthokinetic phenomena arising from particle motion under shear flow and inertial lift of particles, which leads to reduced deposition on the membrane surface (Sethi and Wiesner, 1995).

Determining the critical flux of surface waters for low pressure hollow fiber system is more complicated because of polydisperse particles sizes, and TMP changes along the length of a hollow fiber (Choi and Dempsey, 2005). Therefore, the critical flux for most surface waters systems is the operating flux that separate slow fouling from rapid fouling (Choi and Dempsey, 2005). It is therefore desirable to operate low pressure membrane systems at a sustainable flux in which fouling is minimized to avoid frequent cleaning (Bacchin et al., 2006).

2.3.2 Ultrafiltration process design and system concepts

UF membrane systems usually include pre-treatment in the form of particulate screening and/or chemical pre-treatment; the membrane units; product (or permeate) post-treatment and storage, and possible concentrate (or retentate) waste stream treatment. UF membrane systems for water treatment applications are usually composed of membrane modules installed in parallel to give greater flexibility in production output rates and to allow cost-effective incremental expansions. Recovery is defined as the ratio of net water production (volume of water fed to membrane minus volume of water used during backwashing) to gross water production over a filter run (MWH, 2005). Typical recoveries for UF systems range from 85 percent to 95 percent. The staging of UF membranes are often carried out to optimize the feed water recovery (Anselme and Jacobs, 1996). The overall recovery of a system can sometimes be improved by recycling backwash water after solids removal (Bergman, 2005). According to Anselme and Jacobs (1996), by staging UF systems, recoveries as high as 98 percent can be achieved.

The two basic types of UF processes used in water treatment are the pressure type where the membranes are housed in pressure vessels and the vacuum types where the membranes are submerged in non-pressurized tanks. Although spiral wound UF membranes are available in the market, most drinking water treatment UF membrane applications use systems comprised of hollow fiber membranes.

Submerged hollow fiber systems consist of hollow fiber modules suspended in basins containing the feed water. The basins are open to the atmosphere; hence the pressure on the influent side is limited to the static pressure provided by the water column. The transmembrane pressure is developed by a pump that develops suction on the permeate side of the membrane. The net positive suction head (NPSH) limitations on the permeate pump restrict the submerged membrane systems to a maximum transmembrane pressure of about 7.4 psi. These membranes systems generally operate at a transmembrane pressure of 3 to 6 psi. The system is operated by extracting clean water from the feed basin through the membranes. As a result, the solids concentration in the feed tank can be significantly higher than the source water thus increasing the rate of membrane fouling (MWH, 2005). The two basic techniques used for maintaining proper solids concentration in the feed tank are the "feed and bleed approach" and the "semibatch approach". In the feed and bleed approach, a small waste stream is continuously drawn from the feed tank while in the semibatch an overflow is used to remove excess water/solids during the backwash stage (Zeman and Zydney, 1996; and MWH, 2005).

The pressure-vessel configuration is a pressure-driven process by which colloids, particulates, and high-molecular-mass soluble species are retained by a mechanism of

size exclusion (Anselme and Jacobs, 1996). Transmembrane pressure is developed by a feed pump that increases the feedwater pressure, while the permeate stays at near-atmospheric pressure. Pressure-vessel systems typically operate at transmembrane pressure between 6 and 15 psi (MWH, 2005).

Two filtration approaches have been developed to influence the flow regime for the pressure-vessel configuration; cross-flow filtration and dead-end filtration. In cross-flow filtration, the feedwater is pumped at a high flowrate through the lumen of inside-out membranes at a velocity of 0.5 to 1 m/s. The cross-flow velocity which is parallel to the membrane surface creates a shear force that reduces the development of a surface cake. Since many solids are carried away with the retentate instead of accumulating on the surface of the membrane, the system can operate at a higher flux or with longer periods between backwashes. Because the permeate flow is typically less than 25 % of the feed flow, the retentate is recirculated to the feedwater (MWH, 2005). Due to recirculation the solid content of the feed will increase and must be control by the feed-and-bleed or the semibatch procedure.

The dead-end filtration on the other hand operates without a cross-flow component to the feed stream. The feedwater flow is perpendicular to the membrane surface, so all the solids accumulate on the membrane during the filtration cycle and are removed during the backwash cycle (Zeman and Zydney, 1996; and MWH, 2005). Hence, average flux values may be lower than those achieve with cross-flow filtration. In contrast to many industrial UF applications the dead-end flow regime is most common in membrane filtration for water treatment (MWH, 2005).

Pilot testing is a valuable tool used to determine appropriate operation and design criteria for membrane systems. The pilot testing procedure establishes the basis for evaluating the range of reasonable operating parameters to establish design criteria while meeting finished water quality objectives. Such matters as microbial removal efficiency, finished water quality, operations and maintenance, as well as capital and operating costs are developed from the data collected during the pilot test (Hugaboom and Crozes, 2005). Pilot testing are also often used to gain an insight into system recovery; solute and particle rejection efficiency; pre-treatment requirement, critical operating flux; water temperature; pumping requirement; backwashing and chemical cleaning requirement; and post treatment requirement.

Process design should also include ability to ensure that membranes remained intact and continue to provide a barrier between the feedwater and the permeate. Membrane integrity testing includes turbidity monitoring, particle counting, air pressure decay testing, bubble testing, sonic wave sensing and visual inspection (Jacangelo and Noack, 2005).

2.3.3 Turbidity and microbial removal

Several researchers affirmed that UF membranes are very successful in removing turbidity (Speth and Reiss, 2005; Duranceau and Losch, 2001; Glucina et al., 1998; Lipp and Baldauf, 2002; Heijman et al., 2005). Speth and Reiss (2005) stated that UF membranes produced filtrate with turbidity values less than 0.1 NTU. Duranceau and Losch (2001) stated that turbidity can be lowered to below 0.05 NTU on a consistent basis for variable feedwater quality. The primary characteristic and function of UF systems is the ability to consistently provide a filtrate that is low in turbidity. The ability

to consistently provide a low-turbidity filtrate makes UF compliant with the Surface Water Treatment Rule (SWTR) and its derivatives, such as the Interim Enhanced Surface Water Treatment Rule (IESWTR), that requires finished water turbidity levels of 0.3 NTU or less for 95 percent of the samples collected within a month. In addition, the excellent barrier provided by UF systems, results in a consistent filtrate quality regardless of the fluctuations in feedwater quality (Speth and Reiss, 2005).

The removal of microorganisms by a membrane depends of several factors, one of which is the formation of a dynamic cake layer on the membrane surface which improve the removal efficiencies for most pathogens over the filter cycle (Jacangelo et al., 1995). Cyst forming bacteria and protozoa (Giardia lamblia and cryptosporidium parvum) along with viruses can be effectively removed from a water supply by UF. UF membranes strain particles from water based on the pore size associated with the specific membrane material. Giardia and Cryptosporidium cysts diameters approximately two (2) to three-and-half orders of magnitude greater than typical UF nominal pore diameters (USEPA, 2001b). Since UF membranes pore sizes ranging from 0.005 to 0.2 μm which is smaller than all types of microorganism thus ensuring their complete removal. UF membranes are used for removing particulate matter, protozoa (Giardia and Cryptosporidium), bacteria and viruses. Jacangelo et al. (1991) studied the removal of Giardia by MF and UF and demonstrated removal greater than 4 logs, with no cysts measured in the filtrate. Jacangelo et al., (1995) also studied the removal of Cryptosporidium, Giardia, and MS2 virus by MF and UF hollow fiber systems. The study showed that all the hollow fiber membranes evaluated removed Giardia muris cysts and Cryptosporidium parvum oocysts to below their detection limit.

Bacteria encompass many different species of various shapes and sizes ranging from spherical to almost thread-like in shape and from 0.1 μm to 100 μm in size. However, in general most species of bacteria are larger than the exclusion characteristics of common MF and UF membranes and are completely removed by these membranes (USEPA, 2001b). According to USEPA (2001b), studies conducted on the removal of total coliform in river water using UF membranes resulted in removals greater than 4 logs. Jacangelo et al. (1997) also studied total coliform removals in surface water using UF membranes and reported log removal below detection limit.

Viruses are much smaller than protozoan cyst and bacteria. Viruses range in sizes from 0.005 μm to 0.1 μm which is similar to the entire range of UF and the lower end of MF pores. Viruses are removed by a number of mechanisms including size exclusion (sieving), adsorption onto the membrane surface, filtration by the cake layer particles, adsorption onto particles in the cake layer and sieving as a result of the constriction of membrane pores due to irreversible fouling (Jacangelo et al., 1995). Virus removal by UF membranes varies depending on the pore size of the UF membrane used. For membranes with MWCO of 100,000 Da (approximately 0.01 μm) or tighter, researchers showed that viruses were frequently reduced to less than detection limit (USEPA, 2001b). Jacangelo et al. (1991) and Jacangelo et al. (1997) studied removal of the MS2 bacteriophange virus from seeded deionised water using UF membranes with MWCO of 100,000 Da. The studies showed virus removal was greater than 6 logs. According to USEPA (2001b), similar studies showed virus removal of 1.0 to 6.5 logs for UF membranes with MWCO of 100,000Da and 6.2 to 6.8 logs for UF membranes with MWCO of 10,000 Da.

2.3.4 Integrated process applications

Combining low-pressure membranes filtration operation with other water treatment unit operations has expanded rapidly in recent years to address water quality and treatment goals beyond particulate and microbial removal. These systems are becoming the predominant type of membrane-based water treatment plant because most surface waters contain both dissolved and particulate contaminants (Lozier, 2005).

Where source waters have high or variable turbidity or where total organic carbon (TOC) levels are high, it is more practical to precede membrane filtration with conventional pre-treatment (coagulation, flocculation and sedimentation). The coagulation/flocculation process reduced turbidity and TOC concentration through various mechanisms such as charge neutralization and sorption onto flocs while sedimentation reduces the solids loading to the low-pressure membrane system thus averting consequent fouling (Kabsch-Korbutowicz, 2005; and Lozier, 2005). By providing an influent that is low in turbidity and TOC, the MF/UF system is able to operate at increased flux with longer filtration cycles which reduces cleaning frequency, thereby reducing operating costs (Lozier, 2005). According to Lozier (2005), in-line coagulation is also employed before membrane filtration to reduced arsenic and natural organic matter (NOM).

Membrane filtration is also employed in conjunction with lime softening to provide enhance microbial removal from surface waters with a high degree of hardness. In this application membrane filtration replaces conventional granular media filtration (Lozier, 2005).

UF by itself cannot remove a very significant amount of natural or synthetic organic compounds hence powered activated carbon (PAC) adsorption is sometimes combined with UF. Granular activated carbon (GAC) is also occasionally used in conjunction with UF. Placing the GAC after low pressure membrane treatment eliminates particulate loading on the GAC media and reduces the frequency of backwashing (Lozier, 2005). In PAC-membrane integrated systems, MF and UF are used to remove both particulate matter and PAC with the adsorbed organics (Lozier, 2005; and Clark et al., 1996). Where persistent taste and odour problem exist in a surface water supply and turbidity and NOM content is low, membrane filtration is often preceded by ozonation and biological filtration (Lozier, 2005). Ozonation/biological filtration provides effective taste and odour control, while MF/UF provides excellent particulate and microbial removal. Membrane filtration can also be added as a polishing step to treat the effluent of a conventional treatment plant where enhanced microbial removal is necessary (Lozier, 2005).

Integrating membrane systems exploit the excellent particulate removal capability of low-pressure membrane systems to ensure that utilities have a cost-effective approach to meet ever more stringent drinking water regulations. They also have the potential to explore water resources of lower quality water than those relied upon previously to meet increasing water resources demands (Mallevialle, 1996; and Lozier, 2005).

2.4 Membrane fouling

One of the major factors limiting the successful application of membrane systems for water treatment is membrane fouling. Membrane fouling is caused by specific physical

and/or chemical interaction between the membrane and various components in the source water and cause a rapid and often irreversible loss of flux through the membrane (Zeman and Zedney, 1996; Katsoufidou et al., 2005). Nakatsuka et al. (1996) defines membrane fouling as a phenomenon where substances in the source water, such as suspended inorganic particles, bacteria, viruses, and organic molecules (e.g., humic substances) are deposited onto the surface of the membrane; adsorbed onto the wall of the pores; or plug the opening of the pores. The deposition eventually forms a gel or cake layer on the membrane surface causing a decline in flux for constant pressure systems or an increase in transmembrane pressure (TMP) for constant flux systems.

Cheryan (1998) characterized membrane fouling by an irreversible decline in flux. However, Anselme and Jacobs, (1996) and MWH (2005) characterized fouling as reversible or irreversible. The latter characterization will be adopted for this thesis. During the initial filtration operation a decline in specific flux occurs, and a portion of this flux loss cannot be recovered during backwashing and chemical cleaning operations. This permanent flux loss is called irreversible fouling, and depends on the source water quality as well as the type of membrane used. For full-scale membrane filtration operations, the period between backwashes varies from 30 to 90 minutes while the period between chemical cleaning varies from one to six months (MWH, 2005). As filtration progressed, the specific flux may decline further, but may be recovered by backwashing and cleaning. This recoverable loss of flux is called reversible fouling. The specific flux loss which occurs between backwashes is due to the accumulation of particulate matter on the membrane surface, which is usually carried away during the backwash cycle. The

specific flux loss between cleaning cycles is due to slow adsorption and clogging by materials within the membrane matrix, which may be removed during chemical cleaning.

In addition to fouling, several other phenomenons are also responsible for specific flux decline including membrane compaction, and concentration polarization. Membrane compaction is a function of the membrane physical characteristics and occurs when the membrane is exposed to pressures that will cause the membrane material to deform and reduce the size of the pores. Concentration polarization is due to the accumulation of solutes close to or on the membrane surface that causes an increase in resistance to solvent transport across the membrane forming thus forming a boundary layer. The impact of concentration polarization may be minimized by decreasing the transmembrane pressure, lowering the feed concentration or increasing the cross-flow velocity or turbulence adjacent to the membrane (Cheryan, 1998).

2.4.1 Fouling mechanisms

Since fouling results from the specific interactions between the membrane and the solutes in the feed stream, it is difficult to predict and hence a general rule with universal application cannot be established (Cheryan, 1998). However, it is therefore helpful to have an understanding of the blocking laws that governs fouling.

Fouling can be caused by different solute and particle depositions. Bowen et al. (1995) described four different types of fouling mechanisms as follow: complete blocking (pore sealing), intermediate blocking (pore sealing with superposition), standard blocking (internal pore constriction) and cake filtration (boundary layer resistance). Complete blocking occurs when some pores are completely sealed at the membrane surface by

incoming particles. The fraction of blocked pores is proportional to the amount of permeate flow. Intermediate blocking is an extension of the complete blocking filtration law and presumed that each particle can settle on other particle previously arrived and already blocking some pores or it can also directly block some membrane area. Standard blocking takes place when particles or dissolved matter adsorbs to the wall of the pores, and fouling occurs because of the reduced cross-sectional area of the pores. In cake filtration, the membrane is completely unaffected by incoming particles. However, these particles form a separate layer on the surface of the membrane. Fouling occurs since water has to flow through two layers (the cake and the membrane), each of which offer resistance to flow (Bowen et al., 1995 and MWH, 2005) (Figure 2.4).

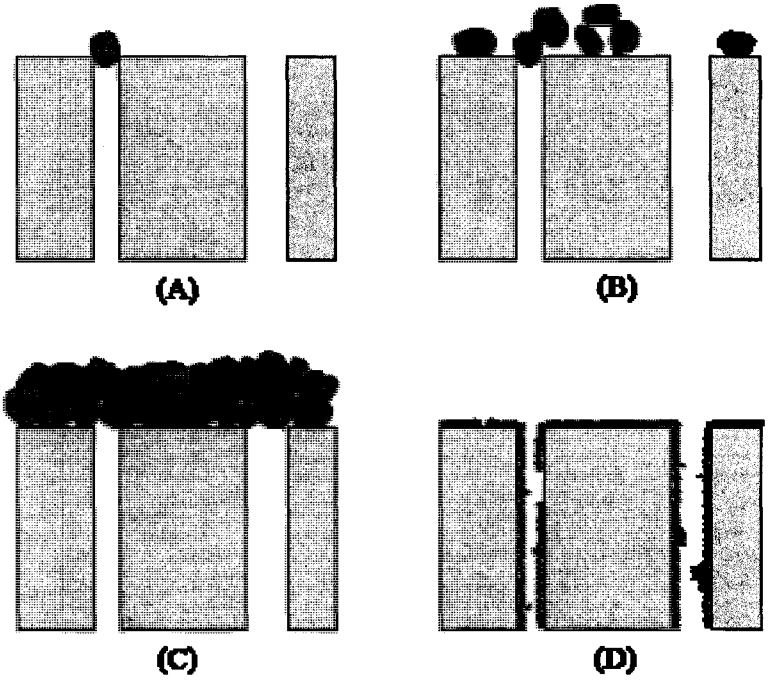

Figure 2.4 Fouling mechanisms according to Bowen et al. (1995) (A) complete blocking, (B) intermediate blocking, (C) cake filtration, (D) standard blocking

Since fouling in its true sense is a result of specific interaction between the membrane and various solutes in the feed stream (Cheryan, 1998), and given the different materials

and pore size distribution of asymmetric membranes in conjunction with the different feed solution characteristics, it is reasonable to assume that membrane fouling occurs through a combination of different mechanisms (Bowen et al., 1995; Katsoufidou et al., 2005).

Several researchers have demonstrated that membrane fouling occurs through more than one fouling mechanisms. Costa et al. (2006) studied fouling of colloidal natural organic matter in UF and found that at the earlier stages of filtration, the dominant fouling mechanism was pore blocking and that as filtration progressed, there was a transition from pore blocking to cake formation. Ho and Zydney (2000) developed a combined pore blockage and cake filtration model for protein fouling during microfiltration. The model accounts for the simultaneous pore blockage and cake formation, with the cake layer forming only over those regions of the membrane surface that have been previously blocked. Yuan et al., (2002) conducted an analysis of humic acid fouling during microfiltration using a pore blockage–cake filtration model based on the theoretical approach developed by Ho and Zydney. They demonstrated that the flux decline during MF of humic acid through 0.2 μm pore size MF membranes was very well described using a modified form of the combined pore blockage and cake filtration model developed by Ho and Zydney. They suggested that the initial fouling was due to pore blockage caused by the physical deposition of large humic acid aggregates on the surface of the MF membrane followed by cake formation over those regions of the membrane that have been previously covered. From their study they also demonstrated that there is a flux below which cake formation becomes negligible (critical flux). Other authors assuming that membrane fouling occurs through a combination of different mechanisms

include (Song, 1998; Duclos-Orsello et al., 2006; Liu and Kim, 2007). The following section will look at some of the major foulants affecting membrane application in the treatment of natural waters.

2.4.2 Foulants in natural waters

Since fouling can be caused by different solute and particle depositions from the feed stream, it is important to understand the nature of these foulants and how they affect membrane application in water treatment. The major types of foulants in natural waters that affect membrane application include particulate matter, dissolved inorganic substances, dissolved organic substances and biological materials.

2.4.2.1 Particulate fouling

During membrane filtration, particulate matter collects on the membrane surface in a porous mat called a filter cake. Cake formation occurs when a suspension contains particles that are too large to enter the pores of the membrane (Chellam and Zander, 2005). In a typical membrane filtration operation, particles larger than 200 μm are usually prefiltered to protect the membrane, so the cake is initially composed of material between 200 μm and the membrane retention rating (MWH, 2005). The cake layer acts as a dynamic filter, retaining additional smaller material but also generating hydraulic resistance to filtration that increases with operating time and causes transmembrane (TMP) pressure to increase (constant flux operation) or equivalently, the permeate flux to decline (constant pressure operation) (Chellam and Zander, 2005). Particulate fouling is largely reversible by periodic backwashing.

2.4.2.2 Dissolved inorganic substances

There is a wide range of inorganic substances that can cause significant fouling in membrane filtration operations. Many of these compounds are often present in natural waters. Zeman and Zedney (1996) presented a list of inorganic species that can cause fouling. They include calcium sulphate, calcium carbonate, calcium phosphate, silica, metal oxides and hydroxides (particularly of iron and aluminium), colloidal sulphur, and other inorganic particulates. Fouling by salts and metal compounds generally occurs by precipitation or flocculation on or within the porous structure of the membrane (Zeman and Zedney, 1996).

According to Anselme and Jacobs (1996), UF processes in contrast to NF and RO, do not usually allow significant dissolved salt retention, which can lead to mineral precipitation on the membrane surface due to salt concentrations higher than their respective solubility products. However, the precipitation of certain minerals in UF processes has been identified as one of the causes of fouling. Anselme and Jacobs (1996) stated that in water treatment, precipitation is mainly due to calcium carbonate precipitation or to precipitation of dissolved metals such as iron and manganese due to oxidation and hydrolysis during the filtration process. They stated that this leads to the formation of an iron and manganese oxide cake on the membrane and are often responsible for inorganic fouling in membrane filtration systems. Fouling caused by iron and manganese oxide is reversible by backwashing (Anselme and Jacobs, 1996). Calcium precipitation can be reduced by acidifying the water, i.e., lowering the pH or by adding calcium-sequestering agents to the feedwater (Zeman and Zedney, 1996). Colloidal silica is a notorious foulant and is present in many natural waters. The solubility of silica is a function of temperature

and pH and excess silica concentration in the feed stream is generally associated with severe silica deposition (Zeman and Zedney, 1996).

2.4.2.3 Dissolved organic substances

Dissolved naturally occurring organic substances have been recognized as one of the major causes of fouling in the membrane filtration of natural waters. The two types of organic foulants that have been studied extensively are protein and natural organic matter (NOM). Zeman and Zedney (1996) found that the significant increase in hydraulic resistance of MF membrane after protein filtration is due to the formation of a relatively thick protein deposit on the upper surface of the membrane. They also stated that the hydraulic resistance brought about by the protein deposit is a function of solution, pH, and ionic strength and that this was due to changes in the protein packing density associated with electrostatic repulsive forces between charged proteins within the deposit. Protein fouling in drinking water treatment membrane applications is not very significant; however, protein fouling models are often used in the study of fouling by NOM and other organic foulants.

NOM has been alluded to by several researchers as a mayor membrane foulant in drinking water treatment. As was mentioned previously, natural organic matter is an extremely complex mixture of macro-organic molecules including humic substances, and polysaccharides. NOM that occur in natural water ranges in molecular weights from 5,000 to 50,000 Dalton (Maartens et al., 1999). NOM can be fractionated into three segments: hydrophobic (humic substances), hydrophilic (non-humic fraction) and transphilic fractions. According to Zularisam et al. (2006), the hydrophobic fraction, which comprises of the larger molecular weight macromolecules represents close to 50%

of dissolved organic carbon as depicted in Figure 2.5. They stated that the hydrophilic fraction comprises of 25–40% lower molecular weight dissolved organic carbon (DOC) including polysaccharides, amino acids and protein and that the transphilic fraction comprised of approximately 10–25% DOC with molecular weight ranging between the hydrophobic and hydrophilic fractions. As depicted in Figure 2.5 and reported by other researchers such as Cheryan (1998) and Fan et al. (2001), the largest fraction of the NOM arises from humic substances. Cheryan (1998) suggested that humic substances could represent up to 80% of the total organic carbon of natural water. Zularisam et al. (2006) also suggested that humic substance could represent 60–90% of the DOC in natural waters. Fan et al. (2001) stated that humic substances (humic and fulvic acids) comprise over 50% of the dissolved organic carbon (DOC), and are mainly responsible for the colour in natural waters. According to Cheryan (1998) and Zularisam et al. (2006), humic substances are weak acidic polyelectrolyte with negatively charged carboxylic acid ($COOH^-$), methoxyl carbonyls (C=O) and phenolic (OH^-) functional groups. Humic substance can be divided into three categories: humic acid (HA), fulvic acids (FA) and humin. HA is soluble at higher pH (normally pH 10) while fulvic acid is soluble in water at all pH levels. Humin usually exists as a black coloured substance and is not soluble in water (Zularisam et al., 2006).

According to Farahbakhsh et al. (2004), the mechanisms of NOM fouling on membrane systems may be divided into three categories: cake formation, surface adsorption-deposition, and adsorption-deposition in the membrane pores. Anselme and Jacobs (1996) suggested that natural organic matter (NOM) in waters can lead to membrane fouling, either by surface adsorption; on the particles making up the filtration cake,

thereby giving the cake cohesion; or by adsorption in the membrane matrix. They stated that this type of fouling depends mainly on the affinity that the NOM have for the membrane material. Anselme and Jacobs (1996) also suggested that this adsorption may be considered a dynamic equilibrium phenomenon with a slow kinetic rate, which leads to progressive saturation of adsorption sites of the membrane material.

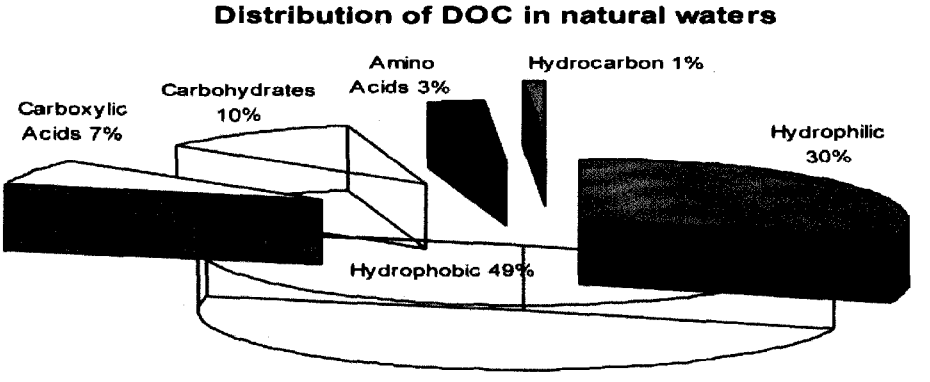

Figure 2.5 Fraction of NOM according to Zularisam et al. (2006)

There have been extensive studies on the impact of NOM on fouling in membrane filtration. In their study on membrane filtration of NOM, Cho et al. (2000) identified non-charged NOM fractions (hydrophilic and hydrophobic neutrals/bases) as the main foulants for negatively charged polyethersulfone (PES) membranes. Fan et al. (2001) reported from their study on the influence of the characteristic of NOM on the fouling of MF membranes that the low-aromatic hydrophilic neutral compounds were the main cause of flux decline. They also showed that the higher the aromaticity of the NOM the greater the flux decline, and that the aromatics mainly resided in the hydrophobic acids fraction. They suggested that the fouling mechanism controlling the flux decline involved the combined effects of adsorptive and colloidal fouling by the hydrophilic neutral fraction in the internal pore structure of the membrane. Fan et al. (2001) also reported

that the order of fouling potential of NOM fractions for the three waters studied was hydrophilic neutral > hydrophobic acids > transphilic acids > hydrophilic charged. They also reported that hydrophobic membranes had greater fouling effect than hydrophilic membranes of similar size. Yuan and Zydney (1999) during their study of humic acid fouling during microfiltration observed that the initial fouling in their system was determined almost entirely by the convective deposition of large particles or aggregates on the membrane surface and that the initial deposits accelerated the subsequent rate of fouling, possibly serving as a nucleation site for the deposition of humic acids macromolecules with little internal pore adsorption. Schafer et al. (2001) in their study of microfiltration of colloids and natural organic matter observed that HA caused a 78% decline in flux compared to FA (15%). Although most researchers concluded that humic fraction of NOM is largely responsible for fouling, others such as Lin et al (1999); Cho et al (2000a); Cho et al (2000b); and Lee et al (2004) claimed that the non-humic fraction of NOM (hydrophilic and neutrals) was responsible for flux decline.

Solution chemistry, including pH, ionic strength and divalent cation concentration, such as Ca^{2+}, may also govern the extent of membrane fouling (Cho et al, 2000b). According to (Zularisam et al. 2006), NOM particles agglomerate more at low pH. Several researchers have shown that membrane flux decreased substantially with lower pH, high ionic strength and high divalent cation concentration. In their study on the effect of pH on UF membrane fouling, Dong et al., (2006) found that a decrease in pH was effective in enhancing NOM removal but significant fouling was observed as a result. They suggested that this fouling could be ascribed to the decrease in the size and negative charge of the NOM which promote the adsorption of NOM in the membrane matrix.

Schäfer et al. (1998) in their study on the fouling of NF membrane by NOM and the influence of multivalent ions reported that fouling was detrimental at high calcium ion concentrations due to the formation of calciumhumate complexes. Hong and Elimelech (1997) studied the chemical and physical aspects of NOM fouling of NF membranes and observed that the presence of divalent cations, such as calcium and magnesium, has marked effect on NOM fouling. They found that fouling increased substantially with high ionic strength, low pH and increasing divalent cations concentration. According to (Zularisam et al. 2006) this behaviour could be due to the changes of intra and intermolecular electrostatic gradients of the functional groups (-COO and -COOH). They stated that increasing ionic concentration changed rejection by buffering or shielding the charge on the solute molecules which encouraged coiling and aggregation of NOM. In addition, Wiesner and Aptel, (1996) stated that higher calcium concentrations and lower pH tend to increase the hydrophobicity of humic materials thus favouring their adsorption.

The interaction of NOM with the membrane material depends on both the characteristics NOM in the feed stream, such as molecular weight, functional groups and charge (Wiesner and Aptel, 1996), and the membrane properties, such as pore size, surface charge, surface roughness and hydrophobicity (MWH, 2005; Nguyen, 2005 and Zularisam et al. 2006). According to MWH (2005), one major membrane characteristic that influences membrane fouling is hydrophobicity. Hydrophobicity is a reflection of the interfacial tension between water and the membrane material. Several authors (including Cheryan M., 1998; and Laîné et al., 1989) have expressed that hydrophilic materials, which like contact with water, tend to have low fouling tendencies whereas hydrophobic

materials may foul extensively. Hydrophobicity is quantified by contact angle measurements, in which a droplet of water is placed against a membrane surface, and the angle between the membrane surface and water droplet surface is measured. Hydrophobic surfaces generally have high contact angle whereas hydrophilic surfaces have low contact angle. Hydrophobicity is affected strongly by the chemical composition of the polymer comprising the material (MWH, 2005). For instance, polymers that have ionized functional groups, polar groups, or oxygen-containing and hydroxyl tend to be very hydrophilic (MWH, 2005).

Laîné et al (1989) in their study of the effect of UF membrane composition observed that higher permeability occurred for the more hydrophilic membranes than for the hydrophobic ones. The study done by Nakatsuka et al. (1996) demonstrated that hydrophobic membranes have greater fouling tendencies thus causing greater flux reduction than hydrophilic membranes. They found that cellulose acetate membranes which are hydrophilic had twice the flux than the more hydrophobic polyethersulfone during the UF of river water. However, there is also contradictory evidence (Dang et al., 2006) possibly because the contact angle measurements may also be influenced by the topography and surface roughness.

Membrane surface charge can also have a significant impact on fouling and flux reduction. Membranes with negative charge have been found to reduce flux decline when the solute is also negatively charged. Wiesner and Aptel (1996) gave an example of organic solutes with negatively charged function groups (e.g., fulvic and humic acids) that can be repelled by negatively charged membrane surfaces. This agrees with the results of Cho et al. (2000). They found that UF membranes with a negatively charged

surface had a greater NOM rejection than expected. Carroll et al. (2000) found that the major contribution to fouling was attributed to the NOM fraction comprising neutral (uncharged) hydrophilic compounds. According to Zularisam et al. 2006, humic substances possess negative charges which prevent them from being adsorbed onto negatively charged membrane surface. They also mentioned that in many studies the foulants were found to be hydrophobic materials (Nilson and DiGiano, 1996; Yuan and Zydney, 1999; Jones and O'Melia, 2000). They suggested that in these circumstances hydrophobic interactions overcome the electrostatic repulsion force between NOM and the membrane and caused fouling.

2.4.2.4 Biological growth

Fouling by biological material (biofouling) is problematic in membrane filtration systems (MWH, 2005). Ridgeway and Flemming (1996) defined biofouling as a loss of system performance due to the formation of biofilm. During the filtration operation, microorganisms are transported to the membrane surface, where they can attached with sufficient force as to prevent removal during backwashing (MWH, 2005). According to Chellam and Zander (2005), the process of microbial attachment may be roughly categorized into three different stages: (1) microoganisms loosely approach the surface of the membrane through various transport mechanisms (such as gravity, diffusion, and convection); (2) microorganisms reside within the viscous sub-layer forming weak bonds with the membrane surface; and (3) microorganisms form irreversible bonds with the membrane surface. Once the microbial cell is attached to the surface of the membrane, it uses nutrient from the feedwater to grow and reproduce thus forming a film (biofilm) (Chellam and Zander, 2005).

Biofouling is favoured by several factors including reduced feed water cross-flow velocities, elevated operating pressures and temperatures, high feed water concentrations of organics, small feed channels, and membrane materials with enhanced bacterial affinities (Ridgway and Flemming, 1996).

Biofouling has several adverse effects on a membrane systems including flux decline, reduced solute rejection, enhanced mineral scaling, increased module differential pressure, permeate contamination, membrane biodegradation and reduced membrane life (Ridgway and Flemming, 1996).

2.5 Membrane fouling control

Since fouling is a complex phenomenon, approaches to reduce fouling can only be described generally and thus each separation problem requires its own specific approach (Mulder, 1996). Mulder (1996) suggested four common methods that can be utilized in the reduction of membrane fouling: (1) pre-treatment of the feed solution; (2) changing membrane properties; (3) optimizing module design and operating parameters; (4) cleaning fouled membranes (hydraulic, cleaning, mechanical cleaning and chemical cleaning).

2.5.1 Hydraulic cleaning

To control the accumulation of solids on the membrane surface, backwashing of the membrane is performed periodically. Unlike conventional media filtration, the backwashing cycle takes only a few minutes. Both liquid and air may be employed in the backwashing of low-pressure membranes. However, inside-out membrane configurations

use only liquid for backwashing. For most low-pressure membranes systems, backwashing is fully automated, initiated when the transmembrane (TMP) pressure reaches a certain set-point; a predetermined period of operation or after a predetermined permeate volume is produced. For most low-pressure systems, backwashing is performed every 30 to 120 min of operation for 1 to 5 min (Jacangelo and Noack, 2005).

Several researches have studied the effect of backwashing in membrane filtration operations. Kim and DiGiano (2006) in their study of fouling rate for an UF membrane reported that that doubling the backwash time from 30 s to 1 min did not decrease the fouling rate, however increasing the frequency of backwashing from once every 15 min to once every 10 min at a backwash time of 30 s reduced the fouling rate. They concluded that backwash frequency was more important than backwash time in the control of fouling rate. In their study of backwash efficiency for hollow fiber MF membranes, Hong et al. (2005) demonstrated that the efficiency of backwashing decreased significantly with increasing solution ionic strength, while backwash efficiency did not vary when particle concentration and operating pressure increased. They suggested that backwash efficiency is closely related to the cake structure. They also suggested that the effective control of membrane fouling in low-pressure membrane operations depends on the mode and efficiency of backwashing and that an increase in backwash frequency and duration significantly reduced membrane fouling. Lipp and Baldauf (2002) showed that for MF/UF systems regular backwash with filtrate supported by air backwash was very effective in minimizing TMP increase. Their investigations also demonstrated that chemical cleaning was still necessary as some irreversible fouling always remains after backwashing.

2.5.2 Chemical cleaning

When foulants can no longer be removed from the membrane surface by backwashing, chemical cleaning is required. After chemical cleaning, partial or full restoration of transmembrane flux or pressure is achieved. Consideration in chemical cleaning includes frequency of cleaning, duration of cleaning, cleaning chemicals and their concentrations, cleaning and rinse volumes, temperature of cleaning solutions, recovery and reuse of cleaning chemicals, and neutralization and disposal of cleaning chemicals (Jacangelo and Noack, 2005).

A variety of chemical cleaning agents can be employed for the cleaning of low pressure membranes, including surfactants, acids, bases, oxidizing agents, sequestering agents, and enzyme cleaners (Jacangelo and Noack, 2005). Chemical cleaning agents work by a number of different mechanisms, including displacement of foulants from the membrane matrix (e.g., by competitive adsorption of appropriate surface active agents); solubilization of the foulants (e.g., by changing the foulant solubility or by providing an appropriate emulsifying or dispersing agent); and chemical modification of the foulants (e.g., oxidation or degradation of proteins, chelating divalent cations, or reaction of metal oxides with appropriate acids) (Zeman and Zydney, 1996). Cleaning is usually initiated after the transmembrane pressure exceeds 10 psi (0.7bar) to 29 psi (2 bars), depending on the particular membrane (Jacangelo and Noack, 2005). Increasing the temperature of cleaning solution to 35 – 40 ^{o}C is often employed to enhance cleaning effectiveness.

Membrane fouling rarely occurs by a single foulant, and the presence of multiple inorganic and organic foulants can complicate the choice of effective chemical cleaning

agents (Zeman and Zydney, 1996). According to Zeman and Zydney, 1996, Bedwell and co-workers examined the cleaning of MF membranes used for municipal water treatment where fouling was due to inorganic precipitates (calcium carbonate and iron oxide) and the deposition of organic material (humic acid). They found that the membranes could be effectively cleaned using surfactants to solubilize the organic material followed by acid cleaning (hydrochloric acid at a pH of 1) to remove the inorganic precipitates. Lee et al. (2000) found that foulants from a hydrophobic NOM source were cleaned more effectively by acid and caustic cleanings in comparison with foulants from a hydrophilic NOM source.

2.5.3 Pretreatment

Traditionally, low-pressure membranes have been used to remove particulate matter including turbidity and microorganisms. However, low-pressure membranes systems (MF and UF) are now being installed in water treatment operations where pretreatment is necessary. As was previously mentioned, membrane filtration is now being combined with existing conventional water treatment plants involving coagulation, flocculation, and sedimentation where MF and UF systems have replaced media filtration. Membrane filtration processes coupled with coagulation are also employed to replace the sedimentation-filtration units (direct membrane filtration). Pretreatment guarantee a much higher water quality in terms of turbidity and microbial removal and also significant increase in flux with very little membrane fouling. As a result of chemical and physical pretreatment, MF and UF membranes are now being considered for treating high turbidity and high NOM waters and source waters containing other contaminants such as arsenic, pesticides, algae, iron and manganese (Farahbakhsh et al., 2004).

Coagulation is the most frequently used chemical pretreatment in MF or UF water treatment facilities to remove NOM. Chemical coagulants used in conjunction with MF and UF membrane systems, include alum, ferric chloride, ferric sulfate and poly aluminum chloride (Farahbakhsh et al., 2004).

The effect of chemical coagulation on membrane fouling has been positive in most instances. Most studies on chemical coagulation have reported a reduction in membrane fouling rate and chemical cleaning frequencies including (Choi and Dempsey, 2004; Kabsch-Korbutowicz, 2005; Kim et al., 2005; Qin et al., 2006; and Jung et al. 2006). Several authors attributed the reduction in fouling rate to the reduced pore plugging by the larger coagulated particulate matter in the raw water. Materials that might otherwise enter the pores and constrict flow are aggregated or sorbed onto flocs of the precipitated metal hydroxide which are rejected at the membrane surface (Wiesner and Laîne, 1996). The filter cake formed from the coagulated matter is easier to remove than particles that plug the membrane thus backwashing is more effective (Farahbakhsh et al., 2004).

In spite of the many evidence supporting the positive impact of coagulation on membrane performance, studies have also shown the contrary. Schäfer et al. 2001 found that coagulation with ferric chloride of water containing NOM; organics are adsorbed on a ferric oxyhydroxide precipitate which is retained by the MF and UF membrane, cause membrane fouling by pore blocking or cake deposition.

2.5.4 Membrane Surface modification

It is well documented that surface chemistry of membranes plays an important role in fouling control. According to Zeman and Zydney (1996), almost 50% of all MF/UF

membranes marketed today are surface-modified. They stated that the common membrane surface modification strategies involve: (1) addition of a compatible modifier (such as a hydrophilic or charged polymer) into the casting solution; (2) adsorption of a modifier onto the membrane surface; (3) chemical or physicochemical post-treatment of the surface (e.g. hydrolysis or gas plasma treatment); and (4) grafting or cross-linking a modifier on the surface.

There have been several initiatives at the laboratory scale to modify membrane surfaces. The majority of the work aimed to make the membrane surfaces more hydrophilic thus making them less susceptible to fouling. Ulbricht and Belfort, (1996) applied low temperature plasma to induced surface modification of polyacrylonitrile (PAN) and polysulfone (PS) ultrafiltration membranes to make them more hydrophilic. They reported that the membranes became more hydrophilic and especially when immersed in water showed good stability of the hydrophilization effect. Pieracci et al. (1999) studied the photochemical modification of 10 kDa polyethersulfone (PES) ultrafiltration membrane by photolysis using ultraviolet light and graft polymerization of hydrophilic monomers onto the membrane surface to create more hydrophilic and lower fouling membrane surfaces. They reported that the modified membranes showed increased hydrophilicity which translated into decreased protein fouling relative to the unmodified (PES) membranes. The membranes also showed higher combined filtration performance compared with commercial low protein adsorbing membranes. They reported that the best filtration results were obtained using PES membranes modified with the monomer N-vinyl-2-pyrrolidinone which resulted in a 50% decrease in fouling and a 4% increase in rejection relative to the unmodified PES membrane. Carroll et al. (2002) modified

polypropylene hollow fiber MF membranes by grafting charged and non-charged hydrophilic polymers as a flexible layer onto the polypropylene membrane surface. They reported that non-ionic and cationic hydrophilic grafts have rates of flux declined by NOM fouling up to 50% lower than ungrafted polypropylene. They stated that these membranes can filter NOM-containing surface water for extended periods without any flux decline due to NOM fouling or without compromising permeate quality.

2.6 Bench-scale systems analysis of fouling by natural organic matter

Bench-scale systems can become a valuable tool in the evaluation of fouling in ultrafiltration systems and thus predict fouling behaviour in large-scale ultrafiltration plants (Heijman et al., 2005a). However, most bench-scale systems fail to simulate the actual operating conditions of low pressure membrane filtration systems. Also, they often fail to include factors that affect membrane performance such as critical operating flux, backwashing frequency, backwashing time, and backwash flux or backwash pressure (Kim and DiGiano, 2006). Most bench-scale systems are designed to operate at constant pressure rather than constant flux and often do not include a backwash cycle (Nakatsuka et al., 1996; Katsoufidou et al., 2005; and Aoustin et al., 2001) . However, constant flux operations are more common in pilot-plant and full-scale systems and according to (Tarabara et al., 1995), there are differences in fouling behaviour between constant pressure and constant flux operations. One major difference observed is the increase in cake resistance during constant flux operations due to compression as transmembrane pressure increase during the filtration cycle (Chellam et al., 1998).

In spite of the widespread use and ease of building constant pressure bench-scale systems, a small number of research groups including (Heijman et al., 2005a; Heijman et al., 2005b; and Kim and DiGiano, 2006) designed and build bench-scale systems that operate at constant flux. Kim and DiGiano (2006) used a two-fiber bench-scale system to investigate fouling rate during the treatment of granular-media filtered secondary wastewater effluent. They maintained constant flux ± 5% of the setpoint flowrate with the use of a positive displacement piston pump and measured fouling rate by the decline in specific flux over several backwash cycles. However, they could not determine backwash efficiency since the system was not equipped with a data acquisition system and pressure measurements were done by visual inspection. Heijman et al. (2005a) used a rather simple and inexpensive equipment to simulate the filtration and backwash cycles of a full-scale system. They maintained constant flux with the use of a piston pump with two syringes to dampen flow fluctuation. The equipment used a four-way-valve to switch between filtration and backwash cycles. The same pump was used for the filtration and backwashing cycles and hence backwashing flux was equal to the filtration flux. Manufactures often recommend a backwashing flux of more than twice the filtration flux and hence the system was deficient in this regard. Heijman et al. (2005b) in their study of heterogeneous fouling in dead-end ultrafiltration used a gear pump to maintain constant flux. The increase in fouling was measured during 12 filtration cycles of 30 min and the backwash flux was twice that of the filtration flux. The system could automatically perform several cycles of filtration and hydraulic cleaning. However, particulate matter can affect the successful operation of gear pumps; hence feed water has to be filtered to acceptable levels thus limiting the use of such a system.

Most constant flux systems although attempted to simulate full-scale plant operations, had several deficiencies. It is therefore the purposes of this work to designed and build a bench-scale hollow fiber ultrafiltration system that mimics the full-scale water treatment plant as close as possible, thus enabling better examination of the effect of operational parameters on membrane performance at the bench-scale level.

Osmonics has established the Osmonics SEPA cell as the standard cell for flat sheet membranes; however there are no standard apparatus for hollow fibers membranes. It is therefore the intent of this work to build a hollow fiber ultrafiltration system of the highest quality that can be used as standard bench-scale equipment since such equipment is lacking for hollow fibers.

2.7 Conclusions of the literature review

NOM in surface waters is considered the major precursor of DBPs during drinking water treatment and a significant membrane fouling agent (Chang and Benjamin, 1996; MWH, 2005; and Katsoufidou et al., 2005). Several authors indicated that membrane fouling restricts the widespread application of membranes in water treatment (Nakatsuka et al., 1996; Chang and Benjamin, 1996; and Smith et al., 2006).

The reduction of membrane fouling can be accomplished by pre-treatment of the feed water; membrane modification; optimizing module design and operating parameters; and cleaning the fouled membranes (Mulder, 1996). To control the accumulation of solids on the membrane surface, backwashing of the membrane is performed periodically. Backwashing during membrane filtration processes has been found to successfully remove most of the reversible component of the fouling layer leading to reduced

transmembrane pressure increases in constant flux systems and permeate flux decline in constant pressure systems thus minimising the severity of fouling (Smith et al., 2006). Backwashing also enables the system to operate for longer periods before stopping for chemical cleaning. Chemical pretreatment is one of the most effective ways to reduce fouling by NOM in membrane filtration. Coagulation is the most frequently used chemical pretreatment in MF or UF water treatment facilities to remove NOM. (Farahbakhsh et al., 2004).

This study will focus on the designing and building a bench-scale system that operates at a constant flux and include a backwash cycle and will also focus on exploring the effect of operating parameters such as backwash frequency, backwash time and operating flux on membrane performance. The study will also investigate the impact of chemical pretreatment on membrane performance. The methodology is detailed in the following chapter.

CHAPTER 3

MATERIALS AND METHODS

This chapter describes the equipment designed for this study (i.e., the membrane characteristics, the module preparation and configuration), the feed water source characteristics, the testing protocols; the experimental design; and the sampling and analytical methods.

The project is divided into five different phases: The first phase involved designing and building a bench-scale, hollow fiber ultrafiltration (UF) system that operates at constant flux and includes a backwash cycle. The second phase involved conducting bench-scale evaluation of critical flux for source and pretreated waters. The third phase involved exploring the effect of operating parameters, such as backwash frequency and backwash time, on membrane performance. The fourth phase of the experiment involved examining the effect of different operating flux on membrane performance. The final phase involved the investigation of the impact of chemical pretreatment on membrane performance.

3.1 Chemicals

The chemicals used in this project were of analytical grade without any further modification. The total organic carbon (TOC) standards were prepared with potassium persulphate (KHP), (BDH Inc., Toronto, ON). Orthophosphoric acid (A.C.S grade, 85% purity, Fisher Scientific, Fair Lawn, NJ) was used as a preservative. TOC reagents were made sodium persulphate (Mallinkrodt Baker Inc, Phillipsburg, NJ) and Orthophosphoric acid (Fisher Chemical A.C.S grade, 85% purity, Fisher Scientific, Fair Lawn, NJ). Alum used in the pretreatment of feed water was prepared from ground aluminium sulphate

($Al_2(SO_4)_3.18H_2O$) (Fisher Scientific, Fair Lawn, NJ). Glassware cleaning was conducted with Chromerge™ (concentrated labware cleaner, VWR International, West Chester, PA) and concentrated sulphuric acid (Fisher Scientific, Fair Lawn, NJ). Reagent-grade water was prepared with a Milli-Q Water System by Millipore (Bedford, MA) using mix bed ion exchange resins, synthetic activated carbon, organic scavengers and UF flatsheet membranes. This ultrapure water is referred to as Milli-Q water.

3.2 Source water

The source water selected for this research is the Ottawa River water (ORW) which is rich in natural organic matter (NOM) and is the source for the Britannia Water Purification Plant which supplies water to the city of Ottawa, Ontario. Water from the intake of the water purification plant was collected at the water plant and stored in a cold room at the University of Ottawa at 4°C to retard biological degradation. One day prior to its use, the water was transferred to the laboratory thus allowing it to reach room temperature (20° C) before the filtration test.

Selected chemical and physical characteristics of the source water collected on September 24, 2007 were measured and are shown in Table 3.1. Source water turbidity, pH, TOC, and UV-254 absorbance were also measured before each filtration test and are also reflected in Table 3.1. The apparent molecular weight distribution (AMWD) of the organic matter within ORW (as determined by Dang 2008) was determined by UF fractionation using a 50 mL Amicon batch stirred UF cell (model 8050, Amicon Corp., Danvers, MA) and regenerated cellulose membranes (Millipore, Bedford MA) with four different nominal molecular weight cut-offs: 5,000, 10,000, 30,000 and 300,000 Daltons.

The major NOM fraction, (humins, hydrophobic acids, hydrophilic acids and transphilic acids within ORW (as determined by Dang 2008) were isolated using XAD 4 and XAD 8 resins (Supelco, Bellefonte, PA) placed in two glass columns (75 cm in length and 2 cm in diameter).

Table 3.1. Raw water quality of ORW

Parameter	Mean
pH	7.49±0.16
Turbidity (NTU)	2.41±0.26
Alkalinity (mg/L as $CaCO_3$)	54
Total Hardness (mg/L as $CaCO_3$)	45.65
Calcium Hardness (mg/L as $CaCO_3$)	43.48
Colour	50
Total Organic Carbon	5.8±0.205
UV254 absorbance (cm^{-1})	0.255±0.018
SUVA (L/mg-m)	4.40

3.3 Ultrafiltration membrane and module configuration

The membrane used in this research is the UltraPES 0.7 hollow fibers from Membrana, Germany. The membrane material is polyethersulfone (PES) with a nominal molecular weight cut-off of 70 kDa. The fibers have an internal diameter of 0.7 mm and outside diameter of 1 mm.

Eight UF hollow fibers were placed within the modules, which were constructed at the University of Ottawa, Faculty of Engineering, Machine shop, consisted of ½ inch O.D. acrylic tubing (¼ inch I.D.) caped at both ends with ½ inch compression brass caps. The

fibers were then sealed at both ends with epoxy resin which harden in 30 min. The eight 26 cm long fibers provided a total surface area of 0.0046 m^2. The module is configured to operate in the inside-out dead-end mode by cutting one of the epoxy bulkheads to permit flow into the inside of the fibers. This configuration was chosen over the cross-flow mode since the pumping costs associated with recirculating feed water through the lumen can be expensive. Detailed construction of the module is shown in (Appendix B). A schematic diagram of the module used in the experiment is presented in Figure 3.1. A pictorial, view of the module is depicted in Figure 3.2.

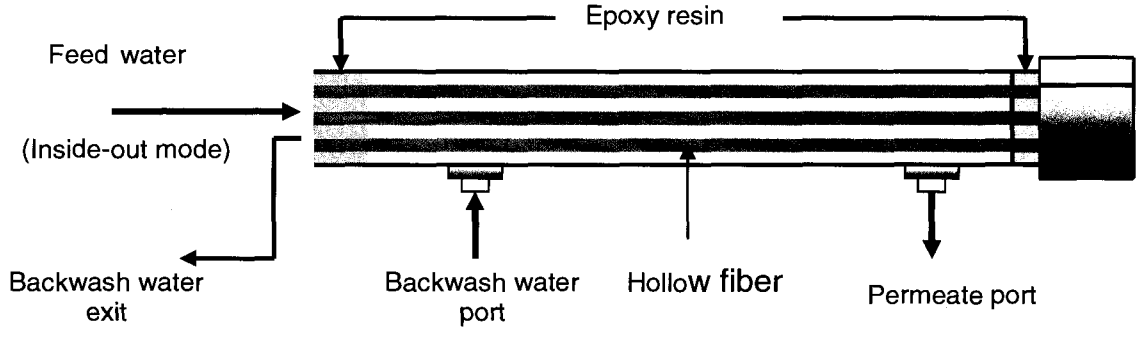

Figure 3.1. Schematic diagram of the inside-out hollow fiber module.

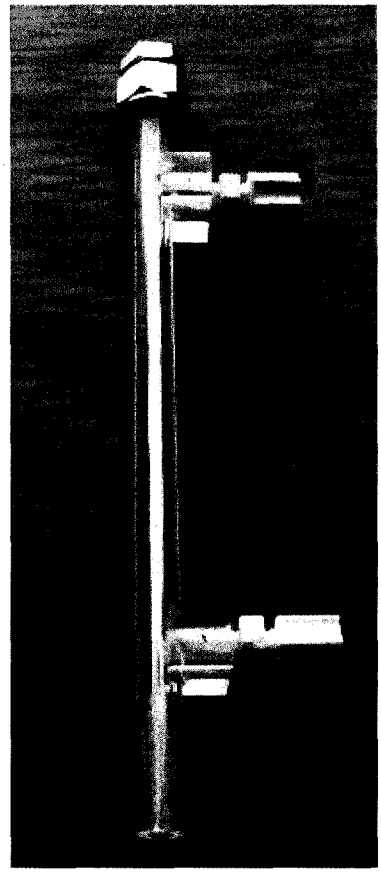

Figure 3.2. Pictorial view of the inside-out hollow fiber module used in the experiments.

3.4 Ultrafiltration system design and set-up

One of the major objectives of this research was to design and build a bench-scale, hollow fiber ultrafiltration (UF) system that operates at constant flux and includes a backwash cycle. Figure 3.3 depicts the ultrafiltration (UF) system designed and built for this research. The system was designed to replicate the filtration and backwash cycles of the full-scale membrane filtration operation.

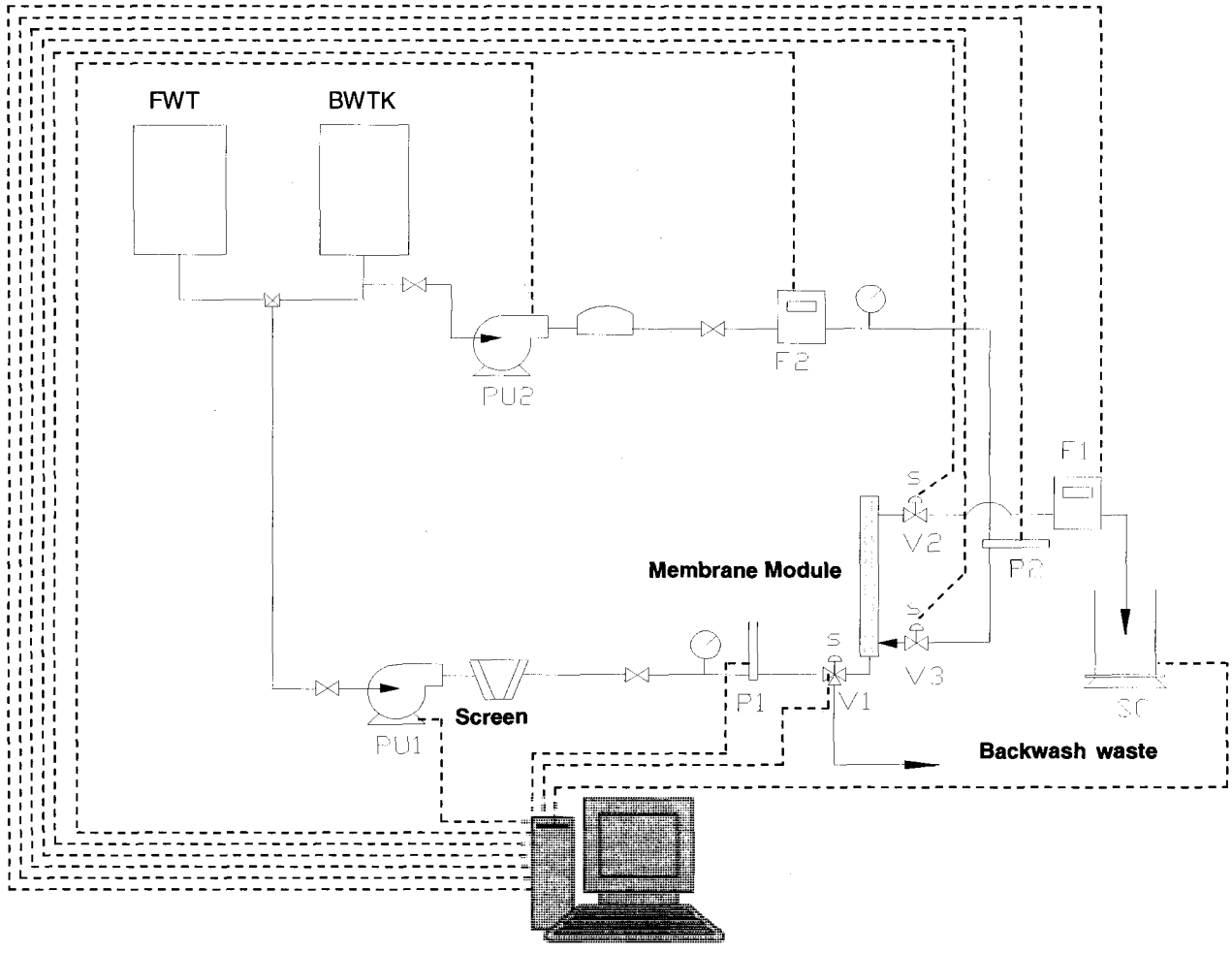

PU1 – Feed water pump
PU2 – Backwash pump
F1 – Filtration flowmeter
F2 – Backwash flowmeter
P1 – Filtration pressure transducer
P2 – Backwash pressure transducer
V1 – 3-way solenoid valve
V2 – 2-way solenoid valve
V3 – 2-way solenoid valve
SC – Scale
FWT – Feed water tank
BWTK – Backwash water tank

---------- Measurement and control electronic connections
——— Fluid lines

Figure 3.3. The ultrafiltration bench-scale system designed for the research

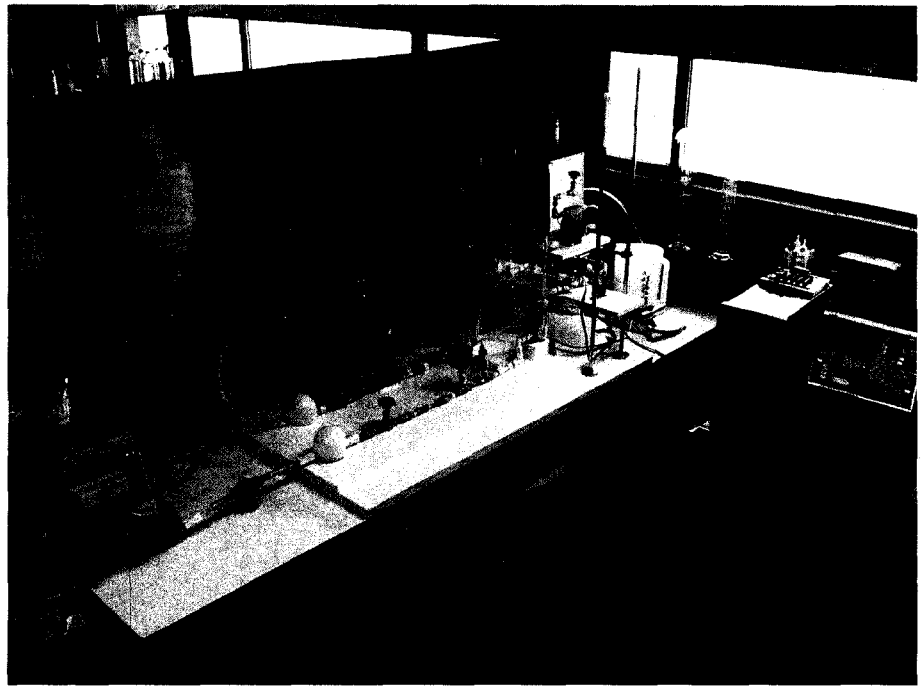

Figure 3.4. Experimental set-up

The UF side of the system was designed to maintain constant flux using a controller to control the feed pump (PU1). The filtration side of the system is comprised of a L/S Easy-Load II peristaltic pump (EW-77200-52, Cole-Parmer, Montreal, QC), a low-profile in-line strainer system with a 178 μm mesh (K-29595-35, Cole-Parmer, Montreal, QC), a gate valve, an inlet pressure gauge, a pressure transducer, a three-way solenoid valve at the base of the membrane module, a two-way solenoid valve on the permeate side of the module and a digital flowmeter (0-20 mL) (L-20CCM-D, Alicat Scientific, Tucson, AZ). The permeate is collected in beakers on a top-loading balance (K-11018-12, Cole-Parmer, Montreal, QC).

The backwashing operation also utilizes a controller and operates at constant flux until the maximum allowable back pressure stipulated by the membrane manufacturer is reached after which the system backwashes at constant pressure. The backwash unit is

comprised of a high pressure peristaltic pump (Maximum pressure 100 psi) (FPUDVS2007, Omega, Laval, QC), a pulsation dampener (EW-30610-37, Cole-Parmer, Montreal, QC) to smooth out flow variations caused by the three roller peristaltic pump, a digital flowmeter (0-50 mL) (L-50CCM-D, Alicat Scientific, Tucson, AZ), an inlet pressure gauge, a pressure transducer, and a two-way solenoid valve at the entrance to the shell side of the module.

The UF system depicted in Figure 3.3 and Figure 3.4 was designed with a LabVIEW interface which enables the input of operating parameters including feed flowrate; filtration cycle length; water temperature; backwash flowrate; backwash time; maximum backwash pressure and running average lengths for permeate weight, flowrate and pressure. The interface also depicts the average of the feed water flowrate. The UF system is automated with a computer initiating both filtration and backwash cycles through the starting and stopping of the feedwater pump and the backwash pump, and through the opening and closing of the three solenoid valves (Figure 3.5). The system is complemented with data acquisition which records the major process outputs including operating time, flowrates and pressures for feed and backwash water, permeate time, balance time and density through an empirical relationship between water temperature and density.

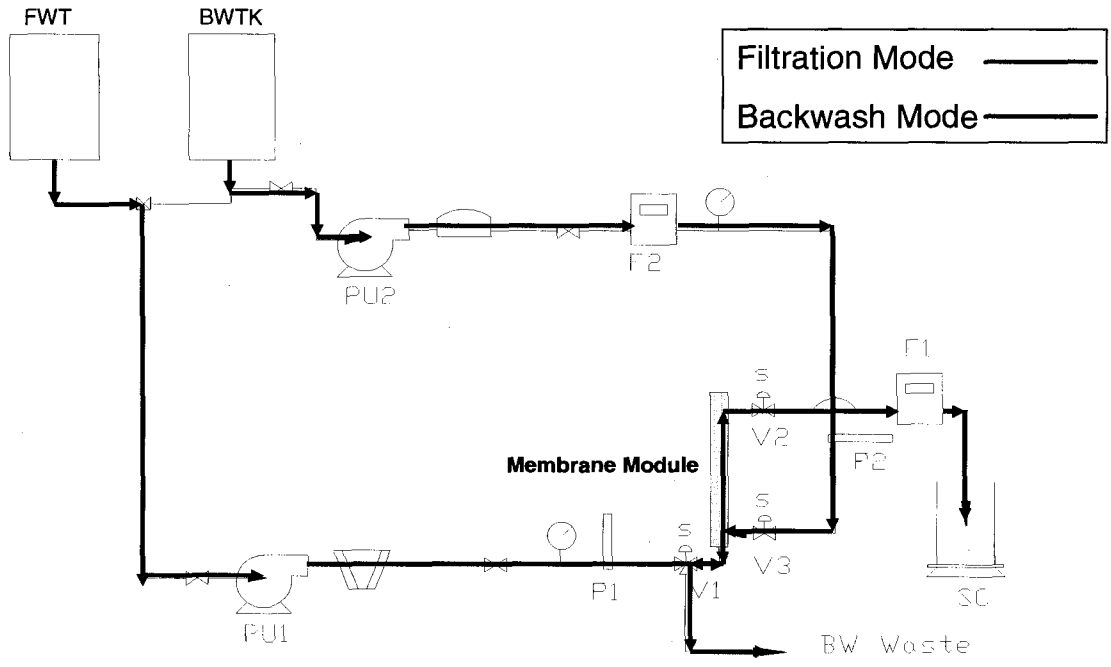

PU1 – Feed water pump
PU2 – Backwash pump
F1 – Filtration flowmeter
F2 – Backwash flowmeter
P1 – Filtration pressure transducer
P2 – Backwash pressure transducer
V1 – 3-way solenoid valve
V2 – 2-way solenoid valve
V3 – 2-way solenoid valve
SC – Scale
FWT – Feed water tank
BWTK – Backwash water tank

Figure 3.5. The ultrafiltration bench-scale system showing filtration and backwash cycles

3.5 Experimental design

Figure 3.6 shows a flow diagram of the general methodology followed in each filtration experiment of Ottawa River water.

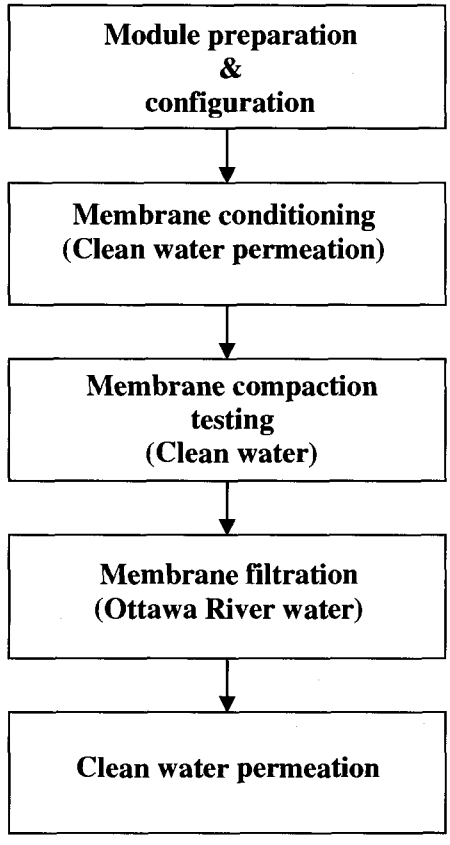

Figure 3.6. Methodology overview

The filtration experiment was conducted in five different stages. The first stage involves the preparation and configuration of the module as described in section 3.3. The second stage involves conditioning the membrane by pumping milli-Q water for an hour through the module at a pump output of 9.25% of maximum output (7 ± 0.35 mL/min). This phase also enables the computation of the initial membrane resistance (Rm_I). This is followed by a clean water test (evaluating transmembrane pressure (TMP) at different

fluxes) to determined the effect of membrane compaction throughout the pressure range during the filtration test. The third stage is the ultrafiltration of Ottawa River water. After the filtration test, milli-Q water is pumped through the module at a pump output of 9.25% (7 ± 0.35 mL/min) for 30 to 60 min and the final membrane resistance (Rm_2) determined. The filtration experiments were conducted in duplicate and a new module was used for each experiment.

3.5.1 Ultrafiltration process description

For each filtration test, Ottawa River water was placed in the feed water tank (FWT) (Figure 3.5) and Milli-Q water in the backwash water tank (BWTK). Filtration cycle length (backwash frequency [BWF]), backwash time (BWT), the desired pump output along with other operating parameters were entered into LabView. Deionized water was use to stabilized the system before switching to river water. During the ultrafiltration test, river water entered the lumen of the fibers at the base of the module and is forced through the side of the fibers (dead-end mode). Permeate flows from the shell side of the module to the top-loading balance where it is collected in beakers. At the end of each filtration cycle which lasted from 15 min to an hour, the computer switched the solenoid valves so as to end the filtration cycle and start the backwash cycle. In the latter the backwash water enters the shell side of the module and forced its way to the inside of the fibers which is the reverse direction of the filtration cycle. The backwash water removed the accumulated filter cake and exits the module via the three-way solenoid valve at the base of the module (Figure 3.5). Milli-Q water was used for backwashing instead of permeate due to the low volume of permeate produced in each experiment.

3.5.2 Bench-scale estimation of critical flux

The experiments were conducted according to the methodology outlined in Figure 3.6. However, instead of operating at a constant flux, filtration experiments for the estimation of critical flux for the feed water and chemical pretreated water were performed using the flux-step method. The experiments involved stepwise increases in permeate flux from approximately 30 $L/m^2/h$ to 110 $L/m^2/h$. Each flux was maintained for a period of 15 minutes. Transmembrane pressure (TMP), operating time, permeate volume, temperature, and density were recorded in LabVIEW throughout the experiments.

3.5.3 Effect of operating parameters on membrane performance

The experiments were conducted according to the methodology outlined in Figure 3.6. The filtration experiments were performed with filtration cycles (backwash frequencies) of 15, 30 and 60 minutes. Each of the cycle was combined with a backwash time of one minute and two minutes, respectively. The experiments were conducted for seven hours at a constant flux of 100 $L/m^2/h$ and transmembrane pressure (TMP), operating time, permeate volume, temperature, and density were recorded in LabVIEW throughout the experiments.

3.5.4 Effect of different operating fluxes on membrane performance

These experiments were also conducted according to the methodology outlined in Figure 3.6. The filtration experiments were performed with a filtration cycle of 30 minutes and a backwash time of one minute. Filtration experiments were performed at constant fluxes of 50, 70, 100 and 120 $L/m^2/h$. All filtration experiments were performed for seven hours

with the exception of the experiment at 120 L/m^2/h flux which was performed for only four hours since the maximum allowable transmembrane pressure of 20 psi was exceeded at which the membranes should had been chemically cleaned but is something that was beyond the scope of this study. Transmembrane pressure (TMP), operating time, permeate volume, temperature, and density were recorded in LabVIEW throughout the experiments.

3.5.5 Effect of chemical pretreatment on membrane performance

Figure 3.7 shows a flow diagram of the methodology followed in each chemical pretreatment filtration experiment.

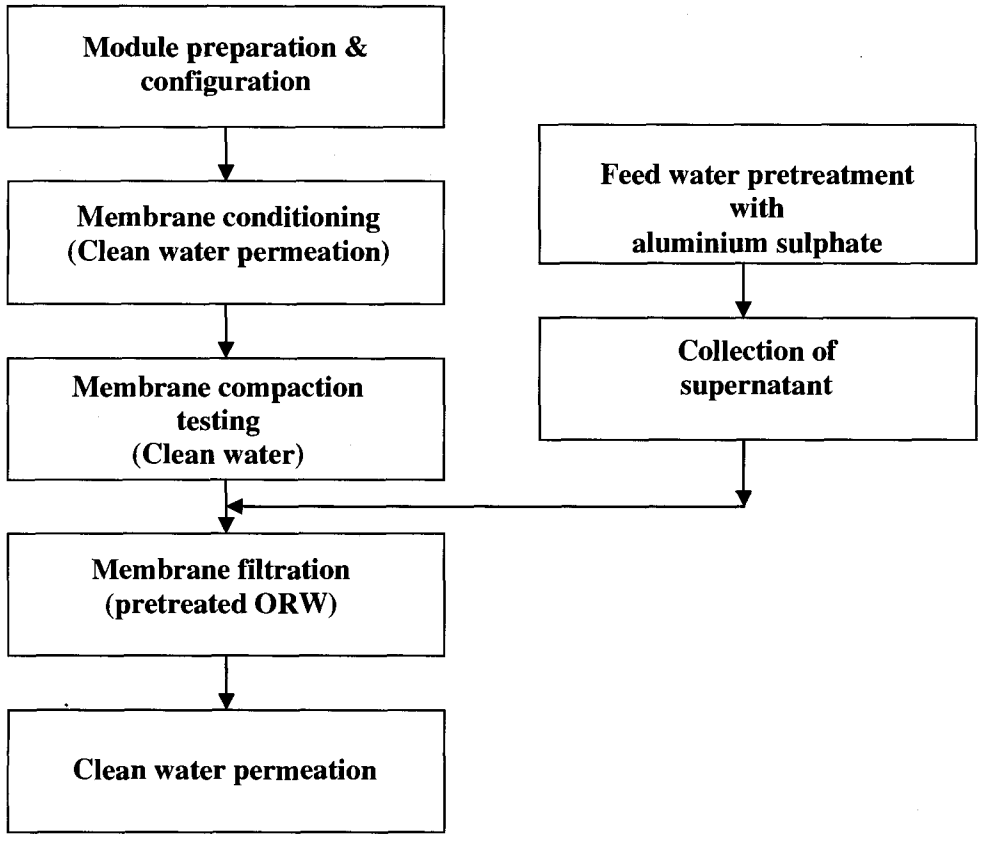

Figure 3.7. Methodology overview for chemical pretreated Ottawa River water

Jar test were carried out with a six paddle Phipps & Bird Jar stirrer to ascertain optimum TOC removal. Different aluminium sulphate concentrations ranging from 10 mg/L to 60 mg/L were added to each of six B-KER[2] laboratory jars. The tests indicated that the optimum TOC removal (54 ± 0.85%) occurred at an aluminium sulphate ($Al_2(SO_4)_3.18H_2O$) (Fisher Scientific, Ottawa, ON) concentration of 40 mg/L equal to 3.24 g Al/m^3 , that was associated with a pH of 6.3. Jar test data and graphs depicting optimum TOC removal are shown in Appendix D. Figure 3.8 depicts the jar testing equipment used in the optimization of TOC removal of ORW.

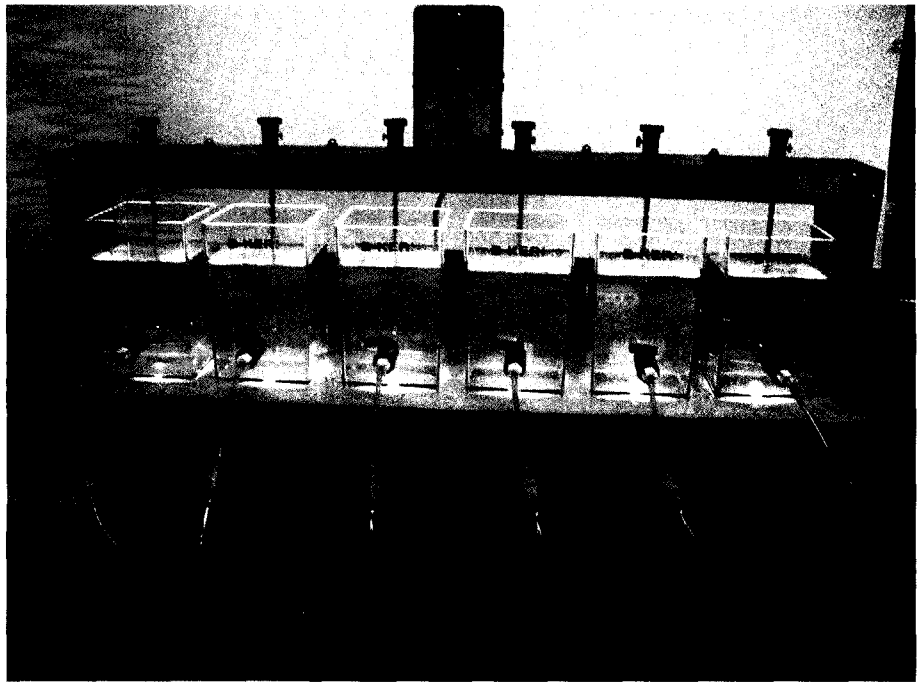

Figure 3.8. Jar test set-up

Chemical pretreatment of Ottawa River water was performed by the jar test method by adding 40 mg/L aluminium sulphate to each of six B-KER [2] (VWR, Mississauga, ON) laboratory jars with sampling port conveniently located at the 10 cm settling-distance level. The jars were then agitated for three minutes at 100 rpm (rapid mix) followed by

slow mixing for 30 minutes at mixing speed of 30 rpm. The jars have a square shape that provide improved mixing and, in many cases, accurately duplicates actual plant conditions. The coagulated water was then settled for 30 minutes. The supernatant was simultaneously withdrawn from the jars simply opening the valves and using the tubing configuration shown in Figure 3.8. The supernatant was then used for the filtration experiment feed water.

The filtration experiments were performed according to the methodology outlined in Figure 3.7. The filtration experiments were performed with a filtration cycle of one hour and a backwash time of one minute. Filtration experiments were performed at constant fluxes of 100 (subcritical flux) and 330 $L/m^2/h$ (supercritical flux). The filtration experiments with the subcritical flux of 100 $L/m^2/h$ were performed for seven hours. However, the filtration experiments with the supercritical flux of 330 $L/m^2/h$ was only performed for two hours since the maximum allowable transmembrane pressure of 20 psi was exceeded. Transmembrane pressure (TMP), operating time, permeate volume, temperature, and density were recorded in LabVIEW throughout the experiments.

3.6 Characterization of chemical pretreated feed water

The apparent molecular weight distribution (AMWD) of the organic matter within the supernatant from the coagulated water was determined by UF fractionation using a 400 mL Amicon batch stirred UF cell (model 8400, Amicon Inc., Beverly, MA) and regenerated cellulose membranes (Millipore, Bedford MA) with five different nominal molecular weight cut-offs: 1,000, 3,000, 5,000 10,000, and 30,000 Daltons. The manufacturer stated that these membranes have a nonionic character and are hydrophilic

with rejection efficiency greater than 98% for specific compounds above the nominal MWCO. The UF characterization technique followed in this study is described in detail by Nilson and DiGiano (1996) and Mosqueda-Jimenez (2003). Figures 3.9 and 3.10 illustrate the stirred UF cell process used in the characterization of permeated ORW and chemically pretreated water respectively.

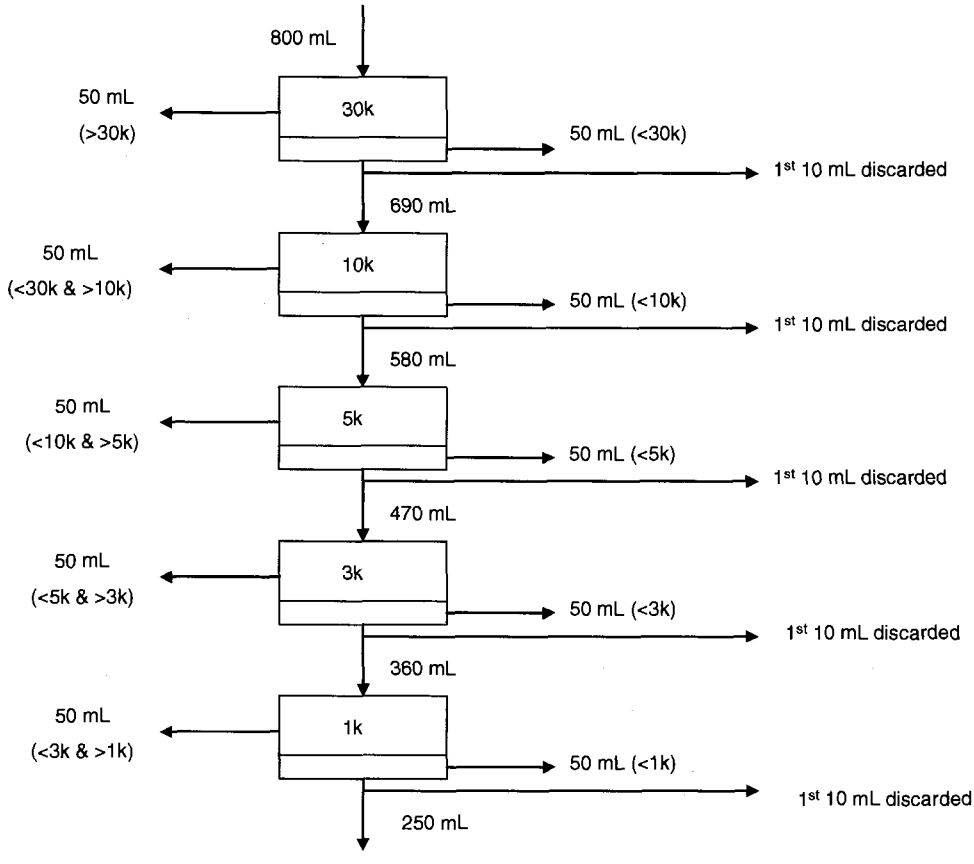

Figure 3.9. Characterization of permeated ORW water

The UF stir cell system consists of a magnetic stirrer and a nitrogen gas pressure source. The membranes were preconditioned by rinsing them floating skin-side down in a beaker with Milli-Q water for 60 minutes changing the water three times. The rinsed membranes are stored in 10% by volume ethanol/water solution and are kept refrigerated at 4 ^{o}C as

suggested by the manufacturer. Prior to use, the membranes were rinsed several times after which Milli-Q water was allowed to filtered through them three times. Two 400 mL sample aliquots were processed for the first molecular weight. Nitrogen gas pressure used ranged from 20 to 50 psig, depending on the permeate flowrate. The stir cell has a maximum operating pressure of 75 psi. The first 10 ml of filtrate were wasted. When 87.5% of the volume was filtered, 50 mL of filtrates and 50 mL retentate were collected and their TOC concentration analyzed. In cases where the feed to the cell is greater than 400 ml, the feed is divided into two equal portions and the retentate combined in pairs.

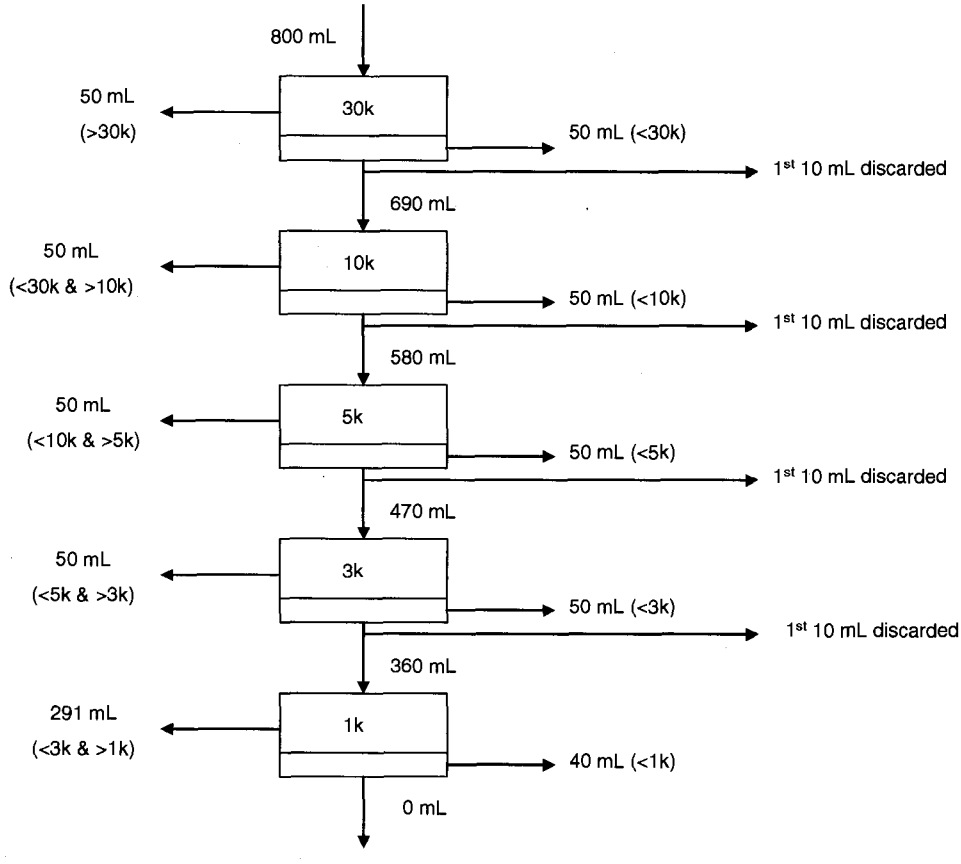

Figure 3.10. Characterization of chemically pretreated ORW

The TOC concentration of a particular molecular weight fraction was calculated

according to the procedure in Nilson and DiGiano (1996) by subtracting the TOC concentration of the filtrate from one membrane from the TOC concentration of the filtrate from the membrane of the next larger nominal MWCO.

3.7 Fraction of chemical pretreated feed water and permeated water

The hydrophobic fraction and a combination of hydrophilic and transphilic fractions of ORW were isolated using XAD 8 resin (Supelco, Bellefonte, PA). The XAD 8 column was prepared according to Storrar (2005) in the following steps:

1. The resin was cleaned according to the manufacturer's recommendations using methanol.

2. The resin was then placed in a glass column (75 cm in length and 2 cm in diameter) and rinsed with 0.1 N sodium hydroxide solution (NaOH) (Fisher Scientific, Hampton, NH) for one to three hours.

3. The column was then rinsed with five column volumes of hot Milli-Q water. At the end of the rinse, the column was removed from the stand and after securing the open end with a stopper, was then shaken vigorously to induce stratification and returned to the stand.

4. The column was then rinsed once with a 10 % 1M hydrochloric acid solution (HCl) (Fisher Scientific, Hampton, NH).

5. Milli-Q water effluent from the column was analyzed using the TOC analyzer. Steps two to five was repeated until the effluent TOC concentration from the column equaled that of the influent Milli-Q water.

After cleaning the column, the fractionation of chemically treated ORW was conducted via the following steps:

1. 100 mL of chemically pretreated ORW was vacuum filtered through a 0.45 μm membrane (Millipore, Billerica, MA) to remove any precipitate. The permeated water was not filtered since it was the product of an UF membrane with pore size less than 0.1 μm.

2. The pH of the samples was adjusted to 2.0 with concentrated HCl (Fisher Scientific, Hampton, NH).

3. The sample was then passed through the column allowing the first 50 mL to go to waste. The remaining 50 mL was then passed through the column three times and stored for analysis. This portion contains a combination of hydrophilic and transphilic fractions.

4. 100 mL of 0.1M NaOH was passed through the column to elute the hydrophobic fraction from the resin.

5. DOC analysis was conducted to quantify the hydrophobic fraction and the combined hydrophilic and transphilic fraction.

3.8 Sample collection and analytical methods

Due to the low flows involved in this experiment hourly composite samples were taken and analyzed for turbidity, pH, total organic carbon (TOC) and UV absorbance at a wavelength of 254 nm (UV_{254nm}).

The analytical methods utilized in this study monitored a variety of parameters in source and permeate waters and are outlined in the following sub-sections.

3.8.1 Total Organic Carbon (TOC)

Due to the high carbon content of NOM, TOC concentration is used as a surrogate for NOM concentration. TOC concentration was measured using UV-persulfate oxidation based TOC analyzer (Model 14-7045-000, Phoenix 8000, Tekmar Dohrmann, Cincinnati, OH) which follows standard method 5310 C, (Standard Methods, 1998). Three measurements were conducted for each sample with the standard deviation in each case less than 0.05 mg/L.

3.8.2 Ultraviolet Absorbance at 254 nm

Ultraviolet absorbance at 254 nm (UV-254) is a useful surrogate for humic substances. Ultraviolet absorbance at 254 nm was measured using a Beckman DU-40 Spectrophotometer. A 10 mm quartz cell was used to house the sample. Measurements were conducted in triplicates.

3.8.3 Colour

The colour of the raw water samples were ascertained using a colour comparator Aqua Tester by Orbeco Analytical Systems Inc. (Farmingdale, NY).

3.8.4 pH

The pH of the raw water and permeate samples were measured using a pH meter (Pinnacle 540, Corning, Lowell, MA).

3.8.5 Turbidity

The turbidity of the raw water and permeate samples were determined using a nephthelometric turbidity meter (HACH 2100AN, Loveland, CO). The turbidimeter was calibrated with the Stablcal Turbidity Standards Calibration Kit (HACH, Loveland, CO) according to manufactures operating manual and (Method 2130 B, Standard Methods, 1998). The following standards were used for the calibration: 200 NTU, 20 NTU, and <0.1 NTU.

3.8.6 Alkalinity

Alkalinity was determined by titration with H_2SO_4 (Method 2320 B, Standard Methods, 1995). Hardness was calculated from titrations with EDTA (Method 2340 C, Standard Methods, 1998).

3.9 Evaluation of flux decline, backwash efficiency, transmembrane pressure, membrane compaction and NOM rejection

All experiments were analyzed on a dimensionless basis to compare multiple data sets obtained under various experimental conditions. The two main parameters used for evaluating membrane performance throughout this study were normalized specific flux J_{NSF} and backwash efficiency (η).

With constant flux (J) operation in all tests, the fouling rate is observed by the decline in normalized specific flux (J_{NSF}). The normalized specific flux (J_{NSF}) was calculated as follow:

$$J_{NSF} = \frac{J/P}{J/P_0} = \frac{P_0}{P} \tag{3.1}$$

where J is the constant operating flux (L/m^2/h), P_0 is the initial TMP (psi), and P the pressure (psi) at any time later in the operation (Kim and DiGiano, 2005).

The backwash efficiency (η) was estimated as follow:

$$\eta = 100\frac{P_f - P_n}{P_f - P_i} \tag{3.2}$$

Where P_f is the final pressure at the end of the filtration cycle, P_i the initial pressure at the start of the same filtration cycle and P_n is the pressure following a backwash (Chellam et al., 1998).

Transmembrane pressure for dead-end filtration was calculated as follow:

$$P_{tm} = P_i - P_p \tag{3.3}$$

where P_{tm} is the transmembrane pressure, P_i is the pressure at the inlet to the module and P_p is the permeate pressure (MWH, 2005). During this experiment the ultrafiltration module discharges to the atmosphere hence the trans-membrane pressure is equal to the pressure at the inlet to the module.

The clean membrane resistances (Rm_1 and Rm_2) were calculated using Darcy's law before and after each filtration experiment.

$$J = \frac{\Delta P}{\mu R_m} \tag{3.4}$$

where J is the volumetric clean water permeate flux through the membrane, μ is the absolute viscosity of water at ambient temperature and ΔP is the transmembrane pressure (Chellam and Jacangelo, 2001).

The fraction of NOM removed from the permeate stream (rejection) is calculated as follow:

$$R = 1 - \frac{C_P}{C_F} \tag{3.5}$$

where R is rejection (dimensionless), C_P is the permeate concentration (mg/L), and C_F is the feed water concentration (mg/L) (MWH, 2005).

CHAPTER 4

RESULTS AND DISCUSSION

In this chapter, an evaluation of the bench-scale hollow fiber ultrafiltration (UF) system and its use to examine the effect of operational parameters and chemical pretreatment on membrane performance was investigated. The chapter is divided into six sections: The first section discusses the design and building of the bench-scale, hollow fiber ultrafiltration (UF) system. The second section describes the source water quality characteristic. The third section presents the results from various techniques used for conducting the bench-scale evaluation of the critical flux for the source water. The fourth section evaluates the effect of operating parameters such as backwash frequency and backwash time on membrane performance. The fifth section examines the effect of different operating flux on membrane performance and the final section investigated the effect of chemical pretreatment on membrane performance.

4.1 Evaluation of hollow fiber ultrafiltration (UF) system

Preliminary UF filtration testing (without backwashing) was conducted with a manually-controlled UF bench-scale system using an L/S Easy-Load II, EW-77200-52, Cole-Parmer, peristaltic feed pump (Appendix K). The system experienced a sharp initial decreased in flowrate for the first 15 minutes of operation (Appendix E), and remained constant thereafter as the transmembrane pressure steadily increased to the maximum allowable transmembrane pressure of 20 psi. A maximum of six percentage (6%) difference in the actual flowrate from the setpoint flowrate was observed in these initial filtration tests. A six percentage (6%) difference in the actual flowrate from the setpoint

flowrate was undesirable since it was the intent of this work to design and build a system that operates with less than five percentage (5%) difference in flowrate from the setpoint. Also, other researchers such as Kim and DiGiano (2006) were reporting a five percentage (5%) difference in actual flowrate from setpoint flowrate.

The UF system described in Chapter 3, Section 3.4, was designed to replicate the filtration and backwash cycles of the full-scale membrane filtration operation. The UF side of the system was designed to maintain constant flux using a controller to control the peristaltic feed pump. The intent to control the feed pump was to reduce the percentage difference between the actual flowrate and the setpoint flowrate observed in the initial UF testing with the manual bench-scale system.

During the filtration test runs of the UF system described in Chapter 3, Section 3.4, it was noted that the digital flowmeters (L-20CCM-D and L-50CCM-D, Alicat Scientific, Tucson, AZ) did not compare well with the actual flowrate. This difference in flowrate measurements was corrected in LabView using Fuzzy Logic operation to force the flowmeter to correspond to the mass of permeate collected over time (corrected for density to yield flowrate) by multiplying the flowrate from the flowmeter by a factor after the system reached steady state. Forcing the flowmeter on the filtration side of the system to correspond to the balance enabled the system to follow the setpoint since the controller takes signal from the flowmeters. From the testing operation, it was also noted that the flowmeters were also affected in a significant way by air bubbles and since the flowmeter on the filtration side of the system was located downstream of two solenoid valves which generate air bubbles each time they open and close. Thus the flowmeter readings were very unsteady. The air bubbles in the flowmeter affects the flowmeter

output and caused the system to deviate from the setpoint. Bleeding the ports, as suggested by the flowmeter manual, was insufficient to correct the problem. The flowmeter was also inverted, as recommended by the manufacturer (Alicat Scientific, Tucson, AZ), but this also proved to be unsuccessful in solving the problem. Attempts were also made to use the scale to control the feed water pump instead of the flowmeters but this was unsuccessful due to the large lag time for the balance (in the order of three seconds). After three months of testing and trying to correct the problems associated with controlling the feed pump, the filtration system became unstable above 15 psi (103 kPa).

Due to the difficulties experienced from trying to control the feed pump with the controller, the filtration system was modified. A high performance peristaltic pump (EW-77250-62, Cole-Parmer, Montreal, QC) with high pressure tubing was used to replace the L/S Easy-Load II peristaltic pump (Appendix E). This pump was operated in the manual mode of the controller since it was capable of maintaining a constant flow within the operating pressure range of the filtration experiments. The high performance peristaltic pump maintained a constant flux within ± 2% of the setpoint flux. The peristaltic L/S Easy-Load II pump could not maintain a constant flowrate was likely due to the fact that the pump was operated at pressures approaching the maximum pressure rating of the pump. The high performance peristaltic pump with a much higher pressure rating provided much more constant flowrates.

Other researchers (including Heijman et al., 2005a; Heijman et al., 2005b and Kim and DiGiano, 2006) have used positive displacement pumps, such as piston pumps and gear pumps to maintain constant flux in their bench-scale fouling experiments but these types

of pumps require pre-filtration of the feed water since they are sensitive to particulate matter. The high pressure, high performances peristaltic pump, a new product from Cole-Parmer, provided a reasonable alternative and in addition permitted the processing of feed waters irrespective of the particulate concentration.

4.2 Water quality characteristics

The characteristics of the source water (Ottawa River water) collected on September 24, 2007 were presented in Chapter 3, Table 3.1. Ottawa River water (ORW) is a light yellow-brown colour water with low hardness and alkalinity. The color arises from the presence of natural organic matter in the water (TOC = 5.80 ± 0.21 mg/l; and UVA_{254} = 0.255 ± 0.018 cm^{-1}). TOC/DOC concentrations are reported with only two decimal places given the accuracy of the measurement. SUVA the specific ultraviolet absorbance, (SUVA= UVA_{254}/TOC) is often used as an indicator of the humic content of NOM. SUVA for ORW was 4.40 L/mg.m during the period in which the experiments were conducted indicating a strong presence of humic acids. For the duration of the experimental work, ORW has turbidity of 2.41 ± 0.26 NTU and pH of 7.49 ± 0.16. The molecular weight distribution and fractionation of NOM for the same batch of ORW conducted by Dang (2008) is depicted in Figure 4.1 and Figure 4.2. Figure 4.1 shows that approximately 13.48% of the NOM was greater than 30,000 Daltons; 44% was in the range of 10,000 to 30,000 Daltons, 29% was between 3,000 to 10,000 Daltons; 10.6% was in the range of 1,000 and 3,000 Daltons; and 2.96% of the NOM was smaller than 1,000 Daltons. The results indicate that 86.52% of the NOM was below 30,000 Daltons.

The molecular weight distribution results were somewhat similar to the results reported by Mosqueda-Jimenez et al. (2004) and Nguyen (2005) for ORW collected at the same location in the months of June and May, respectively. Mosqueda-Jimenez et al. (2004) reported that 95% and of the NOM had molecular weight smaller than 30,000 Daltons while Nguyen (2005) reported that 99% of the NOM had molecular weight smaller than 30,000 Daltons. The slight difference in the results may be due to seasonal variation of the NOM since NOM concentrations are usually higher in the warmer months when biological degradation of plant and animal matter is highest. Since most of the NOM in ORW have molecular weight below 30,000 Daltons, rejection is expected to be low with the UltraPES 0.7 membrane that according to its manufacturer has a nominal molecular weight cut-off of 70 kDa.

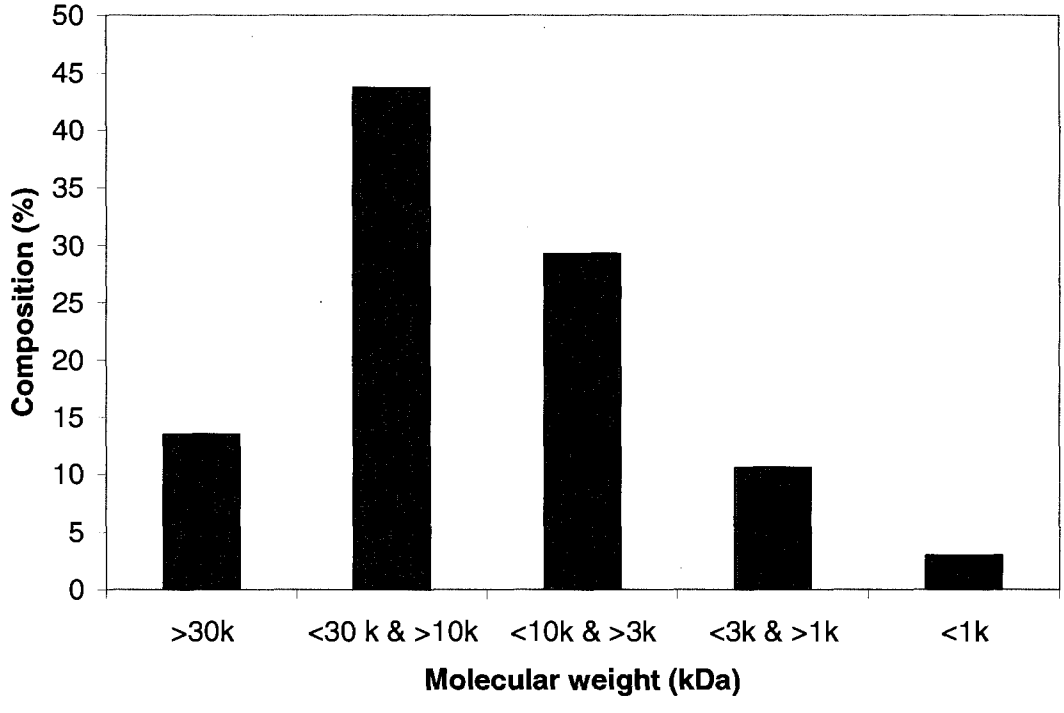

Figure 4.1. Molecular weight distribution of ORW (after Dang, 2008)

The fractionation results of ORW with XAD4 and XAD8 resin are shown in Figure 4.2. The results indicated that hydrophobic acids accounted for 64.4% of the NOM in ORW followed by humins which accounted for 17.6%. Transphilic acids and hydrophilic acids constituted the remainder of the NOM amounting to 10.6% and 7.4%, respectively. The SUVA of 4.40 L/mg.m for ORW supports the results depicted in Figure 4.2 which indicated that hydrophobic acids (humic acids) constitutes a significant portion of the NOM in ORW. The large quantity of hydrophobic acids in ORW is an indication that the foulants are predominantly negatively charged and can severely foul hydrophobic membranes (Cheryan, 1998).

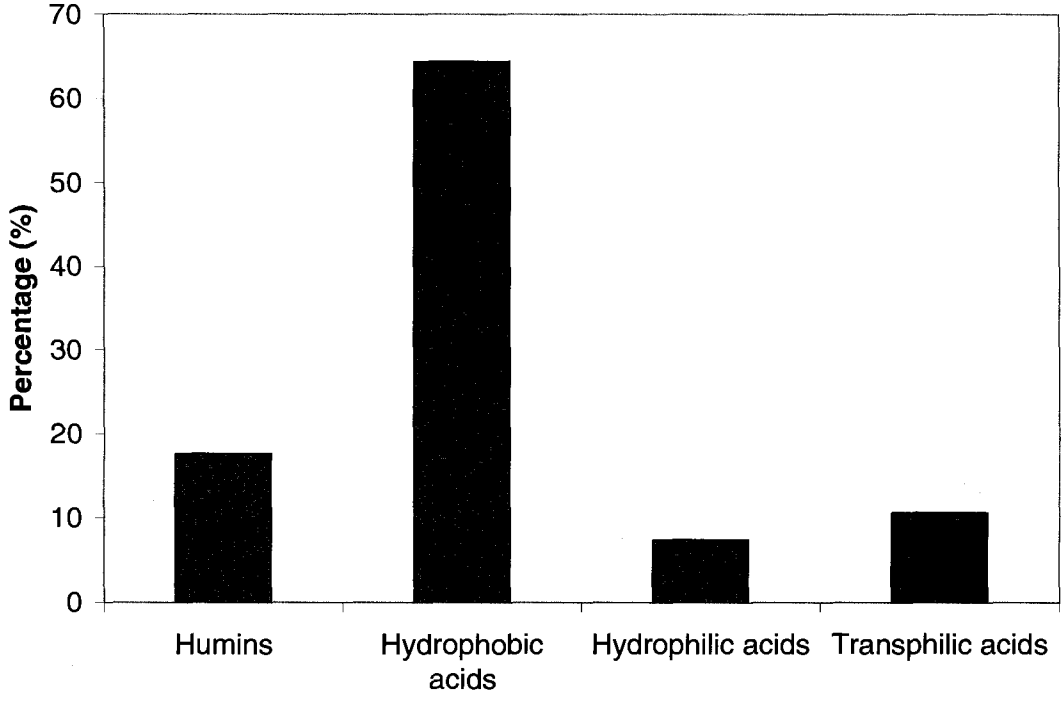

Figure 4.2. NOM fraction of ORW (after Dang, 2008)

4.3 Bench-scale estimation of critical flux

Critical flux is often defined as the flux at which the feed solution line leaves the pure water line during the flux step method (Liu and Kim, 2007). However, low pressure

membrane filtration of surface waters usually results in noticeable increases in TMP with time even for permeate flux well below the critical flux. Huisman et al. (1999); and Chan et al. (2000) defined the critical flux for natural waters as the flux for which there is a rapid increase in TMP when TMP is plotted against permeate flux.

Filtration experiments for the estimation of critical flux for the feed water were performed using the flux-step method. This method involves stepwise increases in permeate flux from approximately 30 $L/m^2/h$ to 110 $L/m^2/h$ and maintaining each flux for a period of 15 minutes as shown in Figure 4.3.

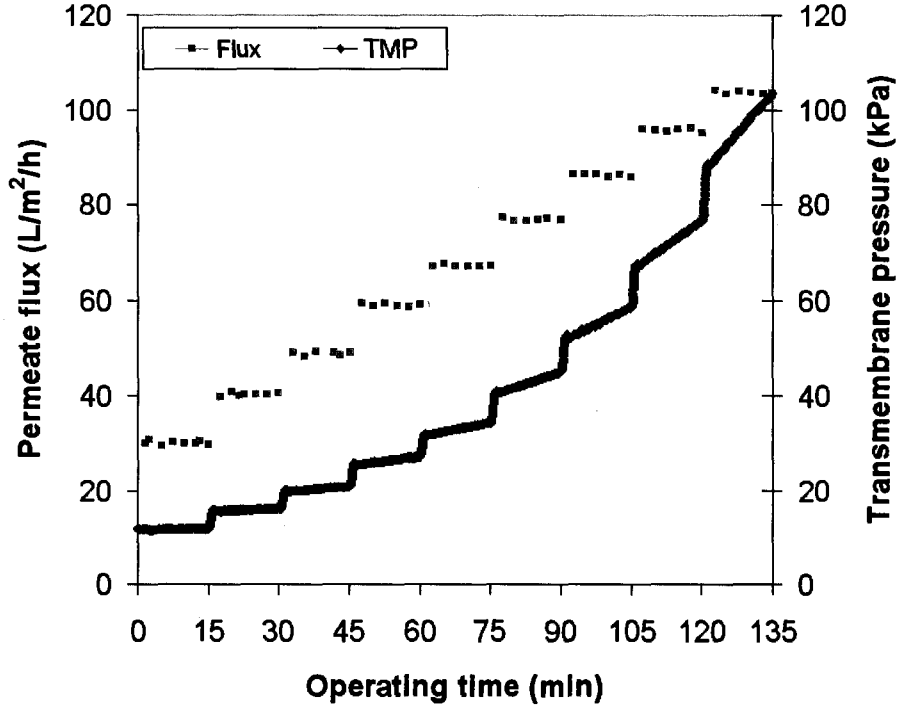

Figure 4.3. Schematic representation of critical flux by the flux-step method

Figure 4.3 shows that the TMP increased slowly for low permeate fluxes and increased rapidly over time for higher permeate fluxes. The last step showed an exponential

increase in TMP. The use of the experimental results from the flux-step method to estimate critical flux is illustrated in Figures 4.4 to 4.6. Two TMP-based parameters were used to estimate the critical flux: average TMP, and rate of change of TMP ($\Delta TMP/\Delta t$). Figure 4.4 shows a plot of the average TMP versus permeate flux for each constant flux condition (i.e., step). From the graph, the slope of line for average TMP versus permeate flux increased significantly when the permeate flux exceeded 75 $L/m^2/h$. This technique for estimating critical flux is consistent with the procedure of Le Clech et al. (2003) and Choi and Dempsey (2005), who also observed a significant increase in the slope of the plot of average TMP versus permeate flux when the flux exceeded the critical value.

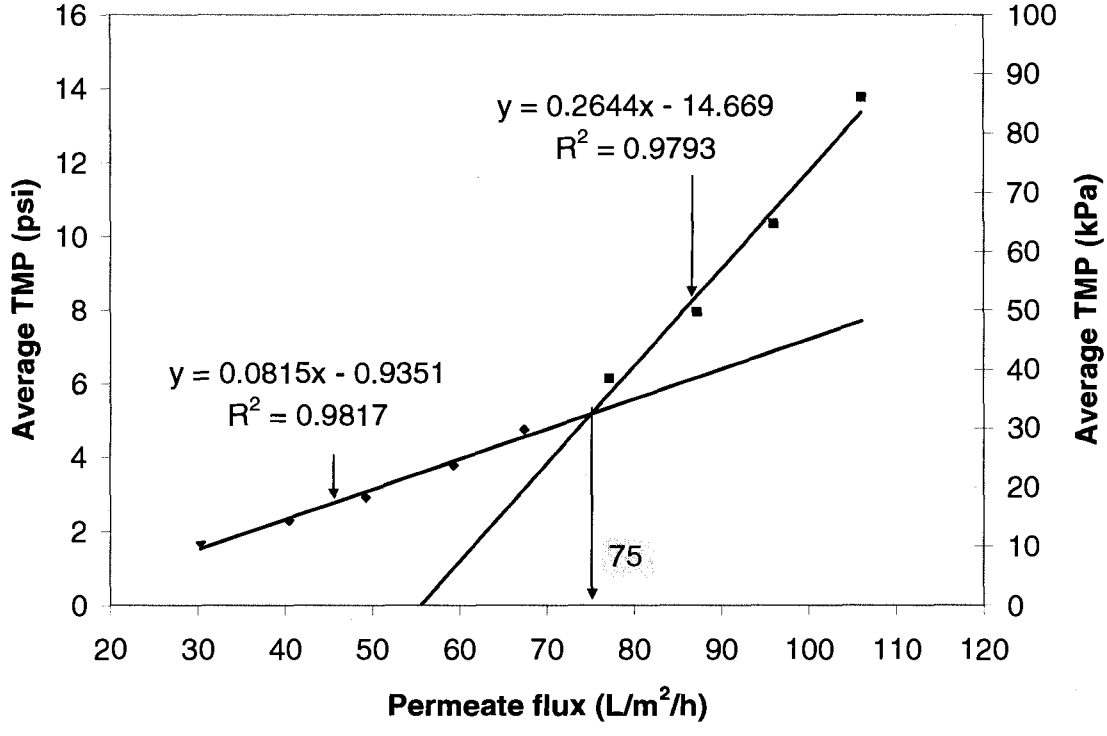

Figure 4.4. Average TMP versus flux to estimate critical flux

The results from the flux-step experiment were also used to plot rate of change of TMP versus permeate flux as depicted in Figure 4.5. The rate of change of TMP was calculated by dividing the difference between the final and initial TMP for each step by the filtration time (i.e., 15 minutes). From the graph, the slope of line for the rate of change TMP versus permeate flux increased significantly when the permeate flux exceeded 75 L/m^2/h. This technique provided a result similar to the result obtained in Figure 4.4 and is an indication that both methods can be used to estimate critical flux. The ΔTMP/Δt versus flux technique for estimating critical flux is also consistent with the procedure of (Le Clech et al. 2003; and Choi and Dempsey, 2005) who also observed a significant increase in the slope of the plot of the rate of change of TMP versus permeate flux when the flux exceeded the critical value.

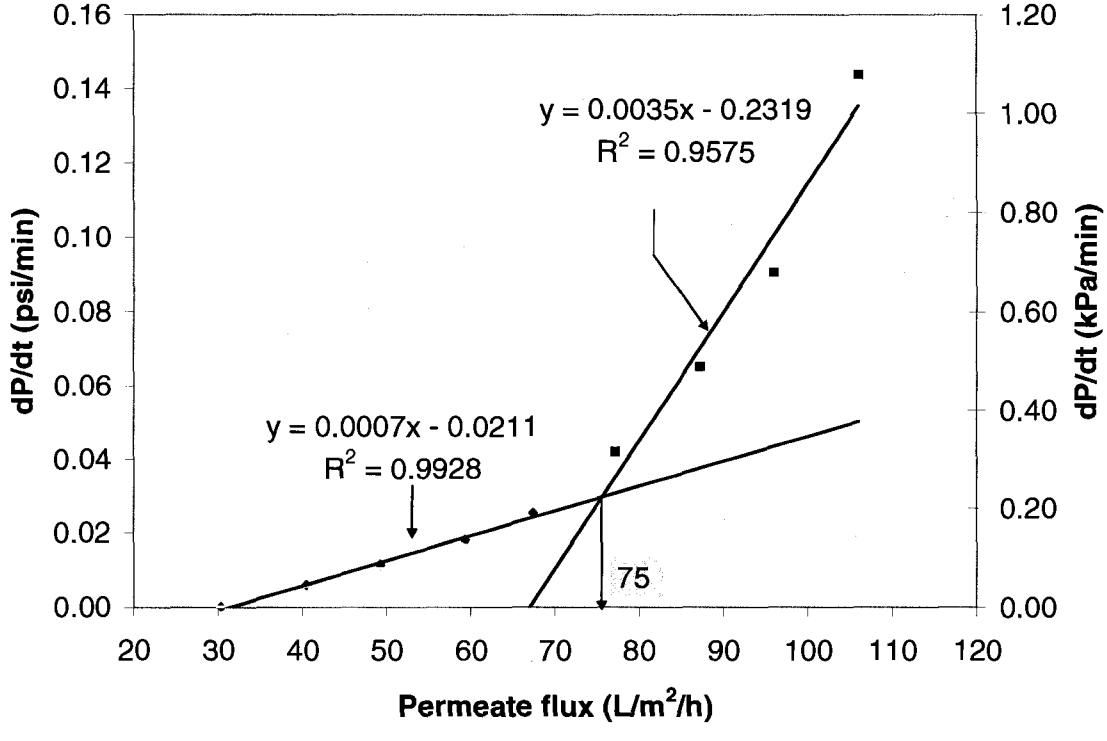

Figure 4.5. ΔTMP/Δt versus flux to estimate critical flux

The results derived from the rate of change of TMP versus permeate flux were further analyzed using two statistical approaches: a) the T-test with p = 0.05 to detect significant deviation between values of ΔTMP/Δt; and b) an F-test to compare variances between successive constant flux steps. Both statistical approaches indicate that a sudden change in ΔTMP/Δt occurred between 0.124 kPa/min (0.018 psi/min) and 0.290 kPa/min (0.042 psi/min) (Appendix L) which correspond to permeate flux values of 59 L/m^2/h and 77 L/m^2/h respectively as illustrated in Figure 4.6. The statistical approaches are therefore not definitive and provide a range in which the critical flux lies and requires other approaches such as the approach depicted in Figure 4.5. The estimation of critical flux using the two TMP-based parameters (average TMP and ΔTMP/Δt) produced results that were similar and are therefore recommended for use in critical flux evaluations.

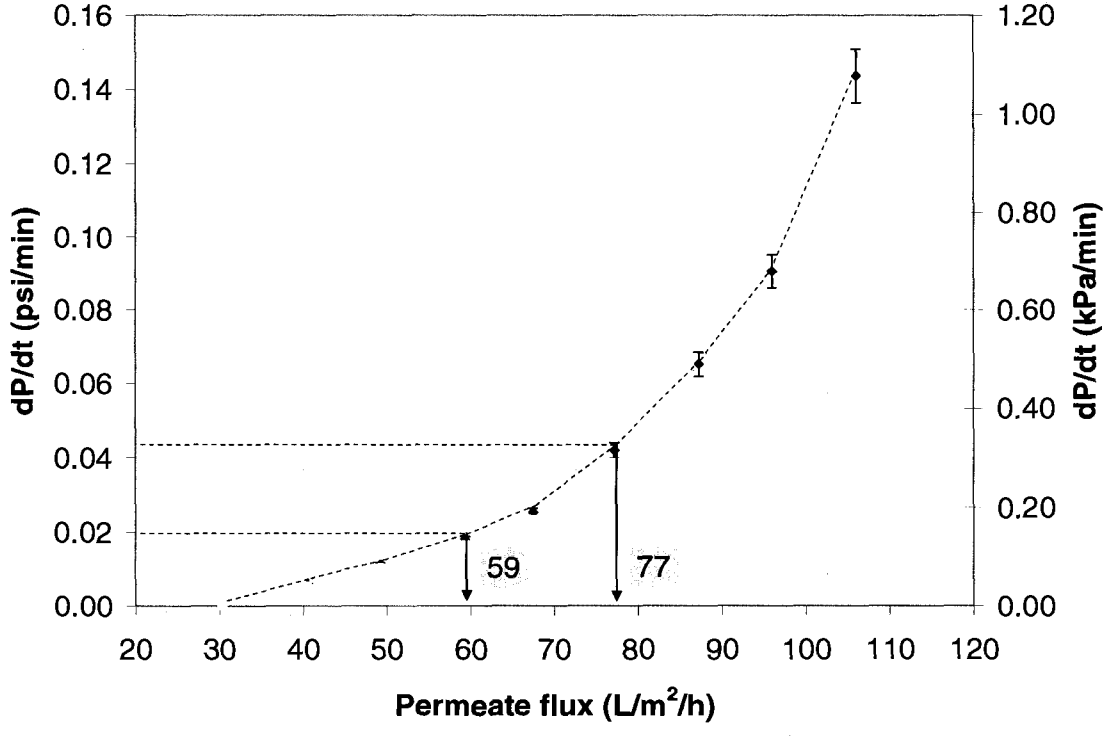

Figure 4.6. ΔTMP/Δt versus flux with critical flux range obtained from statistical analysis

According to the traditional definition of critical flux (Choi and Dempsey, 2005), sub-critical operation is characterised by $\Delta TMP/\Delta t = 0$ (Le Clech et al. 2003). The rate of change of TMP showed gradual increase in the subcritical region indicating the occurrence of fouling. The results from the flux-step method (Figure 4.3 to Figure 4.6) confirms that this traditional definition cannot be applied to natural waters and supports the critical flux definition for natural waters as the flux for which there is a rapid increase in TMP.

The effect of filtration length on critical flux estimation was not explored in these experiments. However, it is reasonable to assume that critical flux will decrease with an increase in filtration time. The longer the filtration time, the more fouling occurs and the greater the TMP. This effect can be estimated by using different time steps for filtration. Choi and Dempsey (2005) in their study observed a decrease in critical flux as the filtration time increased. Therefore, the time steps used to determine critical flux should be similar to the filtration length between backwashes in pilot plants and full-scale membrane filtration operations.

4.4 Effect of operating parameters on membrane performance

All experiments were analyzed on a dimensionless basis to compare multiple data sets obtained under various experimental conditions. The analyses were performed using two main parameters {normalized specific flux (NSF) and backwash efficiency (η)} for accessing membrane performance. With constant flux (J) operation in all tests, the fouling rate was quantified by the decline in normalized specific flux (NSF).

4.4.1 Effect of backwash frequency and backwash time on fouling rate

Figure 4.7 and Figure 4.8 depicts the comparison of normalized specific flux (NSF) decline for a common backwash time (BWT) of one minute and two minutes, respectively, and corresponding backwash frequencies (BWFs) of 15, 30 and 60 minutes, respectively. All filtration experiments were conducted at a flux of 100 L/m^2/h (above the critical flux of 75 L/m^2/h) to observe fouling in a short period. A corresponding backwash flux of 250 L/m^2/h was used based on the manufactures recommendation. Figure 4.7 shows that for a common BWT of one minute the fouling rate decreased substantially by an increase in BWF from 60 to 15 minutes. However, the difference in fouling rate as BWF increase from 60 to 30 minutes was relatively small. The results demonstrated that shorter operation time between backwash cycles results in reduced membrane fouling.

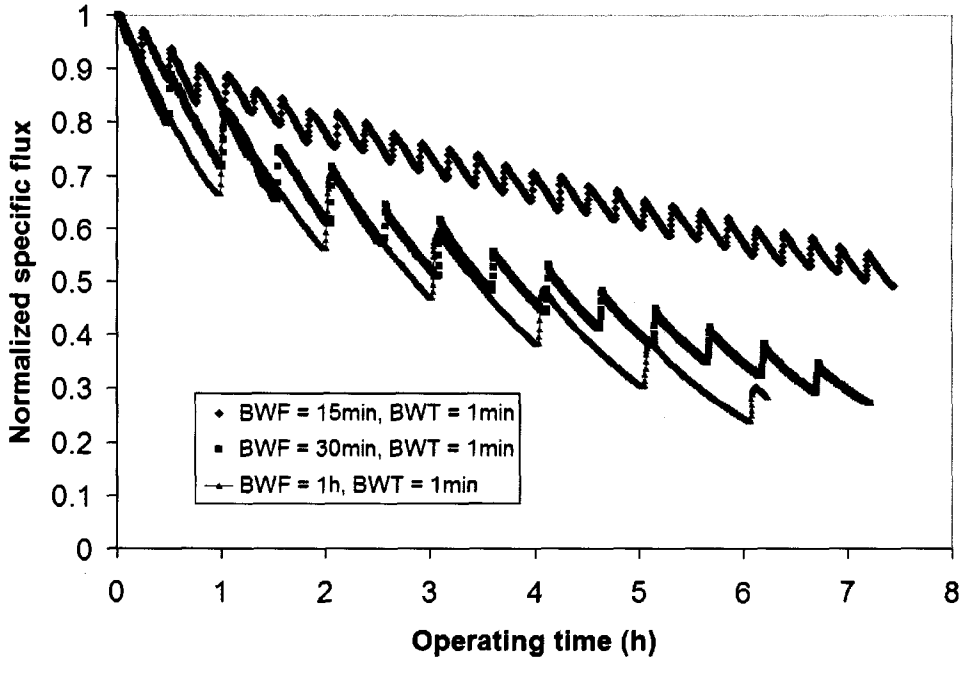

Figure 4.7. Comparison of NSF decline for backwash time of one minute and constant flux of 100 L/m^2/h for ORW using an UltraPES 0.7 membrane

BWT is often perceived as a necessary downtime in low pressure membrane filtration of water. The backwashing process also uses valuable product water, and for the recovery (ratio of net water production to gross water production over a filter run) of membrane filtration to be comparable to rapid gravity filters, recovery in membrane filtration must be in the range of 95% to 98% (MWH, 2005). Therefore, BWT must be minimized for economical membrane operation.

The results from Figure 4.7 and Figure 4.8 indicate that an increase in backwash time from one minute to two minutes decreased the fouling rate to a certain extent but not substantially. The finding agrees well with that of Kim and DiGiano (2005) in their study of fouling rate for UF membrane.

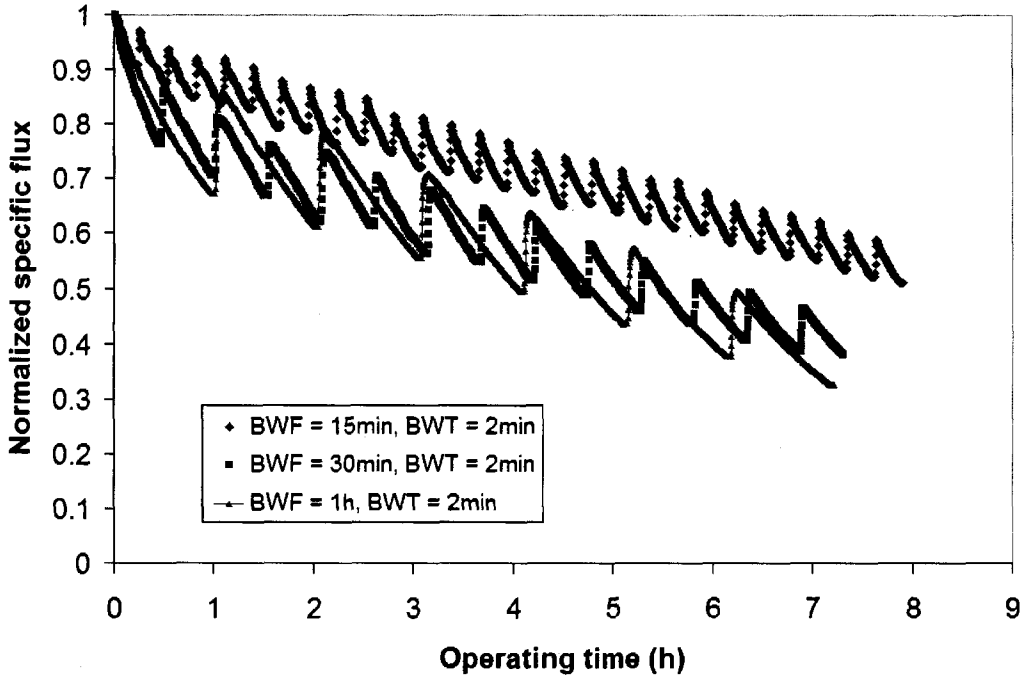

Figure 4.8. Comparison of NSF decline for backwash time of two minutes and constant flux of 100 L/m^2/h for ORW using an UltraPES 0.7 membrane

Figure 4.9, which is a compilation of the data in Figures 4.7 and 4.8, depicts the comparison of NSF decline for a BWT of one minute and two minutes respectively and corresponding BWFs of 15, 30 and 60 minutes. Although increasing the backwash time from one minute to two minutes did not decrease the fouling rate substantially, the figure indicates that BWT has a greater impact as the filtration cycle lengthens. This is reasonable since the longer the filtration cycle, the greater the foulant build-up and the longer the BWT required to clear the accumulated cake layer.

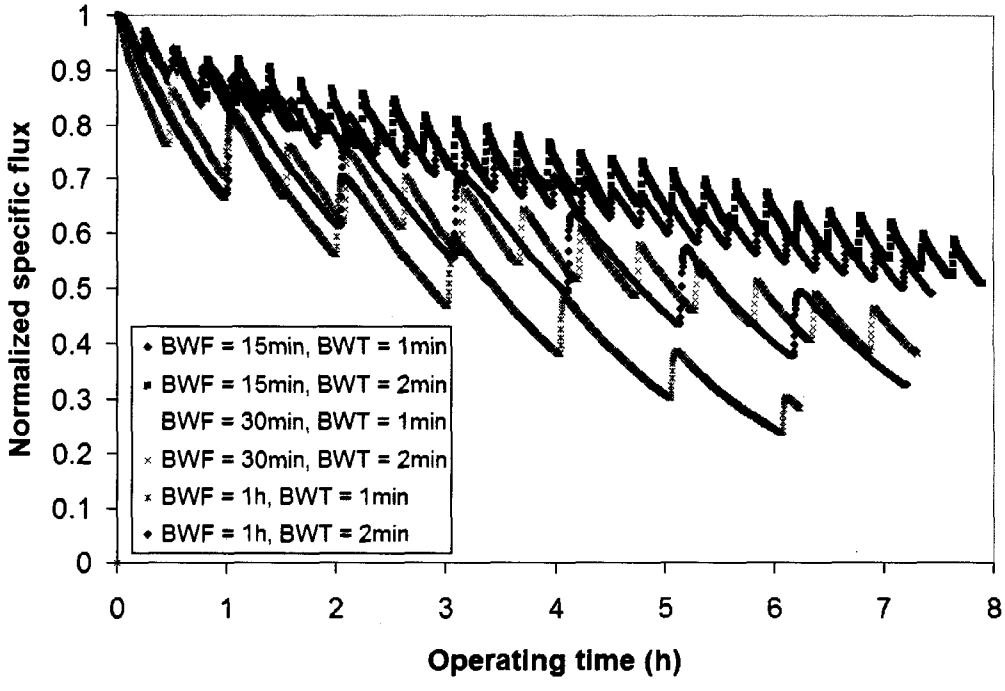

Figure 4.9. Comparison of NSF decline for backwash time of one minute and two minutes and constant flux of 100 L/m^2/h for ORW using an UltraPES 0.7 membrane

From the results depicted in Figure 4.7 and Figure 4.8, it was noted that there was a similarity in fouling rate for the 30 and 60 minuets filtration cycles. This could be due to a combination of different fouling mechanisms. According to Farahbakhsh et al. (2004),

the mechanisms of NOM fouling on membrane systems may be divided into cake formation, surface adsorption-deposition, and adsorption-deposition in the membrane pores. Anselme and Jacobs (1996) suggested that natural organic matter (NOM) in waters can lead to membrane fouling by adsorption on the particles making up the filtration cake, or by adsorption in the membrane matrix. It was therefore assumed that at the beginning of the filtration cycle, pore adsorption is the dominant mechanism and this is evident in the noticeable rapid fouling that occurs at the initial stages of the filtration experiment. The data in the present study demonstrates that backwashing was not very effective in restoring membrane productivity. Pore adsorption is followed by pore blocking and cake formation over those regions of the membrane that have been previously covered. Hence for longer filtration runs cake formation becomes the dominant mechanism. It is therefore possible that the filterability of the cake on the membrane decreases at a slower rate as filtration duration increases giving rise to the similarity in fouling rates for the 30 and 60 minutes filtration cycles.

4.4.2 Effect of backwash frequency and backwash time on backwash efficiency

The backwash efficiency for each filtration experiment was determined according to Equation 3.2 in Section 3.8, Chapter 3. Figure 4.10 depicts combined backwash efficiencies under various operating conditions and represents the mean and standard deviation of duplicate filtration experiments under the same operating conditions. The highest backwash efficiency observed was 85.24% for the 15 minutes filtration cycle and two minutes BWT while the lowest backwash efficiency noted was 62.97% for the one hour filtration cycle and one minute BWT. The results of the filtration experiments demonstrate that backwash efficiency increased with decreasing BWF.

Increasing BWT from one minute to two minutes did not increase the backwashing efficiency substantially. However, as the filtration cycle lengthens, BWT time become more significant as is shown for the 30 minutes and one hour BWFs. This finding agrees well with previous results which indicated that BWT becomes more significant as the filtration cycle lengthens.

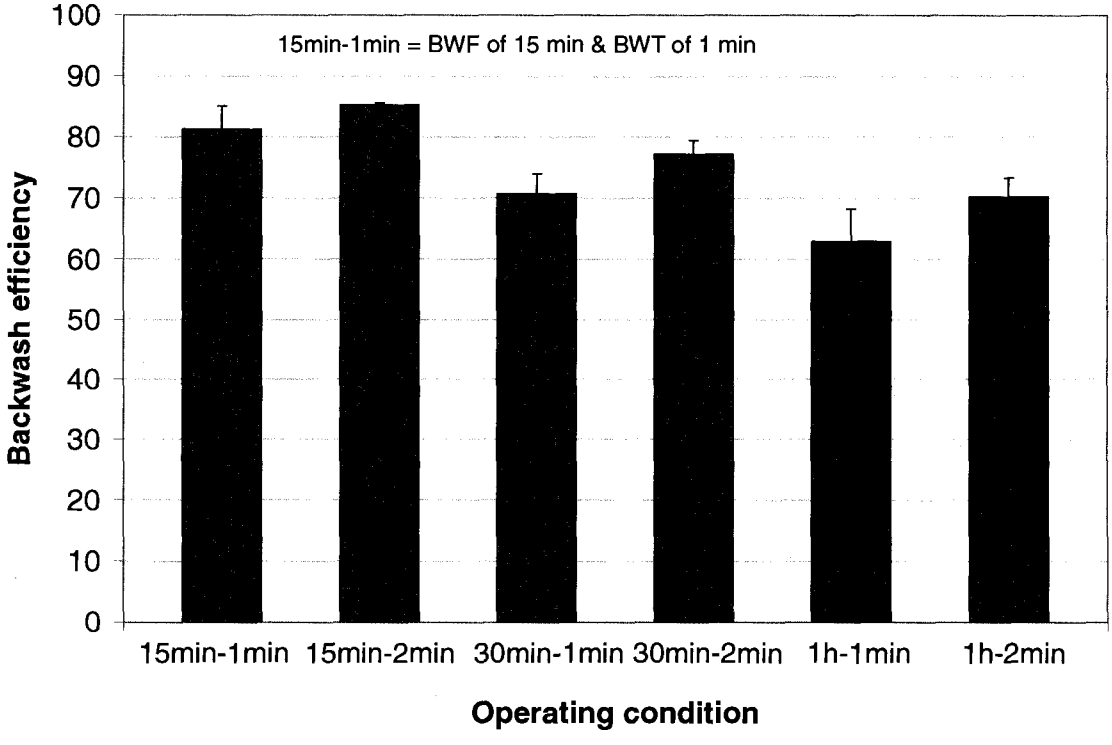

Figure 4.10. Combined backwash efficiencies for different BWF and BWT conditions and constant flux of 100 L/m^2/h

4.4.3 Effect of backwash frequency and backwash time on NOM rejection

Due to the low filtrate volumes produced in these experiments, hourly composite samples were collected to have sufficient volume for turbidity, pH, TOC and UV analysis. Figure 4.11 and Figure 4.12 depict the TOC and UV_{254nm} percentage rejection. The values in these figures are the mean values from duplicate filtration experiments under the same

operating conditions. The results from Figure 4.11 demonstrated that TOC rejection increased as BWF increased from 60 to 15 minutes. With the exception of the 15 min filtration cycle an increase in BWT from one minute to two minutes did not increase TOC rejection. An increase in BWT from one minute to two minutes for the 15 min filtration cycle showed improved TOC rejection likely because NOM sorption is slow and the longer BWT of two minutes allowed for greater desorption during the backwashing, thus liberating some NOM sorption sites (on the membrane) for use in the next filtration cycle. For the longer filtration cycles, NOM become firmly attached to the membrane and thus backwashing has little impact.

According to Figure 4.1, only 13% of the NOM was greater than 30,000 Daltons, the largest pore size membrane used in the fractionation to characterize the NOM. The current hollow fiber system uses a UltraPES 0.7 membrane with nominal MWCO of 70 kDa and unfortunately the NOM fractionation did not include a 70,000 Dalton size membrane. The fact that the NOM rejection of the UltraPES 0.7 membrane with nominal MWCO of 70 kDa was less than 15% (Figure 4.11) seems consistent with the small amount of NOM (i.e., 13%) with molecular weight greater than 30,000 Daltons found in the UF fractionation using flat sheet membranes (Figure 4.1). It can therefore be assumed that membrane surface chemistry and NOM adsorption on filter cake particles or in the membrane pores may be the main NOM removal mechanisms. NOM adsorbed onto the filter cake can be removed by backwashing; however NOM adsorption in the membrane pores is more difficult to remove by backwashing and leads to long term fouling. Accordingly, the later seems to predominate.

Although the differences in the percent rejection for the different filtration cycle lengths

are small, they are statistically significant (Appendix M).

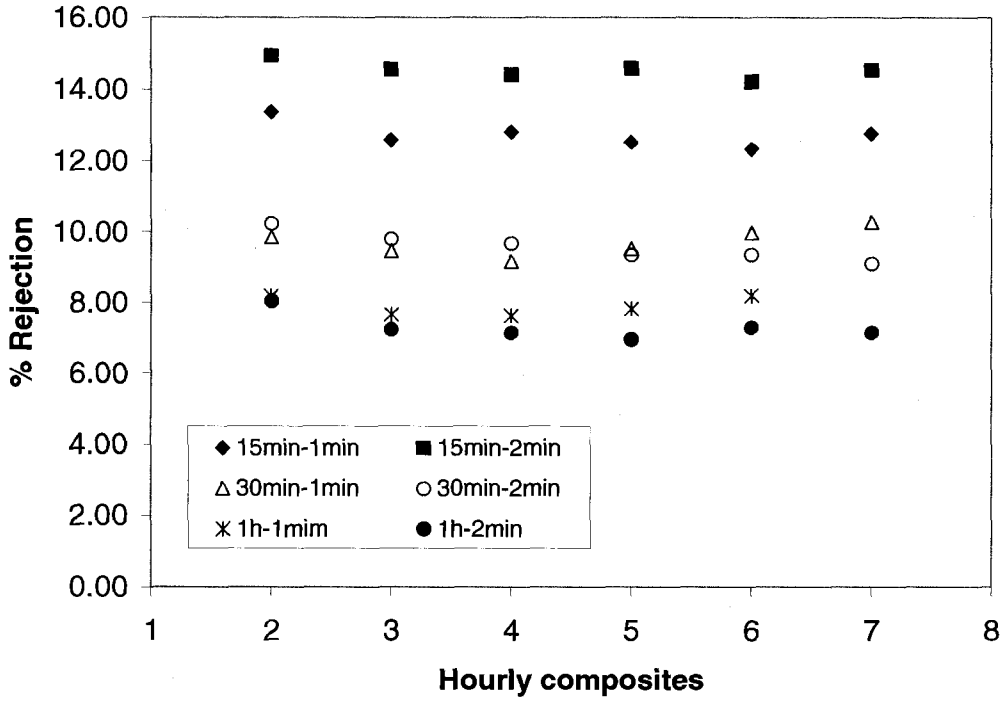

Figure 4.11. Total organic carbon (TOC) percentage rejection for different BWF and BWT conditions and constant flux of 100 L/m^2/h

Ultraviolet absorbance at 254 nm (UVA-254) was used as a surrogate for humic substances. The results from Figure 4.12 demonstrated that UVA254nm rejection increased as BWF increased from 60 to 15 minutes. An increase in BWT from one minute to two minutes did not increase the rejection of the humic content of NOM. Increasing the BWT from one minute to two minutes for the filtration cycle of 15 minute did not increase UV254nm rejection as was observed for TOC rejection. This may due to the competitive adsorption/desorption interactions between the various NOM fractions and since humic substances possess a high adsorptive characteristics due to their great hydrophobic nature, they become firmly attached to the membrane and are more difficult

to remove. Therefore, an increase in BWT from one minute to two minutes may not be effective in improving humic substance rejection.

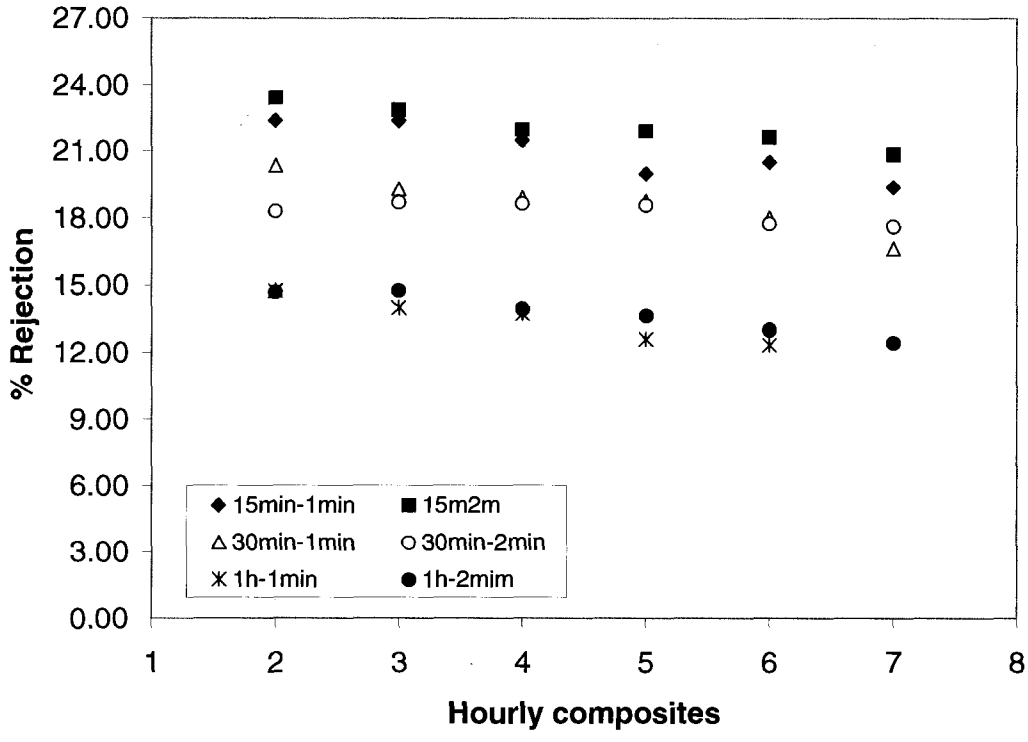

Figure 4.12. Ultraviolet absorption (UVA_{254nm}) percentage rejection for different BWF and BWT conditions and constant flux of 100 $L/m^2/h$

Specific UV absorbance is the UV of a water sample at a given wavelength normalized for total organic carbon (TOC) (Weishaar et al., 2003). SUVA determined at 254 nm is used as an indicator of the aromatic content of NOM. The results depicted in Figure 4.13 demonstrated that composites permeate samples have SUVA values of 3.77 L/mg.m to 4.02 L/mg.m corresponding to a difference in the order of 8.6% to 14.3% when compared with the source water SUVA of 4.4 L/mg.m. The results indicated that a significant portion of the humic substance rejected is aromatic in nature and may be responsible the NSF decline observed in Figure 4.7 to Figure 4.9. It was also observed that the aromatic content of NOM in the composite permeate samples increased as the operating time

increased indicating that with time the membrane become less effective in removing the aromatic component of NOM.

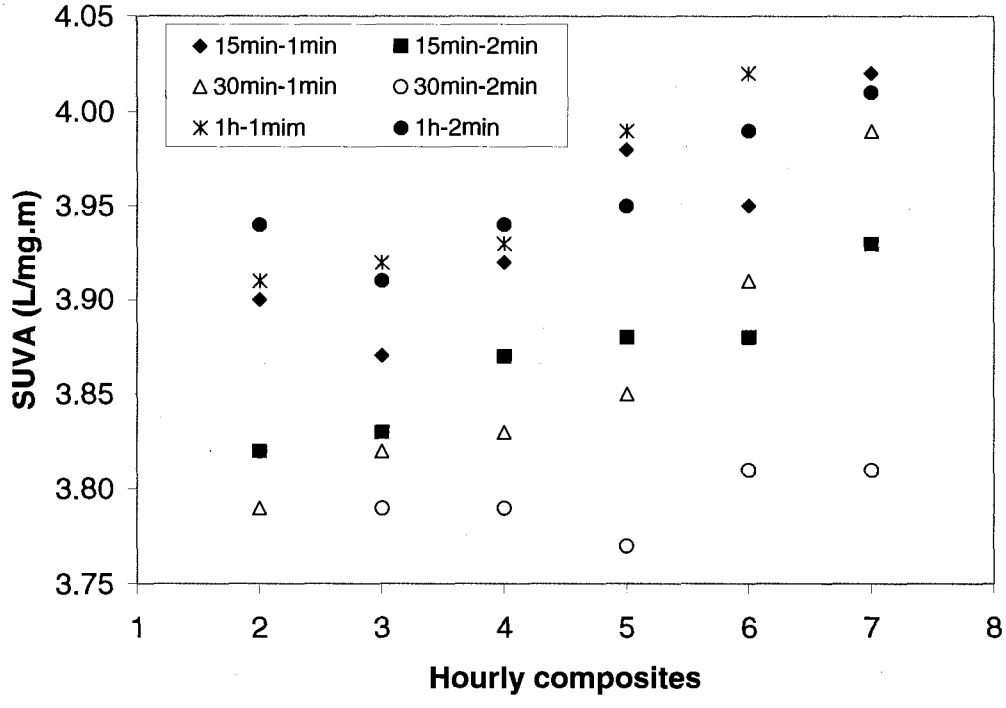

Figure 4.13. Specific ultraviolet absorption (SUVA) for different BWF and BWT conditions and constant flux of 100 L/m^2/h

4.5 Effect of different operating flux values on membrane performance

Normalized specific flux (NSF) and backwash efficiency (η) were also used for accessing membrane performance. With constant flux (J) operation in all tests, fouling was again observed as indicated by the decline in normalized specific flux (NSF).

4.5.1 Effect of different operating flux values on fouling rate

Flux decline patterns are compared for different operating fluxes for a common BWT of one minute and BWF of 30 minutes, respectively, in Figure 4.14. All backwash

operations were performed at constant flux (two and a half times the filtration flux). The figure shows that for a common BWT of one minute and BWF of 30 minutes the fouling rate increased with increasing operating flux from 50 L/m^2/h to 120 L/m^2/h. The system could only be operated for four hours at a flux of 120 L/m^2/h since the maximum allowable pressure of 20 psi (138 kPa) for the system was exceeded in four hours. From Section 4.1, it was determined that the critical flux for the feed water was 75 L/m^2/h. The figure shows vast difference in the fouling rate between the subcritical operations (50 and 70 L/m^2/h) and the supercritical operations (100 and 120 L/m^2/h).

The study therefore indicated that fouling rate is affected by the rate of approach of foulants to the membrane. Fouling was noticed even in subcritical conditions although not as substantial as in the supercritical operations.

Kim and DiGiano (2005) compare specific flux decline patterns for operating flux values of 50 L/m^2/h and 65 L/m^2/h respectively, and found that the extent of specific flux decline was greater for 65 L/m^2/h than for 50 L/m^2/h. Their findings agree well with the result presented in Figure 4.14.

The operating flux for constant flux operations has been shown in other studies to influence other operating parameters such as backwash frequency and backwash time for longer filtration cycles (Kim and DiGiano, 2005). Frequent backwashing however in usually accompanied by an increase in operating cost. Therefore the savings in capital cost that results from operating at a higher flux (thus requiring a smaller membrane surface area) could be offset by the increase in operating cost that accompanies the more frequent backwashing necessary (Kim and DiGiano, 2005).

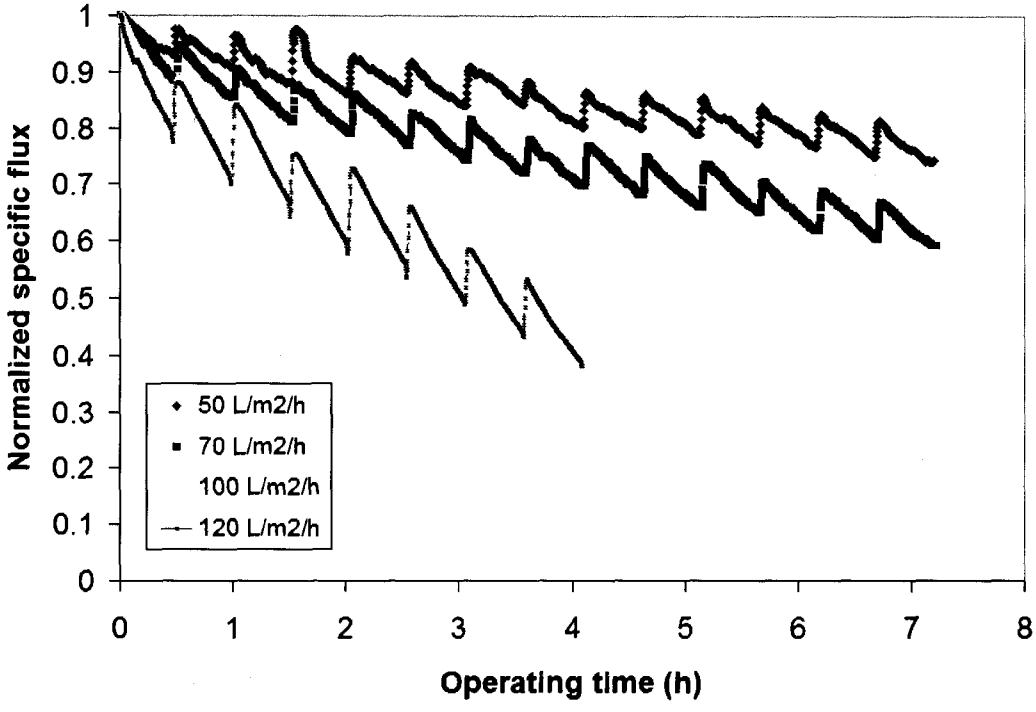

Figure 4.14. Comparison of NSF decline for different operating flux values for BWF of 30 minutes, BWT of one minute and backwash flux at 2.5 times the filtration flux, for ORW using UltraPES 0.7 membrane

4.5.2 Effect of different operating flux values on backwash efficiency

The backwash efficiency was determined according to Equation 3.2 in Section 3.8. Figure 4.15 depicts combined backwash efficiencies for different operating flux values and represents the mean values and standard deviation of duplicate filtration experiments under the same operating conditions. The highest backwash efficiency achieved was 79.18% for the 50 L/m^2/h operating flux while the lowest backwash efficiency obtained was 64.06% for the 120 L/m^2/h operating flux. The results of the filtration experiments demonstrats that backwash efficiency decreased with increasing operating flux. Operating at lower flux values proved to be beneficial since the cake layer was less rigidly attached which results in higher backwashing efficiency. The results again demonstrated that

higher operating flux requires frequent backwashing to adequately clear the accumulated cake layer.

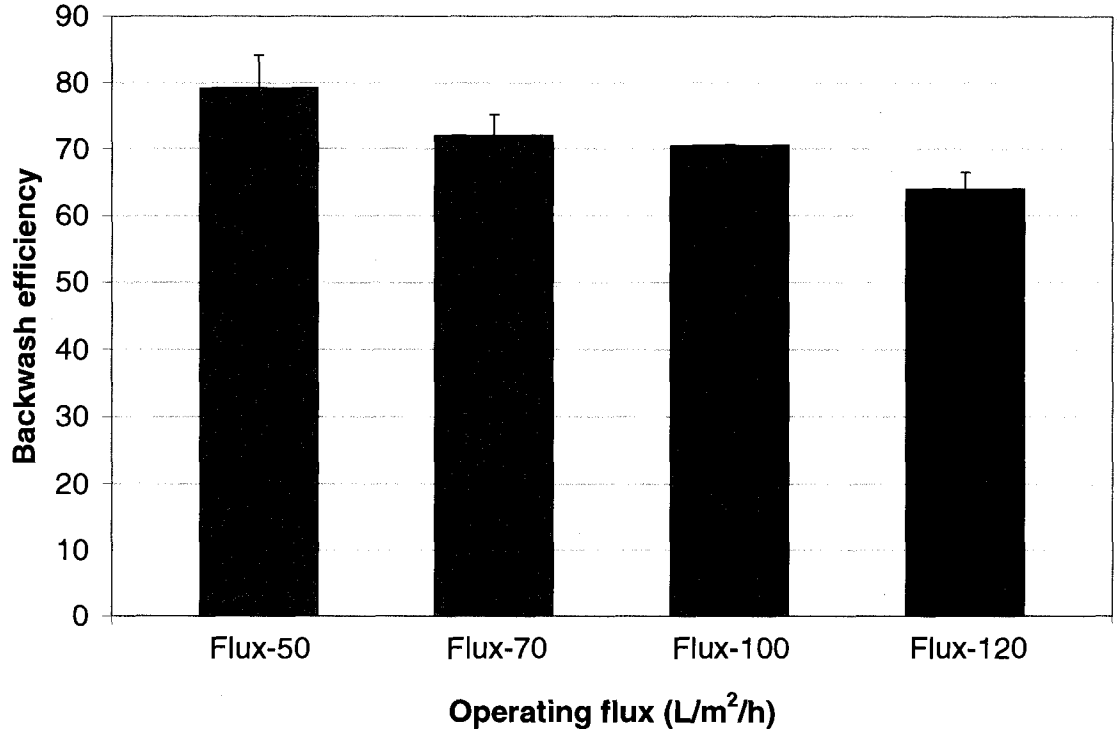

Figure 4.15. Combined backwash efficiencies for different operating flux values and BWF of 30 minutes and BWT of one minute

4.5.3 Effect of different operating flux values on NOM rejection

TOC rejections based on composite permeate samples are presented in Figure 4.16. The figure depicts the mean values from duplicate filtration experiments under the same operating conditions. The results demonstrated that TOC rejection decreased as operating flux increased from 50 L/m^2/h to 120 L/m^2/h. This is very much expected since an increase in permeate flux signifies an increase in the transport of NOM to the membrane surface and a backwash time of one minute may not be sufficient to desorb the adsorbed NOM or to remove the build up of organic matter on the membrane surface at the higher operating flux values which resulted in a decrease in TOC rejection.

Although the differences in the percent rejection for the different flux values are small, they are statistically significant (Appendix M).

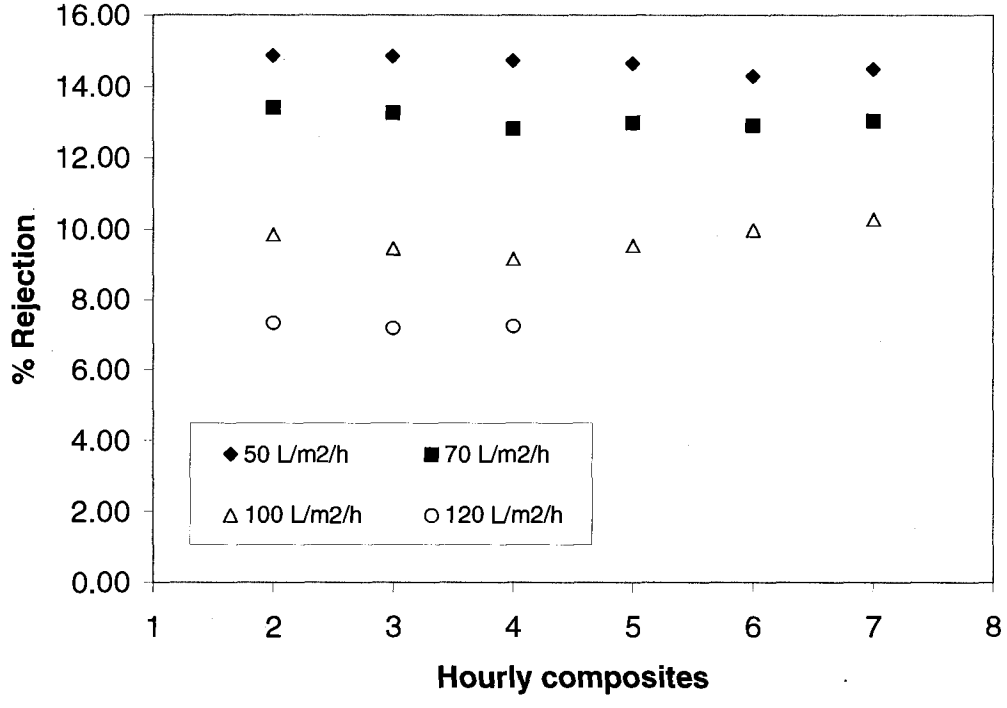

Figure 4.16. TOC percentage rejection for different operating flux values and BWF of 30 minutes and BWT of one minute

4.6 Effect of chemical pretreatment on membrane performance

Jar test were carried out with a six paddle Phipps & Bird Jar stirrer to ascertain optimum TOC removal. Different aluminium sulphate concentrations ranging from 10 mg/L to 60 mg/L were added to each of six square B-KER [2] laboratory jars. The tests indicated that the optimum TOC removal (54 ± 0.85%) occurred at an aluminium sulphate concentration of 40 mg/L equal to 3.24 g Al/m^3. Graphs depicting optimum TOC removal are shown in Appendix D.

Selected chemical and physical characteristics of the chemically pretreated ORW measured prior to the filtration experiments are shown in Table 4.1.

Table 4.1. Chemical pretreated ORW

Parameter	Mean
pH	6.23 ± 0.1
Turbidity (NTU)	0.706 ± 0.1
Alkalinity (mg/L as $CaCO_3$)	10
Total Organic Carbon (mg C/L)	2.81 ± 0.05
UV254 absorbance (cm^{-1})	0.062 ± 0.015
SUVA (L/mg-m)	2.21

From Table 4.1, the chemical pretreatment of ORW resulted in a 68% reduction in the feed turbidity, which is an indirect measure of colloidal particles. TOC was reduced by over 50% while SUVA, an indirect measure of aromatic humic substances was reduced was reduced by 50%. These results show that chemical pretreatment of ORW was effective in reducing colloidal particles and NOM.

4.6.1 Bench-scale estimation of critical flux for chemical water

Filtration experiments for the estimation of critical flux for the chemically pretreated ORW was conducted as described in Section 4.1. The experiments were performed using stepwise increases in permeate flux from approximately 30 $L/m^2/h$ to 350 $L/m^2/h$ and maintaining each flux for a period of 15 minutes. Figure 4.17 and Figure 4.18 show that the TMP remained relatively constant for most of the permeate fluxes and increasing only

slightly for the last two steps. The test was terminated at 350 L/m^2/h since the maximum allowable operating pressure of 20 psi (138 kPa) was reached.

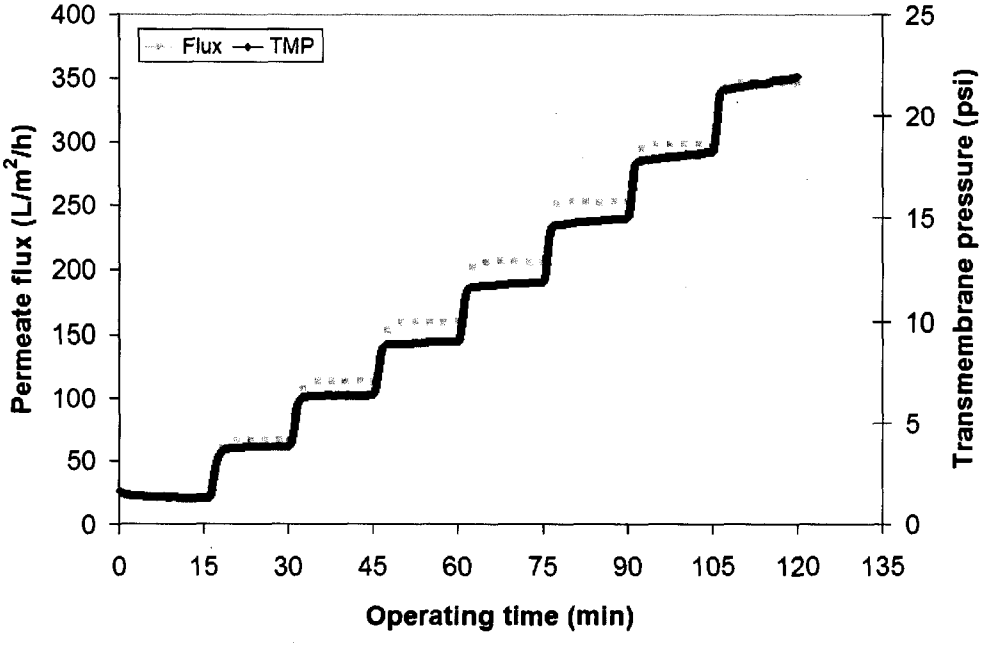

Figure 4.17. Schematic representation of critical flux by the flux-step method

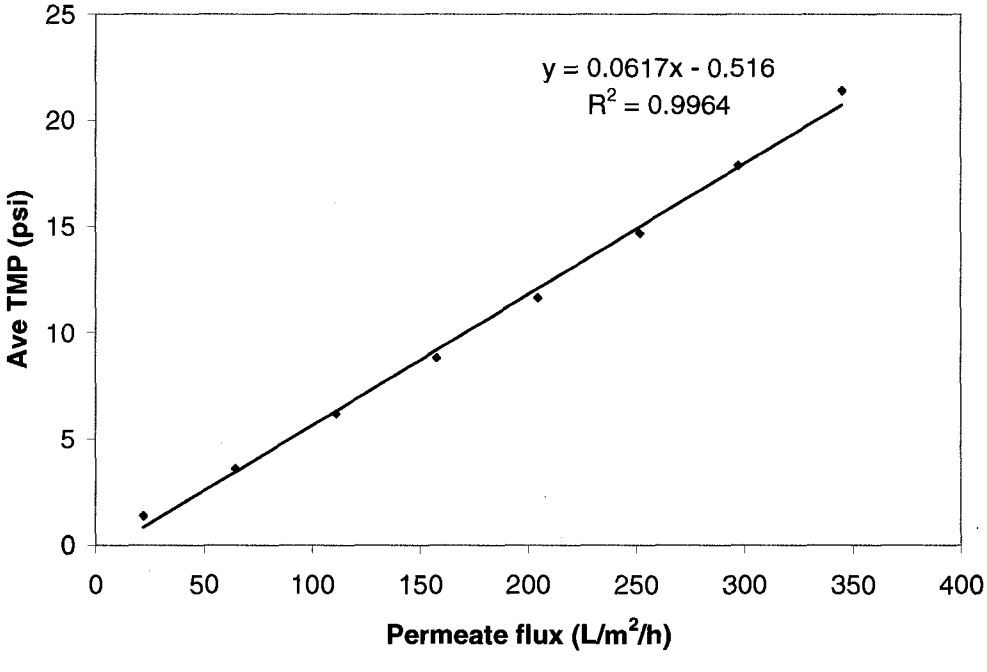

Figure 4.18. Average TMP versus flux for chemical pretreated ORW

Figure 4.18 shows a plot of the average TMP versus permeate flux for each constant flux condition. The data appears to be linear with a R^2 value of 0.9964 and the critical flux seems to be in excess of 350 L/m^2/h. However, the data has a very slight curvature and there may have been a slight transition in fouling trend above 275 L/m^2/h. This is significantly larger than the 75 L/m^2/h critical flux for the raw ORW, so chemical pre-treatment has a large beneficial impact on the membrane performance.

4.6.2 Effect of chemical pretreatment on fouling rate and backwash efficiency

The filtration experiments with chemical pretreated water were performed with a BWF of one hour and a BWT of one minute and constant flux of 100 L/m^2/h (i.e., a sub-critical flux). Backwash conditions were the same for all the experiments. The NSF decline pattern was compared with NSF decline patterns from the filtration of raw (i.e., uncoagulated) ORW with BWF of 15 minutes and BWT of one minute and two minutes, respectively (Figure 4.19). BWF of 15 minutes was chosen for comparison since it represents the optimal BWF for the different operating conditions tested in Section 4.2. Chemically pretreated ORW showed a much lower NSF decline compared with the uncoagulated ORW even though the BWF was four times that of coagulated ORW. The pre-treatment by coagulation resulted in over 50% reduction in TOC which reduces NSF decline. Figure 4.20 indicates that approximately 40% of the hydrophobic matter was removed during the chemical pretreatment of ORW. The other fraction of NOM (hydrophilic and transphilic matter) in ORW, although in smaller proportion when compared with the hydrophobic matter was removed to a much greater extent by the pre-treatment process.

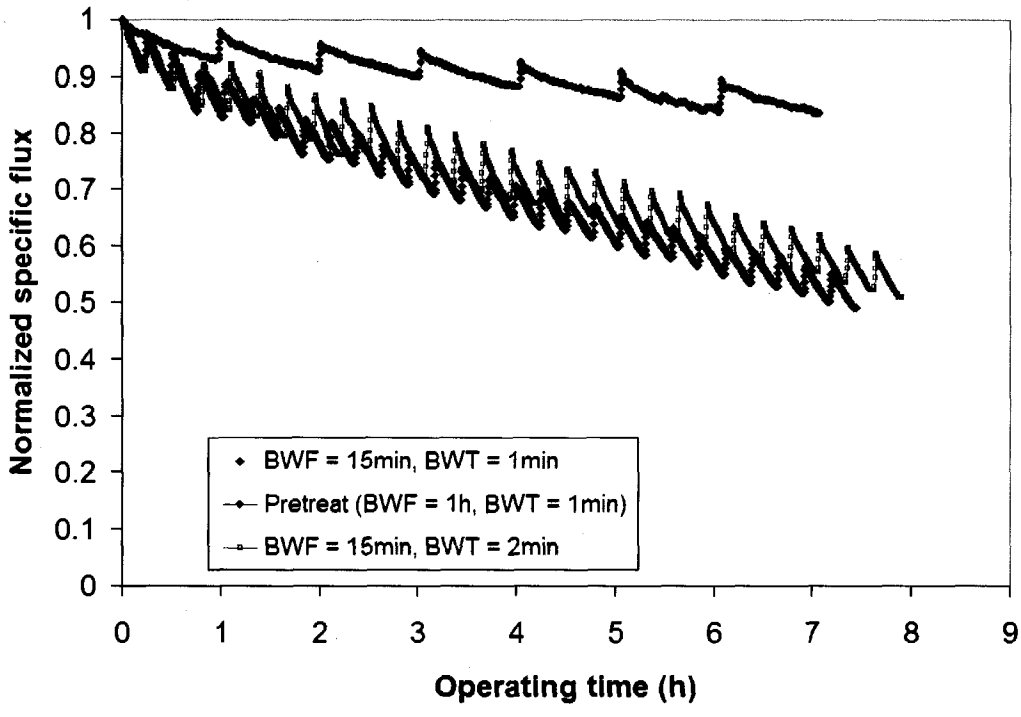

Figure 4.19. Comparison of NSF decline for chemical pretreated ORW and ORW for common operating flux value of 100 L/m^2/h using an UltraPES 0.7 membrane

From Table 4.1, chemically pretreated ORW has a SUVA of 2.21 L/mg-m which is approximately half of the SUVA for ORW (SUVA for ORW = 4.4 L/mg-m). This indicates that chemical pretreatment of ORW removes approximately half of the humic substance that is aromatic in nature. This 50% reduction in humic substance as demonstrated by the difference in SUVA for ORW and chemically treated ORW supported by a 40% removal in hydrophobic matter (figure 4.20), indicates that the reduction in hydrophobic matter may have been responsible for the major reduction in NSF decline. However, the non-hydrophobic fraction of NOM was removed to a great extent by the pre-treatment and could have also played a role in NSF decline of untreated ORW.

Wiesner and Laîne (1996) attributed the reduction in fouling rate to the reduced pore plugging by the larger coagulated particulate matter in the raw water. They stated that materials that might otherwise enter the pores and constrict flow are aggregated or sorbed onto flocs of the precipitated metal hydroxide which are rejected at the membrane surface. In these experiments, a significant portion of the larger macromolecules was removed by sedimentation prior to membrane treatment. In addition, some of the macromolecules that were not removed in sedimentation are sorbed onto the metal hydroxide flocs and are rejected at the membrane surface.

The results from the chemical pre-treatment of ORW compared well with several others authors including (Kabsch-Korbutowicz, 2005a; Kim et al., 2005; Qin et al., 2006; and Jung et al. 2006) who also noticed a significant improvement in NSF after chemical pretreatment of their respective source waters. Kabsch-Korbutowicz (2005a) observed a reduction in TOC of the order of 10 - 69.2% from treating surface water with alum at concentrations from 1.795 – 3.59 g/Al/m^3. Qin et al. (2006) observed DOC removal up to 59.5% from treating reservoir water with alum at a concentration of 5 mg (Al)/L, while Kim et al. (2005) observed TOC removal up to 56% from treating wastewater for reuse with an alum concentration of 100 mg /L.

The backwash efficiency for the chemically pretreated ORW was 93.42 $\pm$ 0.78% compared with 85.1 + 0.26 % for uncoagulated ORW even though the filtration cycles lasted one quarter of those for the coagulated ORW. From these results chemical pretreated ORW showed improved backwash efficiency when compared with uncoagulated OWR. Materials that might otherwise adsorb onto the wall of the pores are removed in sedimentation and at the membrane surface through the rejection of metal

hydroxide flocs. The later likely forms a layer that is more porous and easier to remove, hence making backwashing more effective.

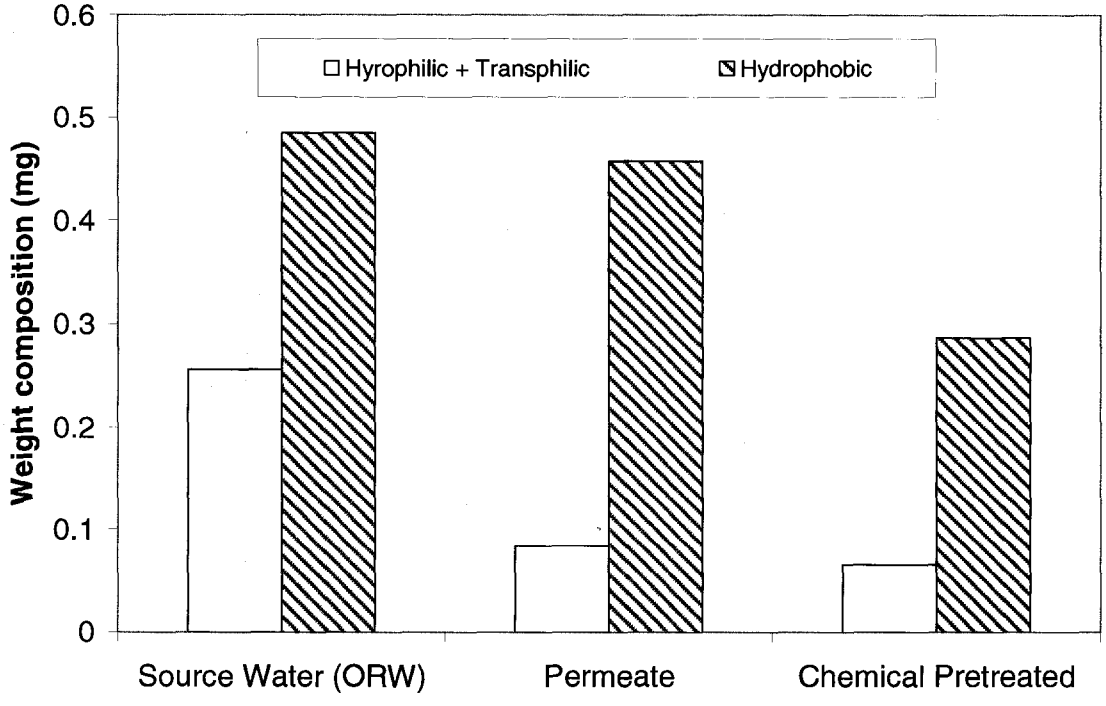

Figure 4.20. NOM fraction comparison of ORW; permeate and chemically pretreated ORW with the same operating conditions of BWF = I h, BWT = 1 min and flux of 100 L/m^2/h

4.6.3 Effect of chemical pretreatment on NOM rejection

Figure 4.21 depicts the TOC percentage rejection for chemically treated ORW with BWF of one hour and BWT of one minute. The figure depicts the mean values and standard deviation from duplicate filtration experiments under the same operating conditions. The results showed that although TOC removal by chemical pretreatment amounts to approximately 54%, TOC rejection by the membrane was still significant (10.4 ± 1.6%). Chemical pretreatment of feed waters are known to remove larger organic

macromolecules and hence the TOC rejection was expected to be relatively low after chemical pretreatment. The comparable rejection achieved may be due to the adsorption of smaller NOM molecules onto the precipitated metal hydroxide flocs comprising the cake layer.

It is therefore evident that chemically pretreatment improved the treatability of ORW thus enhancing membrane performance. The combined effect of chemical pretreatment and ultrafiltration reduced NOM concentration of ORW in excess of 64% compared to a NOM rejection of 14.54% for the ultrafiltration of un-coagulated OWR with BWF and BWT equal fifteen and two minutes, respectively (Figure 4.11). Reduction in NOM concentration signifies a reduction in DBP precursors and hence a reduction in DBP concentration in treated water.

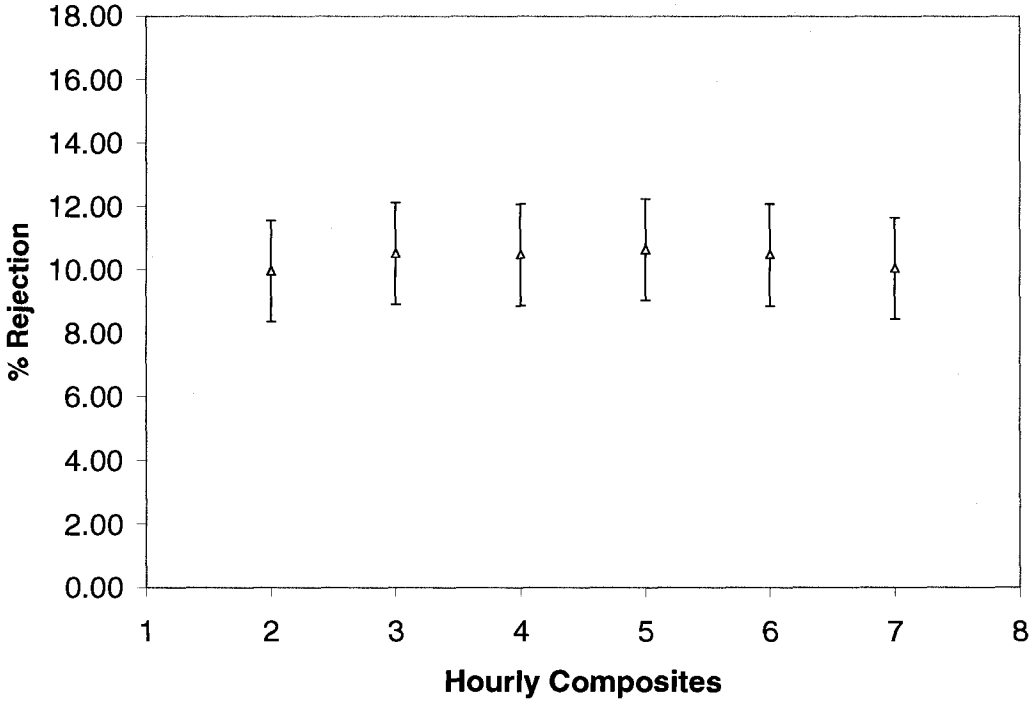

Figure 4.21. Total organic carbon (TOC) percentage rejection for chemically pretreated ORW with BWF of 1 h and BWT of 1 min.

4.7 Relationship between NOM rejection, and membrane characteristics

Attempts were made to investigate the relationship between NOM rejection, and membrane characteristics by performing filtration tests using different commercial membranes. Unfortunately, only one other manufacturer was willing to provide us with hollow fiber membranes, Hydranautics-Nitto Denko Corp. They donated HYDRAcap hydrophilic polyethersulfone (PES) hollow fibers with a nominal MWCO 150 kDa (internal diameter of 0.8 mm and outside diameter of 1.3 mm) from Hydranautics (Nitto Denko Corporation, Oceanside, CA), so they are slightly larger fibers with larger pores than the UltraPES 0.7 hollow fibers membranes used up to this point.

Several attempts were made to pass Milli-Q Water through the HYDRAcap membrane as is customary before the ultrafiltration of ORW, but these attempts were unsuccessful as the TMP kept increasing with no permeation. It was speculated that the surface tension at the membrane-water interphase might have been responsible for the hindered permeation. As a result, the feed was modified by using a solution of Milli-Q water and 20% ethanol to reduce the surface tension at the membrane-water interphase. Several attempts with this solution were also unsuccessful as the TMP kept increasing with no permeation. The manufactures were contacted but were unable to provide any solution.

Permeation through the HYDRAcap membrane, were expected to be excellent since it has a nominal MWCO 150 kDa, twice that of the UltraPES 0.7 membrane with MWCO of 70 kDa. Due to the inability to permeate water through the HYDRAcap membrane, the investigation of its performance was not possible.

CHAPTER 5

CONCLUSIONS AND RECOMMENDATIONS

5.1 Conclusions

The purpose of this study was to design and build a bench-scale hollow fiber ultrafiltration system to examine the effect of operational parameters and chemical pretreatment on membrane performance. The system was used to conduct treatability studies for ORW using commercial hollow fiber membranes. Based on the results presented in Chapter 4, a number of conclusions can be made:

1. The bench-scale, hollow fiber ultrafiltration (UF) system that operates at constant flux and includes a backwash cycle was developed in this study. It is a convenient tool to estimate the critical flux of source waters, and to observe the effect of operating parameters on membrane performance.

2. A great deal of time was spent modifying the system and its control strategy to maintain a constant flux. To a large extent, this proved to be a very difficult task because electronic flowmeters are not reliable.

3. The average TMP and ΔTMP/Δt for estimating the critical flux produced similar results. The flux-step method confirmed that the traditional definition of critical flux which is based on $\Delta TMP/\Delta t = 0$ in the sub-critical region, cannot be applied to natural waters.

4. For a common BWT, the fouling rate decreased substantially by an increase in BWF; BWT was not as significant as BWF but became more significant as the filtration cycle length increased.

5. Backwash efficiency increased as BWF decreased. BWT did not affect backwash efficiency significantly with the exception of the one hour filtration cycle.

6. NOM rejection was affected by BWF as shorter BWF resulted in an increase in NOM rejection, presumably due to the slow sorption of NOM. Shorter BWF allowed for greater desorption during the backwashing, thus liberating some NOM sorption sites on the membrane.

7. Higher operating fluxes increased the rate of approach of foulants to the membrane surface and increasing the fouling rate. This higher rate of approach also resulted in a decrease in NOM rejection. Backwash efficiency also decreased with increasing operating flux.

8. Chemical pre-treatment (Coagulation/flocculation/sedimentation) significantly improved the ultrafiltration of Ottawa River water. The pretreatment not only increased the overall NOM removal to over 64% but also decreased the fouling rate and increased the backwash efficiency.

An increase in BWT from one minute to two minutes for the 15 min filtration cycle showed improved TOC rejection likely because NOM sorption is slow and the longer BWT of two minutes allowed for greater desorption during the backwashing, thus liberating some NOM sorption sites (on the membrane) for use in the next filtration

cycle. For the longer filtration cycles, NOM become firmly attached to the membrane and thus backwashing has little impact.

5.2 Recommendations

1. The controlling of the feed pump should be further explored as this will allow the system to operate at a constant flux irrespective of the power of the peristaltic pump and hence provide a breakthrough at the bench-scale in the designing of constant flux bench-scale systems.
2. The relationship between fouling rate, and membrane characteristics should also be explored to obtain a better understanding of fouling by NOM.

REFERENCE

American Chemistry Council, "A Review of Disinfection Practices and Issues", Chlorine Chemistry Division, Arlington, VA (2003), pp 10-14.

Anselme C., and Jacobs E. P., "Ultrafiltration", chapter 10 in "*Water Treatment Membrane Processes*", J. Mallevialle, P. E. Odendaal and M. R. Wiesner, eds., McGraw Hill; New York, NY, (1996), pp 10.1-10.88.

Aoustin E., Schäfer A.I., Fane A.G., and Waite T.D., "Ultrafiltration of natural organic matter", *Sep. Purif. Technol.*, 22-23, 63-78 (2001).

Aptel P., and Buckley C. A., "Categories of membrane operations", chapter 2 in in "*Water Treatment Membrane Processes*", J. Mallevialle, P. E. Odendaal and M. R. Wiesner, eds., McGraw Hill; New York, NY, (1996), pp 2.1-2.24.

Bacchin P., Aimar P., and Field R.W., "Critical and sustainable fluxes: Theory, experiments and application", *J. Membr. Sci.*, 281, 42–69 (2006).

Bergman R.A., "Membrane Processes", chapter 13 in "*Water Treatment Plant Design*", McGraw Hill; New York, NY, (2005), pp 13.1-13.49.

Blackburn B.G., Craun G.F., Yoder J.S., Hill V., Calderon R.L., Chen N., Lee S.H., Levy D.A., and Beach M.J., "*Morbidity and Mortality Weekly Report*, CDC Surveillance summaries: Surveillance for waterborne disease outbreaks-United States, 2001-2002." U.S. Centers for Disease Control and Prevention, Atlanta, GA, (2004).

Bowen W.R., Calvo J.I., and Hermindez A., "Steps of membrane blocking in flux decline during protein microfiltration", *J. Membr. Sci.*, 101, 153-165 (1995).

Carroll T., Booker N.A., and Meier-Haack J., "Polyelectrolyte-grafted microfiltration membranes to control fouling by natural organic matter in drinking water", *J. Membr. Sci.*, 203, 3–13 (2002).

Chan R., Chen V., and Bucknall M.P., "Ultrafiltration of protein mixtures: measurement of apparent critical flux, rejection performance, and identification of protein deposition", *Desalination*, 146, 83-90 (2002).

Chang Y., and Benjamin M.M., "Iron oxide adsorption and UF to remove NOM and control fouling", *J. AWWA*, 88(12), 74-88 (1996).

Chellam J.C., and Zander A., "Membrane science and theory", chapter 3 in "*Microfiltration and Ultrafiltration for Drinking Water*", AWWA; Denver, CO (2005), pp 35-49.

Chellam S., and Jacangelo J.G., "Critical recovery concept in constant flux microfiltration and effect of operational mode on microfilter performance", chapter 4 in "*Membrane Practice for Water Treatment*", S.J. Duranceau, AWWA; Denver, CO, (2001), pp 43-51.

Chellam S., Jacangelo J.G., and Bonacquisti T.P., "Modeling and experimental verification of pilot-plant scale hollow fiber, direct flow microfiltration with periodic backwashing", *Environ. Sci. Technol.*, 32, 75–81 (1998).

Chen Y., Dong B.Z., Gao N.Y., and Fan J.C., "Effect of coagulation pretreatment on fouling of an ultrafiltration membrane", Desalination, 204, 181-188 (2007).

Cheryan M., "*Ultrafiltration and Microfiltration Handbook*", Technomic Publishing Co., Inc., Lancaster, PA, (1998).

Cho J., Amy G., and Pellegrino J., "Membrane filtration of natural organic matter: comparison of flux decline, NOM rejection, and foulants during filtration with three UF membranes", *Desalination*, 127, 283-298, (2000a).

Cho J., Amy G., and Pellegrino J., "Membrane filtration of natural organic matter: factors and mechanisms affecting rejection and flux decline with charged ultrafiltration (UF) membrane", *J. Membr. Sci.*, 164 89–110, (2000b).

Choi K.Y., and Dempsey B.A., "In-line coagulation with low-pressure membrane filtration", *Water Res.*, 38, 4271-4281, (2004).

Choi K.Y., and Dempsey B.A., "Bench-scale evaluation of critical flux and TMP in low-pressure membrane filtration", *J.AWWA*, 97 (7), 134-143, (2005).

Clark M. M., Baudin I., Anselme C., "Membrane-powered activated carbon reactors", chapter 15 in "*Water Treatment Membrane Processes*", J. Mallevialle, P. E. Odendaal and M. R. Wiesner, eds., McGraw Hill; New York, NY, (1996), pp 15.1-15.22.

Costa R.C., Pinho M.N., and Elimelech M., "Mechanisms of colloidal natural organic matter fouling in ultrafiltration", *J. Membr. Sci.*, 281, 716-725 (2006).

Croue J., Korshin G.V., and Benjamin M., "Executive Summary" in "*Characterization of Natural Organic*, AWWA, Research Foundation, Denver, CO, (2000).

Dang H.T., "*SMM incorporated UF membranes for NOM removal: characterization and cleaning*", PhD thesis in process, Dept. of Civil Engineering, University of Ottawa, Ottawa, ON (2008).

Dang H.T., Narbaitz R.M., Matsuura T., and Khulbe C.K., A comparison of commercial and experimental ultrafiltration membranes via surface property analysis and fouling tests, *Water Quality Res. J. of Canada*, 41 84-93 (2006).

Dong B.Z., Chen Y., Gao N.Y., and Fan J.C., "Effect of pH on UF membrane fouling", *Desalination(Abbreviation?)*, 195, 201-208 (2006).

Duclos-Orsello C., Li W., and Ho C.C., "A three mechanism model to describe fouling of microfiltration membranes", *J. Membr. Sci.*, 280, 856-866 (2006).

Duranceau S. J. and Losch H. J., "Integration of lime softening and ultrafiltration: a powerful water quality combination", chapter 26 in "*Membrane Practices for Water Treatment*", S.J. Duranceau, AWWA; Denver, CO, (2001), pp 447-459.

Fan L., Harris J.L., Roddick F.A., and Booker N.A., "Influence of the characteristics of natural organic matter on the fouling of microfiltration membranes, *Water Res.*, 35, 4455–4463, (2001)

Farahbakhsh K., Svrcek C., Gust R.K., and Smith D.W., "A review of the impac of chemical pretreatment on low-pressure water treatment membranes", *J. Environ. Eng. Sci.*, 3, 237-253 (2004).

Glucina K., Laîne J.M., and Durand-Bourlier L., "Assessment of filtration mode for the ultrafiltration membrane process", *Desalination*, 118, 205-211 (1998).

Gray S. R., Ritchie C.B., and Bolto B.A., "Effect of fractionated NOM on low-pressure membrane flux declines", *Water Sci. and Tech.*, 4, 189-196 (2004).

Hamza A., Pham V. A., Matsuura T., and Santerre J. P. "Development of membranes with low surface energy to reduce the fouling in ultrafiltration applications", *J. Membr. Sci.*, 131, 217-227 (1997).

Heijman S.G.J., Gijsbertsen A., and Amy G., "Water quality test for dead-end ultrafiltration", *AWWA WQTC Conference proceedings,* Denver, CO, (2005a).

Heijman S.G.J., Kennedy M.D., and van Hek G.J., "Heterogeneous fouling in dead-end ultrafiltration", *Desalination*, 178, 295-301 (2005b).

Ho C.C., and Zydney A.L., "A combined pore blockage and cake filtration model for protein fouling during microfiltration", *J. Colloid and Interface Sci.*, 232, 389-399 (2000).

Hong S., and Elimelech M., "Chemical and physical aspects of natural organic matter (NOM) fouling of nanofiltration membranes", *J. Membr. Sci.*, 132, 159-181 (1997).

Hong S., Krishna P., Hobbs C., Kim D., and Cho J., "Variations in backwash efficiency during colloidal filtration of hollow-fiber microfiltration membranes", *Desalination*, 173, 257-268 (2005).

Hrudey S. E., Payment P., Huck P.M, Gillham R.W., and Hrudey E.J., "A fatal waterborne disease epidemic in Walkerton, Ontario: comparison with other waterborne outbreaks in the developed world", *Water Sci. and Tech.*, 47, 7-14 (2003).

Hugaboom D. A. and Crozes G. F., "Pilot testing of membrane system", chapter 7 in "*Microfiltration and Ultrafiltration for Drinking Water*", AWWA, Denver, CO, (2005), pp 147-164.

Huisman I.H., Vellenga E., Trägårdh G., and Trägårdh C., "The influence of the membrane zeta potential on the critical flux for crossflow microfiltration of particle suspensions", *J. Membr. Sci.*, 156, 153-158 (1999).

Jacangelo J.G. and Noack R. K., "System concepts", chapter 4 in "*Microfiltration and Ultrafiltration for Drinking Water*", AWWA, Denver, CO, (2005), pp 51-64.

Jacangelo J.G., Adham S.S., and Laîne J.M., "Mechanism of Cryptosporidium, Giardia, and MS2 virus removal by MF and UF", *J. AWWA*, 87(9), 107-121 (1995).

Jacangelo J.G., Adham S.S., and Laîne J.M., "Membrane filtration for microbial removal report No. 90715", *AWWA Research Foundation*; Denver, CO, (1997).

Jacangelo J.G., Laîne J.M., Carns K.E., Cummings E.W., and Mallevialle J., "Filtration for removing Giardia and microbial indicators ", *J. AWWA*, 83(9), 97-106 (1991).

Jones K.L., and O' Melia C.R., "Protein and humic acid adsorption onto hydrophilic membrane surfaces: effect of pH and ionic strength", *J. Membr. Sci.*, 165, 31–46 (2000).

Jung C.W., Son H.J., and Kang L.S., "Effects of membrane material and pretreatment coagulation on membrane fouling: fouling mechanism and NOM removal", *Desalination*, 197, 154-164 (2006).

Kabsch-Korbutowicz M., "Effect of Al coagulant type on natural organic matter removal efficiency in coagulation/ultrafiltration process", *Desalination*, 185, 327-333 (2005a).

Kabsch-Korbutowicz M., "Application of ultrafiltration integrated with coagulation for improved NOM removal", *Desalination*, 174, 13-22 (2005b).

Katsoufidou K., Yiantsios S.G., and Karabelas A.J., "A study of ultrafiltration by humic acids and flux recovery by backwashing: Experimental and modeling", *J. Membr. Sci.*, 266, 40-50 (2005).

Kennedy M.D., Chun H.K., Yangali V.A.Q., Heijman B.G.J., and Schippers J.C., "Natural organic matter (NOM) fouling of ultrafiltration membranes: fractionation of NOM in surface water and characterization by LC-OCD", *Desalination*, 178, 73-83 (2005).

Kim J., and DiGiano F.A., "A two-fiber, bench-scale test of ultrafiltration (UF) for investigation of fouling rate and characteristics", *J. Membr. Sci.*, 271, 196–204 (2006).

Kim M.H., and Yu M.J., "Characterization of NOM in Han River and evaluation of treatability using UF_NF membrane", *Environmental Research*, 97, 116-123 (2005).

Kim S.H., Moon S.H, Yoon C.H., Yim S.H., and Cho J.W., "Role of coagulant in membrane filtration of wastewater for reuse", *Desalination*, 173, 301-307 (2005).

Kramer, M.H., B.L. Herwaldt, G.F. Craun, R.L. Calderon, and Juranek D.D., "Waterborne Disease: 1993 and 1994", *J. AWWA*. 88(3):66-80 (1996).

Laîné J.M., Hagstrom J.P., Clark M.M., and Mallevialle J., "Effect of ultrafiltration membrane composition", *J. AWWA*, 81(11) 61–67 (1989).

Le Clech P., Jefferson B., Chang I.S., and Judd S.J., "Critical flux determination by the flux-step method in a submerged membrane bioreactor", *J. Membr. Sci.*, 227, 81–93 (2003).

Lee H., Amy G., Cho J., Yoon Y., Moon S.H., and Kim I.S., "Cleaning strategies for flux recovery of an ultrafiltration membrane fouled by natural organic matter", *Water Research*, 35, 3301-3301, (2001).

Lee N., Amy G., Croué J., and Buisson H., "Identification and understanding of fouling in low-pressure membrane (MF/UF) filtration by natural organic matter (NOM)", *Water Research (Abbreviation?)*, 38, 4511-4523, (2004).

Liang J.L., Dziuban E.J., Craun G.F., Hill V., Moore M.R., Gelting R.J., Calderon R.L., Beach M.J., and Roy S.L., "*Morbidity and Mortality Weekly Report*, CDC Surveillance summaries: Surveillance for waterborne disease outbreaks-- United States, 2003-2004." U.S Centers for Disease Control and Prevention, Atlanta, GA, (2006).

Lin C., Lin T., and Hao O.J., "Effects of humic substance characteristics on UF performance", *Water Research*, 34 1097–1106, (1999).

Lipp P., and Baldauf G., "Application of out—in MF/UF systems for drinking water treatment with air supported backwash", *Desalination*, 147, 63-68 (2002).

Liu Q.F., and Kim S.H., "Evaluation of membrane fouling models based on bench-scale experiments: A comparison between constant flowrate blocking laws and artificial neural network (ANNs) model", *J. Membr. Sci.* (2007), doi:10.1016/j.memsci.2007.11.020

Lozier J.C., "Membrane application", chapter 6 in "*Microfiltration and Ultrafiltration for Drinking Water*", AWWA; Denver, CO (2005), pp 101-145.

Maartens A., Swart P., and van Jacobs E.P., "Feedwater pretreatment methods to reduce membrane fouling by natural organic matter", *J. Membr. Sci.*, 163, 51–62 (1999).

MacKenzie W.R., Hoxie N.J., Proctor M.E., Gradus M.S., Blair K.A., Peterson D.E., Kazmierczak J.J., Addiss D.G., Fox K.R., Rose J.B., and Davis J.P., "A massive outbreak in Milwaukee of Cryptosporidium infection transmitted through the public water supply", *N Engl J Med.*, 331, 161-167 (1994).

Mallevialle J., Odendall P.E., and Wiesner M.R., "The emergence of membranes in water and wastewater treatment", chapter 1 in "*Water Treatment Membrane Processes* ", J. Mallevialle, P. E. Odendaal and M. R. Wiesner, eds., McGraw Hill; New York, NY, (1996), pp 1.1-1.10.

Matsuura T., "Synthetic Membranes and Membrane Separation Processes", *CRC Press*, Boca Raton, FL (1994).

Metcalf and Eddy, Inc, "*Wastewater Engineering Treatment and Reuse*", Tchobanoglous G., Burton F.L., and Stensel H.D., e.d., McGraw Hill; New York, NY, (2003).

Minnery J.G., "*The effect of surface modifying macromolecules on pervaporation membranes and the effect of preparation conditions on the morphology of modified membranes*", M.A.Sc. thesis, Department of Chemical Engineering, University of Ottawa, Ottawa, ON (2000)

Mosqueda-Jimenez D. B., "*Impact of manufacturing conditions of Polyethersulfone membranes on final characteristics and fouling reduction*", PhD thesis, Department of Civil Engineering, University of Ottawa, Ottawa, ON (2003).

Mosqueda-Jimenez D. B., Narbaitz R. M., and Matsuura T.. "Membrane fouling test: apparatus evaluation", *J. Env. Eng.*, 130, 90-99 (2004).

Mulder M., "*Basic Principles of Membrane Technology*", Kluwer Academic Publishers, Dordrecht, The Netherlands, (1996).

MWH (Montgomery Watson Hamza), "*Water Treatment Principles and Design*", Crittenden J.C., Trussell R.R., Hand D.W., Howe K.J., Tchobanoglous G., ed., John Wiley & Sons, Inc., Hoboken, NJ, (2005).

Nakatsuka S., Nakate I., and Miyano T., "Drinking water treatment by using ultrafiltration hollow fiber membranes", *Desalination*, 106, 55-61 (1996).

Nguyen H. A., "*Membrane fouling reduction by the incorporation of hydrophilic surface modifying macromolecules in ultrafiltration membrane manufacture*", M.A.Sc thesis, Dept. of Civil Engineering, University of Ottawa, Ottawa, Ontario (2005).

Nilson J.A., and DiGiano F.A., "Influence of NOM composition on nanofiltration", *J. AWWA.*, 88(5), 53–66 (1996).

PID Control Toolset User Manual, National Instruments LabVIEW Nov 2001 Part No. 322192A-01

Pieracci J., Crivello J.V., and Belfort G., "Photochemical modification of 10 kDa polyethersulfone ultrafiltration membranes for reduction of biofouling", *J. Membr. Sci.*, 156, 223–240 (1999).

Qin J.J., Oo M.H., Kekre K.A., Knops F., and Miller P., "Reservoir water treatment using hybrid coagulation—ultrafiltration", *Desalination*, 193, 344-349 (2006).

Ridgway H. F., and Flemming H-C., "Biofouling" chapter 6 in "*Water Treatment Membrane Processes*", J. Mallevialle, P. E. Odendaal and M. R. Wiesner, eds., McGraw Hill; New York, NY, (1996), pp 6.1-6.59.

Sethi S., and Wiesner M.R., "Performance and cost modeling of ultrafiltration", *J. Env. Eng.*, 121, 874-883 (1995).

Schäfer A. I., Fane A. G., and Waite T. D., "Cost factors and chemical pretreatment effects in the membrane filtration of waters containing natural organic matter", *Water Res.*, 35, 1509-1517 (2001).

Schäfer A.I., Fane A.G., and Waite T.D., "Nanofiltration of natural organic matter: removal, fouling and the influence of multivalent ions", *Desalination*, 118, 109-122 (1998).

Seungkwan H., and Elimelech M., "Chemical and physical aspects of natural organic matter (NOM) fouling of nanofiltration membranes", *J. Membr. Sci.*, 132, 159–181 (1997).

Seungkwan H., Krishna P., Hobbs C., Kim D., and Cho J., "Variation in backwash efficiency during colloidal filtration of hollow-fiber microfiltration membranes", *Desalination*, 173, 257-268 (2005).

Smith P.J., Vigneswaran S., Ngo H.H., Ben-Aim R., and Nguyen H., "A new approach to backwash initiation in membrane systems", *J. Membr. Sci.*, 132, 159–181 (1997).

Song L., "Flux decline in crossflow microfiltration and ultrafiltration: mechanisms and modeling of membrane fouling", *J. Membr. Sci.*, 139, 183-200 (1998).

Speth T.F. and Reiss C.R., "Water quality", chapter 2 in "*Microfiltration and Ultrafiltration for Drinking Water*", AWWA; Denver, CO (2005), pp 7-34.

"*Standard Methods for the Examination of Water and Wastewater*", 20th Edition., L.S Clesceri, A.E. Greenberg and A.D. Eaton (1998)

Stirling R., Aramini J., Ellis A., Lim G., Meyers R., Fleury M., and Werker D., "North Battleford, Saskatchewan Spring, 2001 Waterborne Cryptosporidiosis Outbreak", Health Canada, Ottawa, Ontario, (2001).

Storrar M.D., "*Adsorption and Desorption Characteristics of Natural Organic Matter (NOM) in Natural Waters on Granular Activated Carbon (GAC)*", M.A.Sc thesis, Department of Civil Engineering, University of Ottawa, Ottawa, ON (2005).

Tarabara V.V., Hovinga R.M., and Wiesner M.R., "Constant transmembrane pressure vs. constant permeate flux: effect of particle size on crossflow membrane filtration", *Environ. Eng. Sci.*, 19, 343–355 (2002).

Ulbricht M., and Belfort G., "Surface modification of ultrafiltration membranes by low temperature plasma II. Graft polymerization onto polyacrylonitrile and polysulfone", *J. Membr. Sci.*, 111, 193–215 (1996).

USEPA (United States Environmental Protection Agency). "Stage 1 Disinfectants and Disinfection Byproducts Rule", EPA 815-F-98-010, Office of Ground and Drinking Water, Washington, D.C., (December 1998).

USEPA. "Microbial and Disinfection By-product Rules Simultaneous Compliance Guidance Manual", EPA 815-R-99-015, Office of Ground and Drinking Water, Washington, D.C., (August 1999).

USEPA. "Stage 1 Disinfectants and Disinfection By-products Rule: A Quick Reference Guide", EPA 816-F-01-010, Office of Ground and Drinking Water, Washington, D.C., (2001a).

USEPA. "Low Press Membrane Filtration for Pathogen Removal", EPA 815-C-01-001, Office of Ground and Drinking Water, Washington, D.C, (2001b).

USEPA. "Stage 2 Disinfectants and Disinfection By-products Rule: A Quick Reference Guide for Schedule 1 Systems", EPA 816-F-06-001, Office of Ground and Drinking Water, Washington, D.C., (2006).

Weishaar J.L., Aiken G.R., Bergamaschi B.A., Fram M.S., Fujii R., and Mopper K., "Evaluation of specific ultraviolet absorbance as an indicator of the chemical composition and reactivity of dissolved organic carbon", *Environ. Sci. Technol.*, 37, 4702-4708 (2003).

Wiesner M. R. and Buckley C. A., "Principles of rejection in pressure-driven membrane processes", chapter 5 in "*Water Treatment Membrane Processes*", J. Mallevialle, P. E. Odendaal and M. R. Wiesner, eds., McGraw Hill; New York, NY, (1996), pp 5.1-5.17.

Wiesner M. R., and Aptel P., "Mass transport and permeate flux and fouling in pressure-driven processes", chapter 4 in "*Water Treatment Membrane Processes*", J. Mallevialle, P. E. Odendaal and M. R. Wiesner, eds., McGraw Hill; New York, NY, (1996), pp 4.1-4.28.

Wiesner M. R., and Laîne J.M., "Coagulation and membrane separation", chapter 16 in "*Water Treatment Membrane Processes*", J. Mallevialle, P. E. Odendaal and M. R. Wiesner, eds., McGraw Hill; New York, NY, (1996), pp 16.1-16.11.

Yuan W., and Zydney A.L., "Humic acid fouling during microfiltration", *J. Membr. Sci.*, 157, 1–12 (1999).

Yuan W., Kocic A., and Zydney A.L., "Analysis of humic acid fouling during microfiltration using a pore blockage–cake filtration model", *J. Membr. Sci.*, 198, 51-62 (2002).

Zeman J. L., and Zydney L. A., "*Microfiltration and Ultrafiltration: Principles and Applications*", Marcel Dekker, New York, NY (1996).

Zularisam A.W., Ismail A.F., and Salim R., "Behaviours of natural organic matter in membrane filtration for surface water treatment—a review", *Desalination*, 194, 211-231 (2006).

APPENDIX A

CLEANING OF GLASSWARE

Since the work in this thesis involved water samples of relatively low TOC values, the cleaning of the glassware was performed according to Storrar (2005).

The cleaning of the glassware was conducted in the follow steps:

1. The glassware was rinsed with distilled water then soaked with 5% Contrex Alkaline Liquid Detergent (Fisher Scientific, Fair Lawn, NJ) and Milli-Q water mixture for six hours.

2. The glassware was then rinsed with Milli-Q water and dried in a Fisher ISO TEMP laboratory oven (Fisher Scientific, Fair Lawn, NJ) overnight at 110°C

3. The glassware was then allowed to cool to room temperature and then filled with a solution of Chromerge™ (concentrated labware cleaner, VWR International, West Chester, PA) and concentrated sulphuric acid (Fisher Scientific, Fair Lawn, NJ), (25 mL bottle of chromerge to 4.1 kg container of concentrated sulphuric acid) for two hours.

4. The glassware was then rinse with Milli-Q water ten times and dried overnight in a Fisher ISO TEMP laboratory oven t at 110°C.

APPENDIX B

ULTRAFILTRATION MODULE CONSTRUCTION

The membrane modules used throughout the filtration experiments were constructed as follow:

1. Acrylic tubing, 12 inches in length, ¼ inch inside diameter and ½ inch outside diameter supplied by Canus Plastic Inc, Ottawa, was washed with 5% Contrex Alkaline Liquid Detergent and dried at room temperature.
2. Tubing facing was fabricated in the machine shop from acrylic plastic sheets ¾ inch in thickness. The acrylic plastic sheets were cut in 1 ¼ inch strips and drilled on ½ x ⅝ inch centers with a ½ inch diameter drill bit (see Figure B.1). The facing were then obtained by cutting the 1 ¼ inch strips in two halves (⅝ inch each) then cutting these halves into 1 inch lengths.
3. Two acrylic facings were then cemented onto each 12 inches acrylic tubing with acrylic cement, 50 mm and 80 mm, respectively, from each end of the tubing and dried for 24 hours.
4. The cemented acrylic facing were then drilled and tapped to accommodate ⅛ inch NPTM x ¼ inch pipe reducer fittings.
5. Compression brass caps, (½ inch in diameter) were then tighten onto each end of the tubing. The tubing was then drilled on the opposite side of the facing, ½ inch from the brass caps on both ends to be able to introduce the epoxy resin.
6. The brass caps were then removed and the outside and inside of the tubes scrubbed with a brush and allowed to dry at room temperature.

7. Eight hollow fibers were then cut in equal lengths, inserted in the tubes and then epoxy was added. The hollow fibers were held in place for 30 minutes for the epoxy resin to dry and harden.
8. After the epoxy is dried, the module is cut to the desired length and the lumen of the fibers cleared.

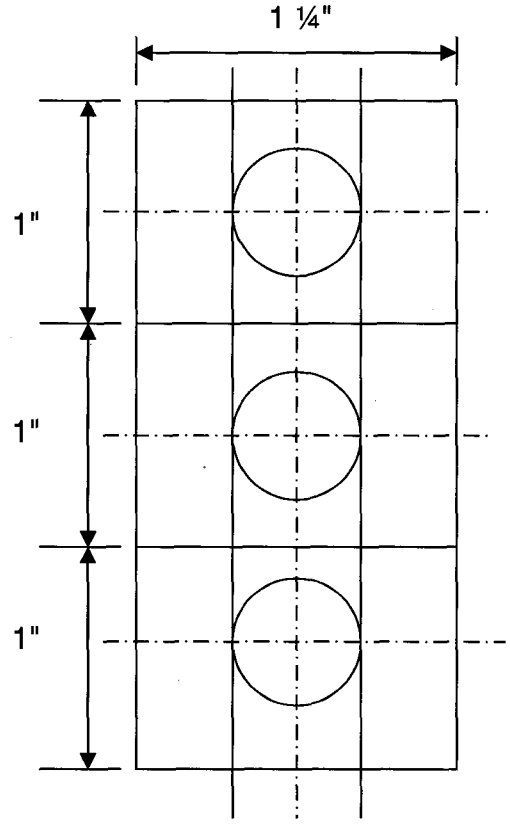

Figure A.1. Acrylic plastic sheets cut in 1 ¼ inch strips and drilled on ½ x ⅝ inch centers

APPENDIX C

PID TUNING PARAMETERS

An integral part of operating the system depicted in Chapter 3, Figure 3.3 and Figure 3.4 in a stable and suitable manner is determining the appropriate PIDs (P-Proportional, I-Integral, D-Derivative) tuning parameters. The PIDs controlling the feed pump and backwash pump were calibrated using the open-loop step test tuning procedure (Ziegler-Nichols tuning method). The procedure assumes that any process can be modeled as a first-order process with a lag. The procedure involves observing the pump output (% output) and the process variable (PV) which is the flowrate on a strip chart that shows time on the x-axis. The controller is positioned in the manual mode and the output is set to a nominal operating value. The flowrate (PV) is allowed to settle completely. The flowrate (PV) and output values were recorded. A step change is made in the pump output and the new pair of values (flowrate and % pump output) recorded after the flowrate settled. Figure C.1 depicts an example of an output and process variable strip chart used to tune the controllers.

The measured values T_d (deadtime in minutes), T (Time constant in minutes) and K the process gain (K= change in output/change in PV) are then multiplied by the factors (quarter-decay ratios) shown in Table C.1. K_c (proportional gain), T_i (integral or reset time) and T_D (derivative or rate time) (PID parameters) were then determined from T_d and Equation (C.1).

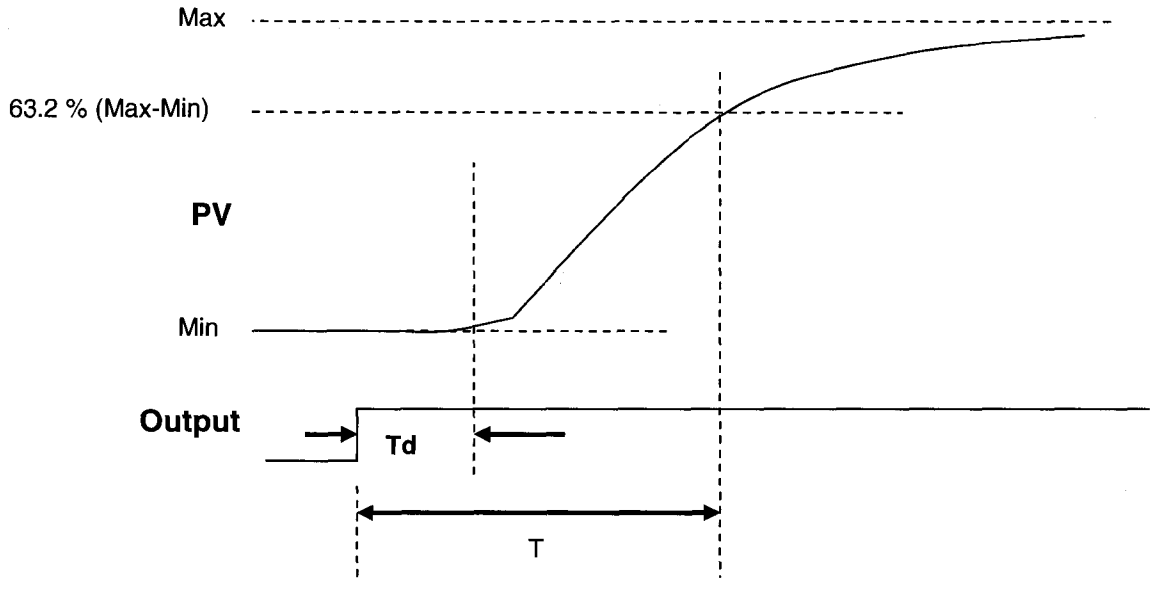

Figure C.1. Output and process variable strip chart (NI LabView, 2001)

Table C.1. Open-loop quarter decay ratio values (NI LabView, 2001)

Controller	PB (percent)	Reset (T_i) (minutes)	Rate (T_D) (minutes)
P	$100\frac{KT_d}{T}$	—	—
PI	$110\frac{KT_d}{T}$	$3.33T_d$	—
PID	$80\frac{KT_d}{T}$	$2.00T_d$	$0.50T_d$

$$PB = 100/K_c \qquad (C.1)$$

Typical steps used for tuning the PID controllers are as follows: K_c was used to decrease rise time (time taken for PV to rise beyond 90% of the desired level for the first time); T_D was used to reduce overshoot and settling time (height of peak above steady-state and time taken for system to converge to steady-state respectively) ; and T_i was used to

eliminate steady-state error (difference between the steady-state output and the desired output).

APPENDIX D

JAR TEST RESULTS

Table D.1 depicts duplicate Jar testing results for the optimization of TOC removal for ORW.

Table D.1. Jar testing results for ORW

Parameter	Alum concentration (mg/L)	pH Sample 1	pH Sample 2	TOC (mg/L) Sample 1	TOC (mg/L) Sample 2
Raw	0	7.35	7.21	5.58	5.62
Blank	0	7.33	7.21	5.75	5.67
Sample 1	20	6.79	6.92	2.67	2.95
Sample 2	30	6.58	6.58	2.67	2.63
Sample 3	40	6.34	6.26	2.41	2.43
Sample 4	50	5.77	5.76	2.40	2.46
Sample 6	60	5.16	5.05	2.36	2.56

Figure D.1 and Figure D.2 show plots of TOC concentration versus alum dosage. The plots represent the data depicted in Table D.1 and showed that the optimum TOC removal occurred at approximately 40 mg/L.

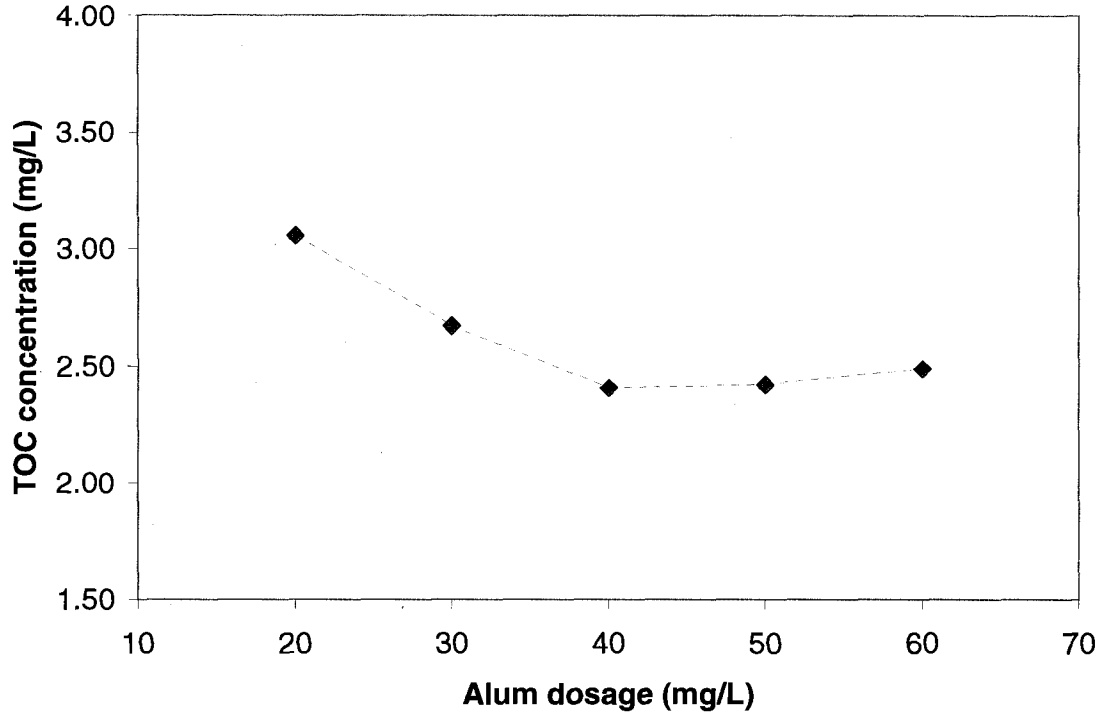

Figure D.1. Optimum TOC removal for Jar Test No. 1

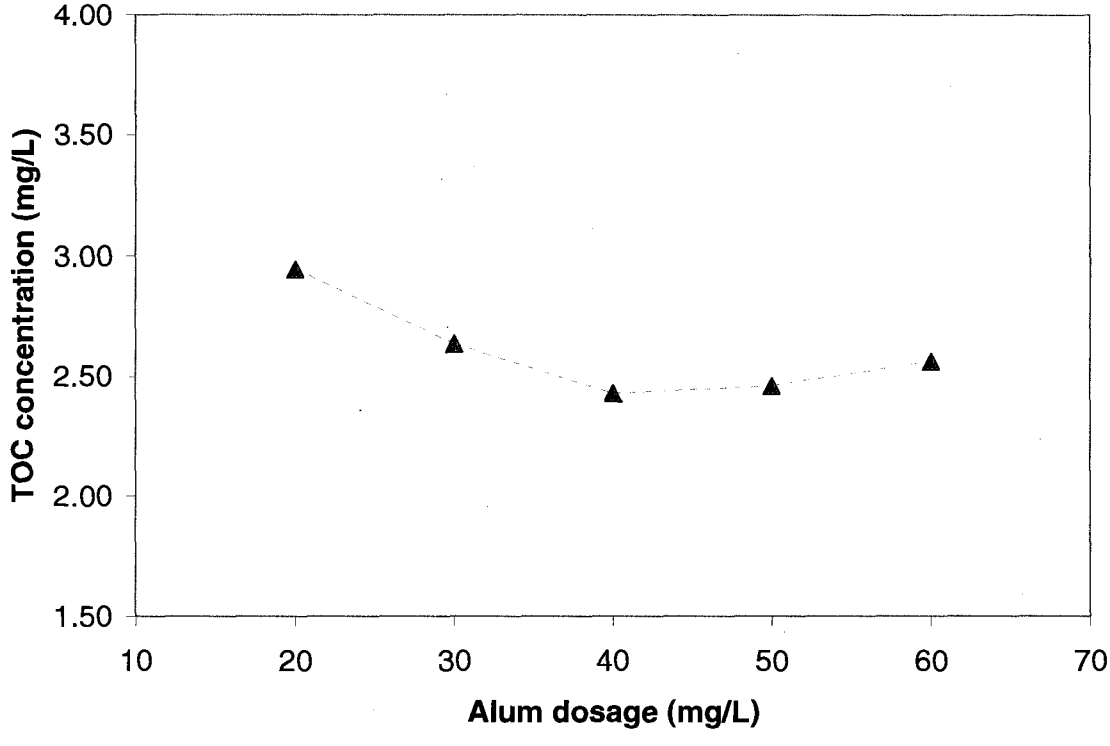

Figure D.2. Optimum TOC removal for Jar Test No. 2

APPENDIX E

ULTRAFILTRATION PUMP TEST

Figures E.1 and E.2 depicts preliminary UF filtration testing (without backwashing) for the initial feed pump (peristaltic L/S Easy-Load II, EW-77200-52, Cole-Parmer, Montreal, QC) and the high performance peristaltic replacement pump (EW-77250-62, Cole-Parmer, Montreal, QC).

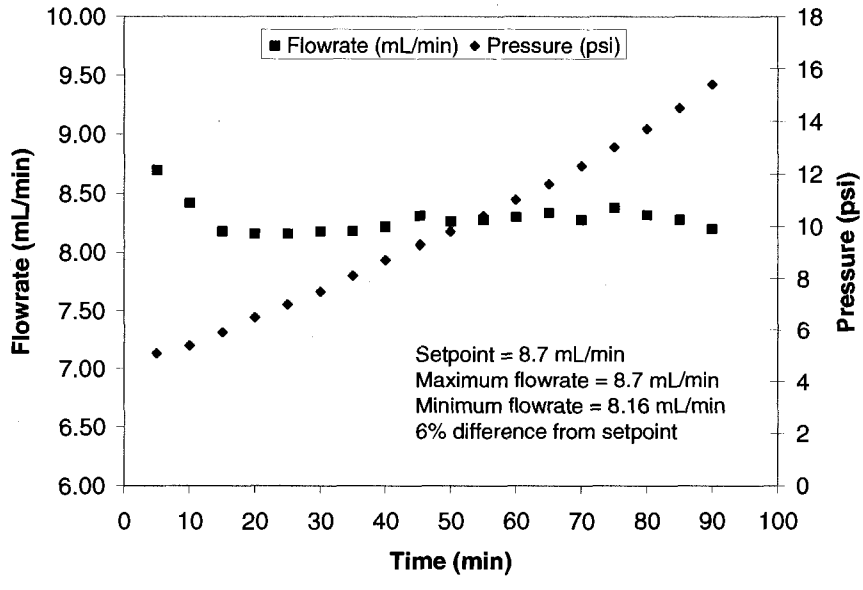

Figure E.1. Preliminary UF pump test results for peristaltic pump (L/S Easy-Load II, EW-77200-52, Cole-Parmer, Montreal, QC)

Figure E.1 shows that the flowrate from the peristaltic L/S Easy-Load II pump experienced a sharp initial decreased in flowrate for the first 15 minutes of operation, and remained constant thereafter as the transmembrane pressure steadily increased to the maximum allowable transmembrane pressure of 20 psi (138 kPa). A maximum of six percentage (6%) difference in the actual flowrate from the setpoint flowrate was observed in these initial filtration tests. The high performance peristaltic pump, depicted in Figure E.2, showed superb performance in maintaining a constant flow when compared with the

peristaltic L/S Easy-Load II pump. The peristaltic L/S Easy-Load II pump could not maintain a constant flowrate was likely due to the fact that the pump was operated at pressures approaching the maximum pressure rating of the pump. The high performance peristaltic pump with a much higher pressure rating provided much more constant flowrates.

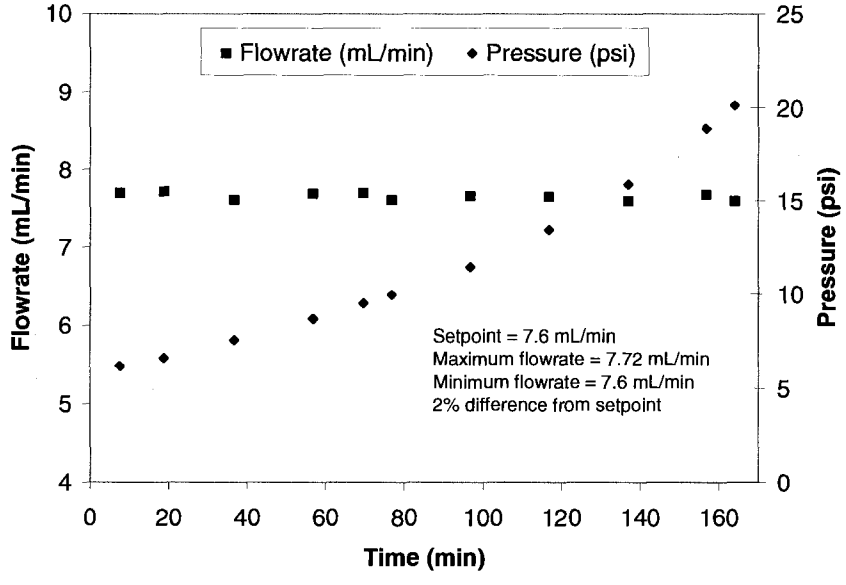

Figure E.2. UF pump test results for high performance peristaltic pump (EW-77250-62, Cole-Parmer, Montreal, QC)

APPENDIX F

LINEAR REGRESSION FOR STEP-FLUX RESULTS OF ORW

Table E.1. Step-flux results for ORW

Mean Flux ($L/m^2/h$)	Mean TMP (psi)
30	1.70
40	2.28
49	2.92
59	3.78
67	4.75
77	6.14
87	7.95
96	10.34
106	13.76

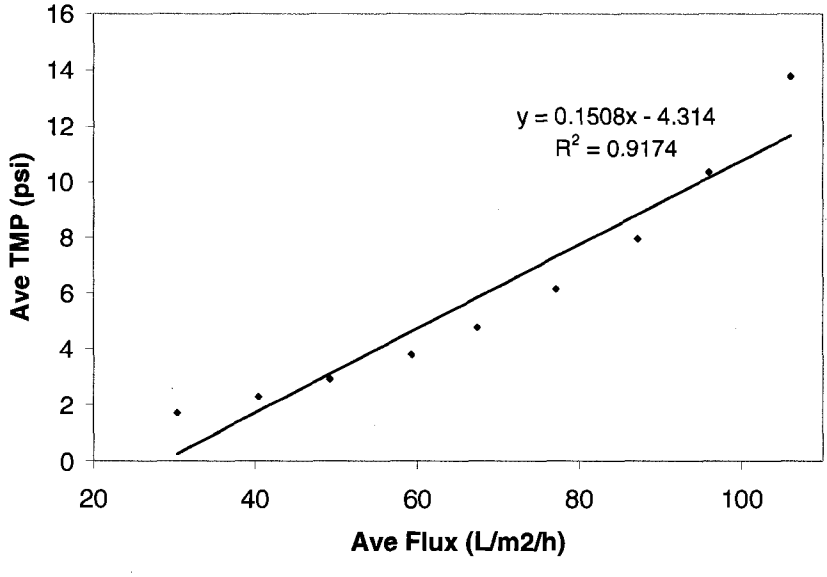

Figure E.1. Linear regression of the results from the step-flux results for ORW

APPENDIX G

ULTRAFILTRATION ANALYTICAL RESULTS

Date: October 16, 2007

Operating flux = 100 /m^2/h

BWF = 15 min

BWT = 60s

Table G.1. Ultrafiltration results - Test 1a

Sample ID	Turbidity NTU	pH	TOC mg/L	TOC % Rejection	Ave UV254 cm^{-1}	UV254 % Rejection	SUVA L/mg.m
Filtered MilliQ Water	0.063	5.47	0.20	96.33	0.001	99.58	0.50
Composite 1	0.066	7.13	4.38	20.38	0.169	29.29	3.86
Composite 2	0.065	7.29	4.82	12.44	0.186	22.18	3.86
Composite 3	0.064	7.37	4.84	11.93	0.185	22.59	3.82
Composite 4	0.067	7.41	4.83	12.14	0.189	20.92	3.91
Composite 5	0.062	7.33	4.84	11.97	0.195	18.41	4.03
Composite 6	0.064	7.44	4.84	11.96	0.192	19.67	3.96
Composite 7	0.067	7.43	4.84	11.95	0.195	18.41	4.03
Source Water	1.87	7.41	5.50		0.239		

Date: October 23, 2007

Operating flux = 100 /m^2/h

BWF = 15 min

BWT = 60s

Table G.2. Ultrfiltration results - Test 1b

Sample ID	Turbidity NTU	pH	TOC mg/L	TOC % Rejection	Ave UV254 cm^{-1}	UV254 % Rejection	SUVA L/mg.m
Filtered MilliQ Water	0.061	5.55	0.11	98.01	0.002	99.16	1.84
Composite 1	0.054	7.00	4.24	22.63	0.168	29.71	3.96
Composite 2	0.061	7.19	4.71	14.11	0.185	22.59	3.93
Composite 3	0.065	7.27	4.75	13.23	0.186	22.18	3.91
Composite 4	0.059	7.26	4.74	13.51	0.186	22.18	3.93
Composite 5	0.058	7.28	4.76	13.07	0.187	21.76	3.93
Composite 6	0.064	7.27	4.78	12.71	0.188	21.34	3.93
Composite 7	0.063	7.28	4.73	13.61	0.191	20.08	4.04
Source Water	2.42	7.46	5.48		0.239		

Date: October 18, 2007

Operating flux = 100 /m^2/h

BWF = 15 min

BWT = 2 min

Table G.3. Ultrafiltration results - Test 2a

Sample ID	Turbidity NTU	pH	TOC mg/L	TOC % Rejection	Ave UV254 cm^{-1}	UV254 % Rejection	SUVA L/mg.m
Filtered MilliQ Water	0.051	5.47	0.13	97.66	0.002	99.17	1.51
Composite 1	0.059	7.11	4.35	23.12	0.169	30.17	3.89
Composite 2	0.062	7.26	4.80	15.08	0.185	23.55	3.85
Composite 3	0.061	7.33	4.84	14.48	0.186	23.14	3.84
Composite 4	0.06	7.38	4.83	14.63	0.186	23.14	3.85
Composite 5	0.058	7.39	4.82	14.86	0.188	22.31	3.90
Composite 6	0.056	7.39	4.84	14.43	0.188	22.31	3.88
Composite 7	0.064	7.41	4.83	14.59	0.191	21.07	3.95
Source Water	2.25	7.33	5.66		0.242		

Date: October 21, 2007

Operating flux = 100 /m^2/h

BWF = 15 min

BWT = 2 min

Table G.4. Ultrafiltration results - Test 2b

Sample ID	Turbidity NTU	pH	TOC mg/L	TOC % Rejection	Ave UV254 cm^{-1}	UV254 % Rejection	SUVA L/mg.m
Filtered MilliQ Water	0.053	5.34	0.13	97.65	0.002	99.16	1.50
Composite 1	0.058	7.09	4.39	22.56	0.167	30.13	3.80
Composite 2	0.059	7.3	4.83	14.77	0.183	23.43	3.79
Composite 3	0.055	7.34	4.84	14.59	0.185	22.59	3.82
Composite 4	0.059	7.38	4.86	14.19	0.189	20.92	3.88
Composite 5	0.058	7.41	4.86	14.31	0.188	21.34	3.87
Composite 6	0.056	7.33	4.88	13.98	0.189	20.92	3.88
Composite 7	0.059	7.35	4.85	14.49	0.190	20.50	3.92
Source Water	2.38	7.57	5.67		0.242		

Date: September 25, 2007

Operating flux = 100 /m^2/h

BWF = 30 min

BWT = 1 min

Table G.5. Ultrafiltration Results - Test 3a

Sample ID	Turbidity NTU	pH	TOC mg/L	TOC % Rejection	Ave UV254 cm^{-1}	UV254 % Rejection	SUVA L/mg.m
Filtered MilliQ Water	0.058	5.4	0.22	96.18	0.002	99.18	0.92
Composite 1	0.056	7.19	4.63	18.62	0.174	28.98	3.76
Composite 2	0.055	7.36	5.15	9.44	0.198	19.18	3.84
Composite 3	0.057	7.39	5.18	8.98	0.198	19.18	3.83
Composite 4	0.056	7.29	5.21	8.36	0.200	18.37	3.84
Composite 5	0.057	7.29	5.19	8.66	0.199	18.78	3.83
Composite 6	0.056	7.23	5.13	9.72	0.203	17.14	3.954032
Composite 7	0.06	7.25	5.13	9.86	0.206	15.92	4.018493
Source Water	2.68	7.35	5.69		0.245		

Date: September 27. 2007

Operating flux = 100 /m^2/h

BWF = 30 min

BWT = 1 min

Table G.6. Ultrafiltration results - Test 3b

Sample ID	Turbidity NTU	pH	TOC mg/L	TOC % Rejection	Ave UV254 cm^{-1}	UV254 % Rejection	SUVA L/mg.m
Filtered MilliQ Water	0.054	5.36	0.24	95.73	0.000	100.00	0.00
Composite 1	0.069	6.92	4.55	19.91	0.169	30.45	3.72
Composite 2	0.06	7.2	5.09	10.25	0.190	21.81	3.73
Composite 3	0.069	7.22	5.11	9.94	0.195	19.75	3.81
Composite 4	0.065	7.27	5.11	9.96	0.195	19.75	3.82
Composite 5	0.062	7.29	5.09	10.39	0.197	18.93	3.87
Composite 6	0.059	7.27	5.09	10.24	0.196	19.34	3.85
Composite 7	0.069	7.3	5.07	10.70	0.201	17.28	3.97
Source Water	7.46	7.35	5.68		0.243		

Date: October 1, 2007

Operating flux = 100 /m^2/h

BWF = 30 min

BWT = 2 min

Table G.7. Ultrafiltration results - Test 4a

Sample ID	Turbidity NTU	pH	TOC mg/L	TOC % Rejection	Ave UV254 cm^{-1}	UV254 % Rejection	SUVA L/mg.m
Filtered MilliQ Water	0.067	5.54	0.22	96.13	0.002	99.18	0.90
Composite 1	0.055	6.94	4.70	18.28	0.173	29.39	3.68
Composite 2	0.062	7.15	5.18	9.90	0.200	18.37	3.86
Composite 3	0.067	7.24	5.19	9.78	0.197	19.59	3.80
Composite 4	0.063	7.28	5.20	9.54	0.198	19.18	3.81
Composite 5	0.058	7.31	5.22	9.27	0.199	18.78	3.82
Composite 6	0.055	7.13	5.21	9.29	0.201	17.96	3.85
Composite 7	0.055	7.32	5.24	8.79	0.202	17.55	3.85
Source Water	2.29	7.46	5.75		0.245		

Date: October 4, 2007

Operating flux = 100 /m^2/h

BWF = 30 min

BWT = 2 min

Table G.8. Ultrafiltration results - Test 4b

Sample ID	Turbidity NTU	pH	TOC mg/L	TOC % Rejection	Ave UV254 cm^{-1}	UV254 % Rejection	SUVA L/mg.m
Filtered MilliQ Water	0.053	5.47	0.23	95.95	0.006	97.49	2.57
Composite 1	0.058	6.95	4.63	19.58	0.173	27.62	3.74
Composite 2	0.059	7.22	5.15	10.55	0.195	18.41	3.79
Composite 3	0.056	7.24	5.19	9.81	0.196	17.99	3.78
Composite 4	0.056	7.25	5.19	9.81	0.196	17.99	3.78
Composite 5	0.063	7.31	5.21	9.43	0.194	18.83	3.72
Composite 6	0.058	7.26	5.21	9.42	0.197	17.57	3.78
Composite 7	0.066	7.3	5.21	9.44	0.196	17.99	3.76
Source Water	2.25	7.46	5.76		0.239		

Date: November 11, 2007

Operating flux = 100 /m^2/h

BWF = 1 h

BWT = 1 min

Table G.9. Ultrafiltration results - Test 5a

Sample ID	Turbidity NTU	pH	TOC mg/L	TOC % Rejection	Ave UV254 cm^{-1}	UV254 % Rejection	SUVA L/mg.m
Filtered MilliQ Water	0.041	6.07	0.11	98.17	0.003	98.75	2.85
Composite 1	0.055	6.98	4.75	17.30	0.184	23.33	3.87
Composite 2	0.054	7.09	5.22	9.17	0.207	13.75	3.96
Composite 3	0.055	7.14	5.25	8.64	0.207	13.75	3.94
Composite 4	0.056	7.24	5.23	9.05	0.207	13.75	3.96
Composite 5	0.058	7.2	5.25	8.68	0.212	11.67	4.04
Composite 6	0.06	7.22	5.23	9.08	0.212	11.67	4.06
Source Water	2.4	7.22	5.75		0.240		

Date: December 4, 2007

Operating flux = 100 /m^2/h

BWF = 1 h

BWT = 1 min

Table G.10. Ultrafiltration results - Test 5b

Sample ID	Turbidity NTU	pH	TOC mg/L	TOC % Rejection	Ave UV254 cm^{-1}	UV254 % Rejection	SUVA L/mg.m
Filtered MilliQ Water	0.05	5.99	0.09	98.40	0.001	99.59	1.08
Composite 1	0.057	7.00	4.83	16.29	0.185	24.49	3.83
Composite 2	0.058	7.09	5.35	7.21	0.206	15.92	3.85
Composite 3	0.057	7.11	5.38	6.69	0.210	14.29	3.90
Composite 4	0.058	7.16	5.41	6.22	0.211	13.88	3.90
Composite 5	0.057	7.18	5.37	6.95	0.211	13.88	3.93
Composite 6	0.054	6.93	5.34	7.33	0.213	13.06	3.99
Source Water	2.5	7.18	5.77		0.245		

Date: October 25, 2007

Operating flux = 100 /m^2/h

BWF = 1 h

BWT = 2 min

Table G.11. Ultrafiltration results - Test 6a

Sample ID	Turbidity NTU	pH	TOC mg/L	TOC % Rejection	Ave UV254 cm^{-1}	UV254 % Rejection	SUVA L/mg.m
Filtered MilliQ Water	0.045	5.45	0.16	97.19	0.002	99.16	1.27
Composite 1	0.058	7.00	4.62	17.38	0.184	22.36	3.99
Composite 2	0.06	7.17	5.11	8.55	0.203	14.35	3.97
Composite 3	0.061	7.31	5.14	8.00	0.201	15.19	3.91
Composite 4	0.055	7.28	5.15	7.79	0.203	14.35	3.94
Composite 5	0.055	7.29	5.19	7.16	0.205	13.50	3.95
Composite 6	0.052	7.3	5.17	7.38	0.205	13.50	3.96
Composite 7	0.058	7.3	5.18	7.34	0.208	12.24	4.02
Source Water	2.38	7.43	5.59		0.237		

Date: November 13, 2007

Operating flux = 100 /m^2/h

BWF = 1 h

BWT = 2 min

Table G.12. Ultrafiltration results - Test 6b

Sample ID	Turbidity NTU	pH	TOC mg/L	TOC % Rejection	Ave UV254 cm^{-1}	UV254 % Rejection	SUVA L/mg.m
Filtered MilliQ Water	0.043	5.99	0.10	98.27	0.001	99.59	1.02
Composite 1	0.056	7.00	4.73	16.18	0.183	24.07	3.87
Composite 2	0.057	7.12	5.22	7.54	0.204	15.35	3.91
Composite 3	0.063	7.18	5.28	6.46	0.206	14.52	3.90
Composite 4	0.055	7.2	5.28	6.48	0.208	13.69	3.94
Composite 5	0.06	7.21	5.26	6.74	0.208	13.69	3.95
Composite 6	0.057	7.28	5.24	7.19	0.210	12.86	4.01
Composite 7	0.053	7.21	5.25	6.98	0.210	12.86	4.00
Source Water	2.4	7.36	5.64		0.241		

Date: January 14, 2008

Operating flux = 50 /m²/h

BWF = 30 min

BWT = 1 min

Table G.13. Ultrafiltration results - Test 7a

Sample ID	Turbidity NTU	pH	TOC mg/L	TOC % Rejection
Filtered MilliQ Water	0.054	6.79	0.10	98.27
Composite 1	0.052	7	3.93	30.33
Composite 2	0.058	7.14	4.68	17.03
Composite 3	0.06	7.2	4.69	16.86
Composite 4	0.063	7.21	4.74	16.02
Composite 5	0.059	7.23	4.76	15.68
Composite 6	0.055	7.01	4.81	14.73
Composite 7	0.057	7.3	4.80	14.93
Source Water	2.34	7.24	5.64	

Date: January 15, 2008

Operating flux = 50 /m²/h

BWF = 30 min

BWT = 1 min

Table G.14. Ultrafiltration results - Test 7b

Sample ID	Turbidity NTU	pH	TOC mg/L	TOC % Rejection
Filtered MilliQ Water	0.038	5.45	0.08	98.61
Composite 1	0.055	7	4.62	18.21
Composite 2	0.057	7.17	4.93	12.71
Composite 3	0.062	7.31	4.92	12.85
Composite 4	0.062	7.28	4.89	13.42
Composite 5	0.062	7.29	4.88	13.60
Composite 6	0.063	7.3	4.86	13.87
Composite 7	0.062	7.3	4.85	14.04
Source Water	2.38	7.43	5.78	

Date: January 16, 2008

Operating flux = 70 /m^2/h

BWF = 30 min

BWT = 1 min

Table G.15. Ultrafiltration results - Test 8a

Sample ID	Turbidity NTU	pH	TOC mg/L	TOC % Rejection
Filtered MilliQ Water	0.043	6.79	0.42	92.99
Composite 1	0.056	6.91	4.71	22.11
Composite 2	0.055	6.98	5.27	12.76
Composite 3	0.064	7.06	5.25	13.12
Composite 4	0.06	7.14	5.29	12.54
Composite 5	0.061	7.2	5.26	13.05
Composite 6	0.055	7.21	5.25	13.20
Composite 7	0.062	7.11	5.23	13.48
Source Water	2.34	7.28	6.04	

Date: January 17, 2008

Operating flux = 70 /m^2/h

BWF = 30 min

BWT = 1 min

Table G.16. Ultrafiltration results - Test 8b

Sample ID	Turbidity NTU	pH	TOC mg/L	TOC % Rejection
Filtered MilliQ Water	0.049	7	0.29	95.05
Composite 1	0.057	7.27	4.56	21.83
Composite 2	0.056	7.3	5.01	14.07
Composite 3	0.054	7.7	5.05	13.41
Composite 4	0.057	7.37	5.07	13.07
Composite 5	0.058	7.37	5.08	12.92
Composite 6	0.059	7.39	5.10	12.59
Composite 7	0.053	7.09	5.10	12.58
Source Water	2.43	7.56	5.83	

Date: January 20, 2008

Operating flux = 120 /m^2/h

BWF = 30 min

BWT = 1 min

Table G.17. Ultrafiltration results - Test 9a

Sample ID	Turbidity NTU	pH	TOC mg/L	TOC % Rejection
Filtered MilliQ Water	0.048	7	0.21	96.35
Composite 1	0.055	7.11	4.89	14.53
Composite 2	0.053	7.17	5.32	7.07
Composite 3	0.055	7.17	5.35	6.50
Composite 4	0.062	7.15	5.32	7.03
Source Water	2.49	7.13	5.73	

Date: January 21, 2008

Operating flux = 120 /m^2/h

BWF = 30 min

BWT = 1 min

Table G.18. Ultrafiltration Test 9b

Sample ID	Turbidity NTU	pH	TOC mg/L	TOC % Rejection
Filtered MilliQ Water	0.041	6.97	0.13	97.78
Composite 1	0.052	7	4.86	15.44
Composite 2	0.054	7.11	5.31	7.61
Composite 3	0.06	7.08	5.29	7.88
Composite 4	0.053	7.13	5.32	7.45
Source Water	2.4	7.22	5.75	

Date: December 12, 2007

Operating flux = 100 /m^2/h

BWF = 1 h

BWT = 1 min

Table G.19. Results for pretreatment followed by ultrafiltration - Test 10a

Sample ID	Turbidity NTU	pH	TOC mg/L	TOC % Rejection	Ave UV254 cm^{-1}	UV254 % Rejection	SUVA L/mg.m
Filtered MilliQ Water	0.055	5.38	0.08	97.13	0.003	95.16	3.66
Composite 1	0.046	5.96	2.35	17.90	0.052	16.13	2.21
Composite 2	0.044	5.96	2.58	9.98	0.058	6.45	2.25
Composite 3	0.044	5.98	2.59	9.56	0.055	11.29	2.13
Composite 4	0.048	5.97	2.60	9.01	0.055	11.29	2.11
Composite 5	0.046	6.02	2.61	8.74	0.054	12.90	2.07
Composite 6	0.045	6.08	2.62	8.50	0.052	16.13	1.99
Composite 7	0.048	6.17	2.65	7.40	0.054	12.90	2.04
Pretreated Water	0.615	6.13	2.86		0.062		
Source Water	2.12	7					

Date: February 20, 2008

Operating flux = 100 /m^2/h

BWF = 1 h

BWT = 1 min

Table G.20. Results for pretreatment followed by ultrafiltration - Test 10b

Sample ID	Turbidity NTU	pH	TOC mg/L	TOC % Rejection	Ave UV254 cm^{-1}	UV254 % Rejection	SUVA L/mg.m
Filtered MilliQ Water	0.045	6.18	0.1078	96.10	0.003	95.16	2.78
Composite 1	0.066	6.4	2.4663	10.78	0.053	14.52	2.15
Composite 2	0.06	6.37	2.4892	9.95	0.054	12.90	2.17
Composite 3	0.054	6.33	2.4471	11.47	0.055	11.29	2.25
Composite 4	0.065	6.26	2.4338	11.95	0.052	16.13	2.14
Composite 5	0.052	6.24	2.4172	12.55	0.053	14.52	2.19
Composite 6	0.047	6.22	2.4197	12.46	0.052	16.13	2.15
Composite 7	0.048	6.16	2.4128	12.71	0.053	14.52	2.20
Pretreated Water	0.798	6.21	2.7642		0.062		
Source Water	2.34	6.74	5.6339				

APPENDIX H

ULTRAFILTRATION DATA EXTRACT SUMMARY

Date: October 16, 2007

Operating flux = 100 /m^2/h

BWF = 15 min

BWT = 60s

Table H.1. Ultrafiltration Extract Summary -Test 1a

Filtration Cycles	Average Flowrate (mL/min)	Average Flux (L/m^2/h)	Setpoint Flux (L/m^2/h)	Permeate Volume (L)	Cumulative Permeate Volume (L)	Backwash Efficiency (%)
1	7.61	99.25	100	0.0959	0.0959	64.38
2	7.64	99.63	100	0.1143	0.2102	64.96
3	7.66	99.87	100	0.1147	0.3249	67.18
4	7.71	100.56	100	0.1155	0.4404	79.34
5	7.73	100.79	100	0.1155	0.5559	57.72
6	7.65	99.83	100	0.1154	0.6713	80.96
7	7.65	99.72	100	0.1144	0.7858	72.64
8	7.67	100.00	100	0.1137	0.8995	95.39
9	7.65	99.78	100	0.1146	1.0141	75.43
10	7.64	99.71	100	0.1144	1.1285	72.16
11	7.64	99.60	100	0.1146	1.2431	76.87
12	7.65	99.78	100	0.1148	1.3579	84.15
13	7.57	98.74	100	0.1132	1.4712	84.07
14	7.63	99.53	100	0.1147	1.5859	74.38
15	7.65	99.80	100	0.1149	1.7008	82.14
16	7.63	99.57	100	0.1146	1.8154	89.53
17	7.66	99.90	100	0.1153	1.9308	75.12
18	7.65	99.83	100	0.1150	2.0458	86.86
19	7.67	100.05	100	0.1149	2.1607	76.56
20	7.64	99.63	100	0.1149	2.2756	85.45
21	7.63	99.52	100	0.1146	2.3903	83.75
22	7.63	99.55	100	0.1147	2.5050	83.31
23	7.60	99.16	100	0.1143	2.6193	71.26
24	7.65	99.72	100	0.1151	2.7344	90.70
25	7.58	98.88	100	0.1137	2.8482	86.88
26	7.62	99.41	100	0.1148	2.9630	76.17
27	7.62	99.43	100	0.1144	3.0774	81.62
28	7.62	99.45	100	0.1147	3.1922	
					Average	**78.48**

Date: October 18, 2007

Operating flux = 100 /m^2/h

BWF = 15 min

BWT = 2 min

Table H.2. Ultrafiltration Extract Summary - Test 1b

Filtration Cycles	Average Flowrate (mL/min)	Average Flux (L/m^2/h)	Setpoint Flux (L/m^2/h)	Permeate Volume (L)	Cumulative Permeate Volume (L)	Backwash Efficiency (%)
1	7.62	99.45	100	0.1141	0.1141	94.04
2	7.62	99.35	100	0.1143	0.2284	68.17
3	7.64	99.61	100	0.1150	0.3434	88.78
4	7.63	99.51	100	0.1150	0.4584	90.74
5	7.61	99.28	100	0.1148	0.5732	73.37
6	7.61	99.28	100	0.1146	0.6878	88.58
7	7.61	99.32	100	0.1148	0.8026	79.21
8	7.63	99.51	100	0.1148	0.9174	91.74
9	7.56	98.61	100	0.1140	1.0314	85.28
10	7.67	100.09	100	0.1151	1.1465	73.64
11	7.69	100.29	100	0.1159	1.2624	87.07
12	7.65	99.81	100	0.1153	1.3777	97.55
13	7.64	99.69	100	0.1151	1.4928	96.93
14	7.59	98.99	100	0.1143	1.6071	72.53
15	7.64	99.69	100	0.1151	1.7222	85.55
16	7.65	99.79	100	0.1155	1.8377	89.62
17	7.59	98.97	100	0.1143	1.9520	96.47
18	7.61	99.26	100	0.1146	2.0666	85.73
19	7.60	99.18	100	0.1145	2.1812	76.48
20	7.61	99.22	100	0.1144	2.2956	101.07
21	7.62	99.45	100	0.1146	2.4102	76.83
22	7.62	99.44	100	0.1147	2.5249	81.75
23	7.62	99.38	100	0.1148	2.6398	75.54
24	7.60	99.18	100	0.1144	2.7542	103.39
25	7.60	99.13	100	0.1145	2.8687	80.80
26	7.61	99.27	100	0.1144	2.9831	80.76
27	7.61	99.30	100	0.1146	3.0978	85.67
28	7.63	99.46	100	0.1147	3.2125	
					Average	85.46

Date: October 21, 2007

Operating flux = 100 /m^2/h

BWF = 15 min

BWT = 2 min

Table H.3. Ultrafiltration Extract Summary - Test 2a

Filtration Cycles	Average Flowrate (mL/min)	Average Flux (L/m^2/h)	Setpoint Flux (L/m^2/h)	Permeate Volume (L)	Cumulative Permeate Volume (L)	Backwash Efficiency (%)
1	7.62	99.43	100	0.0947	0.0947	64.85
2	7.64	99.70	100	0.1151	0.2097	66.33
3	7.67	100.06	100	0.1153	0.3250	82.01
4	7.65	99.73	100	0.1150	0.4400	101.04
5	7.64	99.66	100	0.1145	0.5545	85.28
6	7.61	99.29	100	0.1147	0.6692	80.39
7	7.64	99.64	100	0.1151	0.7843	85.17
8	7.59	99.06	100	0.1144	0.8987	93.06
9	7.59	99.04	100	0.1145	1.0132	89.77
10	7.57	98.75	100	0.1139	1.1271	71.48
11	7.61	99.28	100	0.1148	1.2419	95.11
12	7.62	99.44	100	0.1146	1.3565	87.23
13	7.52	98.08	100	0.1130	1.4695	86.58
14	7.62	99.44	100	0.1146	1.5841	86.76
15	7.62	99.39	100	0.1147	1.6989	80.31
16	7.62	99.42	100	0.1148	1.8137	91.54
17	7.62	99.46	100	0.1147	1.9284	94.11
18	7.61	99.21	100	0.1147	2.0431	83.40
19	7.62	99.44	100	0.1145	2.1576	84.32
20	7.64	99.65	100	0.1150	2.2727	95.59
21	7.59	98.97	100	0.1140	2.3867	80.62
22	7.59	99.06	100	0.1144	2.5011	79.56
23	7.62	99.35	100	0.1149	2.6160	87.28
24	7.62	99.46	100	0.1148	2.7309	89.71
25	7.60	99.07	100	0.1138	2.8447	88.89
26	7.62	99.39	100	0.1145	2.9592	75.91
27	7.63	99.50	100	0.1149	3.0742	88.52
28	7.59	99.02	100	0.1143	3.1885	
					Average	**84.99**

Date: October 23, 2007

Operating flux = 100 /m^2/h

BWF = 15 min

BWT = 60s

Table H.4. Ultrafiltration Extract Summary - Test 2b

Filtration Cycles	Average Flowrate (mL/min)	Average Flux (L/m^2/h)	Setpoint Flux (L/m^2/h)	Permeate Volume (L)	Cumulative Permeate Volume (L)	Backwash Efficiency (%)
1	7.61	99.31	100	0.0889	0.0889	69.34
2	7.67	100.01	100	0.1150	0.2039	65.23
3	7.68	100.11	100	0.1151	0.3190	78.61
4	7.66	99.90	100	0.1148	0.4338	107.35
5	7.64	99.70	100	0.1140	0.5478	79.52
6	7.59	99.03	100	0.1141	0.6619	82.94
7	7.61	99.30	100	0.1143	0.7763	83.59
8	7.60	99.10	100	0.1142	0.8905	92.79
9	7.66	99.95	100	0.1149	1.0054	85.15
10	7.64	99.70	100	0.1150	1.1204	66.73
11	7.62	99.40	100	0.1146	1.2350	65.16
12	7.60	99.19	100	0.1142	1.3492	91.74
13	7.49	97.67	100	0.1125	1.4617	114.11
14	7.59	99.02	100	0.1143	1.5761	60.36
15	7.56	98.67	100	0.1135	1.6896	65.72
16	7.59	99.02	100	0.1141	1.8037	92.15
17	7.53	98.21	100	0.1132	1.9169	82.04
18	7.55	98.53	100	0.1135	2.0305	82.52
19	7.57	98.68	100	0.1138	2.1443	80.95
20	7.56	98.64	100	0.1137	2.2580	90.71
21	7.62	99.38	100	0.1150	2.3730	113.84
22	7.57	98.68	100	0.1140	2.4871	88.81
23	7.56	98.66	100	0.1140	2.6011	64.29
24	7.57	98.68	100	0.1138	2.7149	97.91
25	7.66	99.91	100	0.1114	2.8264	96.66
26	7.57	98.72	100	0.1137	2.9401	81.90
27	7.57	98.76	100	0.1139	3.0540	85.52
28	7.57	98.69	100	0.1137	3.1678	
						83.91

Date:September 25, 2007

Operating flux = 100 /m^2/h

BWF = 30 min

BWT = 1 min

Table H.5. Ultrafiltration Extract Summary - Test 3a

Filtration Cycles	Average Flowrate (mL/min)	Average Flux (L/m^2/h)	Setpoint Flux (L/m^2/h)	Permeate Volume (L)	Cumulative Permeate Volume (L)	Backwash Efficiency (%)
1.00	7.58	98.82	100	0.2177	0.2177	43.24
2.00	7.57	98.69	100	0.2273	0.4450	79.02
3.00	7.55	98.51	100	0.2258	0.6708	113.58
4.00	7.57	98.74	100	0.2275	0.8983	43.82
5.00	7.61	99.23	100	0.2281	1.1265	92.42
6.00	7.63	99.48	100	0.2295	1.3560	51.81
7.00	7.61	99.26	100	0.2272	1.5832	90.85
8.00	7.58	98.83	100	0.2280	1.8113	83.70
9.00	7.53	98.28	100	0.2261	2.0374	63.46
10.00	7.49	97.64	100	0.2244	2.2619	77.43
11.00	7.35	95.85	100	0.2203	2.4822	69.20
12.00	7.45	97.20	100	0.2261	2.7083	71.41
13.00	7.55	98.54	100	0.2276	2.9359	70.25
					Average	**73.09**

Date: October 4, 2007

Operating flux = 100 /m^2/h

BWF = 30 min

BWT = 2 min

Table H.8. Ultrafiltration Extract Summary - Test 4b

Filtration Cycles	Average Flowrate (mL/min)	Average Flux (L/m^2/h)	Setpoint Flux (L/m^2/h)	Permeate Volume (L)	Cumulative Permeate Volume (L)	Backwash Efficiency (%)
1	7.56	98.60	100	0.2123	0.2123	70.69
2	7.56	98.58	100	0.2271	0.4394	73.52
3	7.58	98.86	100	0.2277	0.6671	85.71
4	7.57	98.78	100	0.2275	0.8946	78.67
5	7.55	98.47	100	0.2264	1.1211	83.60
6	7.57	98.71	100	0.2276	1.3487	67.25
6	7.58	98.93	100	0.2278	1.5765	87.65
8	7.57	98.70	100	0.2276	1.8040	81.68
9	7.57	98.70	100	0.2274	2.0314	72.33
10	7.58	98.88	100	0.2277	2.2590	78.28
11	7.58	98.88	100	0.2276	2.4866	69.02
12	7.58	98.87	100	0.2277	2.7143	97.27
13	7.56	98.63	100	0.2266	2.9409	
					Average	**78.81**

Date: November 11, 2007

Operating flux = 100 /m^2/h

BWF = 1 h

BWT = 1 min

Table H.9. Ultrafiltration Extract Summary - Test 5a

Filtration Cycles	Average Flowrate (mL/min)	Average Flux (L/m^2/h)	Setpoint Flux (L/m^2/h)	Permeate Volume (L)	Cumulative Permeate Volume (L)	Backwash Efficiency (%)
1	7.62	99.41	100	0.4427	0.4427	56.64
2	7.64	99.70	100	0.4369	0.4369	64.28
3	7.59	98.98	100	0.4563	0.8932	62.06
4	7.59	99.01	100	0.4560	1.3492	59.64
5	7.61	99.32	100	0.4576	1.8068	57.44
6	7.62	99.41	100	0.4581	2.2649	55.03
					Average	**59.18**

Date: December 4, 2007

Operating flux = 100 /m^2/h

BWF = 1 h

BWT = 1 min

Table H.10. Ultrafiltration Extract Summary - Test 5b

Filtration Cycles	Average Flowrate (mL/min)	Average Flux (L/m^2/h)	Setpoint Flux (L/m^2/h)	Permeate Volume (L)	Cumulative Permeate Volume (L)	Backwash Efficiency (%)
1	7.66	99.88	100	0.44	0.44	55.09
2	7.65	99.80	100	0.43	0.87	72.00
3	7.64	99.61	100	0.46	1.33	67.81
4	7.63	99.48	100	0.46	1.79	73.80
5	7.65	99.76	100	0.46	2.25	65.90
6	7.64	99.65	100	0.46	2.71	65.95
					Average	**66.76**

Date: October 25, 2007

Operating flux = 100 /m^2/h

BWF = 1 h

BWT = 2 min

Table H.11. Ultrafiltration Extract Summary - Test 6a

Filtration Cycles	Average Flowrate (mL/min)	Average Flux (L/m^2/h)	Setpoint Flux (L/m^2/h)	Permeate Volume (L)	Cumulative Permeate Volume (L)	Backwash Efficiency (%)
1	7.65	99.77	100	0.4039	0.4039	64.44
2	7.63	99.54	100	0.4586	0.8624	68.15
3	7.63	99.52	100	0.4586	1.3210	59.53
4	7.63	99.49	100	0.4584	1.7795	69.90
5	7.63	99.56	100	0.4590	2.2384	75.00
6	7.62	99.37	100	0.4580	2.6964	70.79
7	7.63	99.55	100	0.4590	3.1555	
					Average	**67.97**

Date: November 13, 2007

Operating flux = 100 /m^2/h

BWF = 1 h

BWT = 2 min

Table H.12. Ultrafiltration Extract Summary - Test 6b

Filtration Cycles	Average Flowrate (mL/min)	Average Flux (L/m^2/h)	Setpoint Flux (L/m^2/h)	Permeate Volume (L)	Cumulative Permeate Volume (L)	Backwash Efficiency (%)
1	7.61	99.21	100	0.4457	0.4457	64.10
2	7.63	99.49	100	0.4589	0.9046	78.32
3	7.61	99.24	100	0.4572	1.3618	73.14
4	7.62	99.38	100	0.4581	1.8199	73.79
5	7.63	99.49	100	0.4587	2.2786	75.86
6	7.61	99.26	100	0.4573	2.7359	69.19
					Average	**72.40**

Date: January 14, 2008

Operating flux = 50 /m^2/h

BWF = 30 min

BWT = 1 min

Table H.13. Ultrafiltration Extract Summary -Test 7a

Filtration Cycles	Average Flowrate (mL/min)	Average Flux (L/m^2/h)	Setpoint Flux (L/m^2/h)	Permeate Volume (L)	Cumulative Permeate Volume (L)	Backwash Efficiency (%)
1	3.71	48.40	50	0.0978	0.0978	54.64
2	3.86	50.34	50	0.1151	0.2129	59.40
3	3.83	49.96	50	0.1141	0.3270	38.12
4	3.88	50.60	50	0.1156	0.4426	81.10
5	3.88	50.59	50	0.1164	0.5590	67.52
6	3.85	50.27	50	0.1151	0.6741	110.43
7	3.85	50.19	50	0.1151	0.7893	76.71
8	3.86	50.39	50	0.1157	0.9050	68.00
9	3.80	49.62	50	0.1135	1.0185	80.35
10	3.83	49.92	50	0.1141	1.1327	88.64
11	3.85	50.17	50	0.1153	1.2480	81.03
12	3.85	50.25	50	0.1151	1.3631	78.54
13	3.82	49.80	50	0.1139	1.4771	99.59
14	3.83	49.92	50	0.1142	1.5913	
					Average	**75.70**

Date: January 15, 2008

Operating flux = 50 /m^2/h

BWF = 30 min

BWT = 1 min

Table H.14. Ultrafiltration Extract Summary - Test 7b

Filtration Cycles	Average Flowrate (mL/min)	Average Flux (L/m^2/h)	Setpoint Flux (L/m^2/h)	Permeate Volume (L)	Cumulative Permeate Volume (L)	Backwash Efficiency (%)
1	4.02	52.45	50	0.1041	0.1041	65.26
2	4.01	52.34	50	0.1133	0.2174	82.98
3	3.99	52.07	50	0.1116	0.3290	114.82
4	4.01	52.32	50	0.1131	0.4421	58.42
5	4.00	52.20	50	0.1120	0.5540	86.33
6	4.01	52.34	50	0.1133	0.6673	90.19
7	4.02	52.40	50	0.1133	0.7806	62.25
8	4.04	52.66	50	0.1138	0.8943	77.64
9	3.98	51.91	50	0.1118	1.0061	94.62
10	3.98	51.91	50	0.1124	1.1185	93.46
11	3.95	51.53	50	0.1110	1.2294	79.74
12	3.97	51.81	50	0.1120	1.3414	83.86
13	3.93	51.32	50	0.1106	1.4520	85.11
14	3.96	51.60	50	0.1119	1.5638	
					Average	**82.67**

Date: January 16, 2008

Operating flux = 70 /m^2/h

BWF = 30 min

BWT = 1 min

Table H.15 Ultrafiltration Extract Summary - Test 8a

Filtration Cycles	Average Flowrate (mL/min)	Average Flux ($L/m^2/h$)	Setpoint Flux ($L/m^2/h$)	Permeate Volume (L)	Cumulative Permeate Volume (L)	Backwash Efficiency (%)
1	5.36	69.87	70	0.1532	0.1532	55.71
2	5.37	70.05	70	0.1593	0.3125	54.91
3	5.33	69.52	70	0.1582	0.4708	73.73
4	5.34	69.70	70	0.1588	0.6296	81.52
5	5.34	69.67	70	0.1546	0.7842	66.27
6	5.30	69.07	70	0.1591	0.9434	86.49
7	5.30	69.12	70	0.1593	1.1027	65.16
8	5.29	68.99	70	0.1588	1.2616	88.57
9	5.27	68.70	70	0.1578	1.4194	80.35
10	5.28	68.92	70	0.1589	1.5783	86.78
11	5.27	68.75	70	0.1584	1.7366	65.65
12	5.26	68.67	70	0.1588	1.8954	83.05
13	5.28	68.93	70	0.1590	2.0543	77.79
14	5.27	68.73	70	0.1586	2.2129	
					Average	**74.31**

Date: January 17, 2008

Operating flux = 70 /m^2/h

BWF = 30 min

BWT = 1 min

Table H.16. Ultrafiltration Extract Summary - Test 8b

Filtration Cycles	Average Flowrate (mL/min)	Average Flux (L/m^2/h)	Setpoint Flux (L/m^2/h)	Permeate Volume (L)	Cumulative Permeate Volume (L)	Backwash Efficiency (%)
1	5.28	68.90	70	0.1497	0.1497	46.61
2	5.25	68.51	70	0.1478	0.2976	75.15
3	5.25	68.49	70	0.1578	0.4553	56.43
4	5.25	68.49	70	0.1577	0.6130	71.40
5	5.27	68.74	70	0.1578	0.7708	55.07
6	5.24	68.31	70	0.1573	0.9280	83.52
7	5.22	68.12	70	0.1573	1.0853	73.41
8	5.22	68.08	70	0.1568	1.2420	78.43
9	5.21	67.90	70	0.1565	1.3985	64.99
10	5.22	68.11	70	0.1568	1.5553	69.36
11	5.22	68.15	70	0.1569	1.7121	75.64
12	5.24	68.36	70	0.1576	1.8697	75.72
13	5.21	67.97	70	0.1568	2.0264	80.27
14	5.22	68.15	70	0.1572	2.1836	
					Average	**69.69**

Date: January 20, 2008

Operating flux = 120 L /m^2/h

BWF = 30 min

BWT = 1 min

Table H. 17. Ultrafiltration Extract Summary - Test 9a

Filtration Cycles	Average Flowrate (mL/min)	Average Flux (L/m^2/h)	Setpoint Flux (L/m^2/h)	Permeate Volume (L)	Cumulative Permeate Volume (L)	Backwash Efficiency (%)
1	9.16	119.54	120	0.2500	0.2500	46.59
2	9.18	119.74	120	0.2759	0.5259	78.67
3	9.20	120.01	120	0.2768	0.8027	53.39
4	9.20	119.96	120	0.2761	1.0788	87.04
5	9.18	119.69	120	0.2761	1.3549	65.17
6	9.18	119.71	120	0.2758	1.6307	60.63
7	9.15	119.30	120	0.2746	1.9053	69.48
8	9.20	119.97	120	0.2764	2.1817	
					Average	**65.85**

Date: January 21, 2008

Operating flux = 120 /m^2/h

BWF = 30 min

BWT = 1 min

Table H.18. Ultrafiltration Extract Summary - Test 9b

Filtration Cycles	Average Flowrate (mL/min)	Average Flux (L/m^2/h)	Setpoint Flux (L/m^2/h)	Permeate Volume (L)	Cumulative Permeate Volume (L)	Backwash Efficiency (%)
1	9.12	119.01	120	0.2632	0.2632	52.49
2	9.14	119.16	120	0.2744	0.5376	60.89
3	9.13	119.05	120	0.2739	0.8116	61.30
4	9.11	118.78	120	0.2733	1.0849	67.80
5	9.06	118.19	120	0.2715	1.3564	60.32
6	9.08	118.45	120	0.2742	1.6307	61.71
7	9.16	119.46	120	0.2750	1.9057	71.31
8	9.16	119.46	120	0.2756	2.1814	
					Average	**62.26**

Date: December 12, 2007

Operating flux = 100 /m^2/h

BWF = 1 h

BWT = 1 min

Table H.19. Pretreatment / Ultrafiltration Extract Summary - Test 10a

Filtration Cycles	Average Flowrate (mL/min)	Average Flux (L/m^2/h)	Setpoint Flux (L/m^2/h)	Permeate Volume (L)	Cumulative Permeate Volume (L)	Backwash Efficiency (%)
1	7.61	99.25	100	0.4456	0.4456	51.04
2	7.61	99.32	100	0.3406	0.3406	157.14
3	7.60	99.17	100	0.4562	0.7968	59.85
4	7.59	98.96	100	0.4554	1.2522	119.43
5	7.60	99.08	100	0.4560	1.7083	98.66
6	7.63	99.51	100	0.4574	2.1656	77.78
					Average	**93.98**

Date: February 20, 2008

Operating flux = 100 /m^2/h

BWF = 1 h

BWT = 1 min

Table H.20. Pretreatment / Ultrafiltration Extract Summary - Test 10b

Filtration Cycles	Average Flowrate (mL/min)	Average Flux (L/m^2/h)	Setpoint Flux (L/m^2/h)	Permeate Volume (L)	Cumulative Permeate Volume (L)	Backwash Efficiency (%)
1	7.63	99.48	100	0.4422	0.4422	110.17
2	7.61	99.22	100	0.4549	0.4549	70.32
3	7.63	99.53	100	0.4564	0.9113	91.20
4	7.63	99.58	100	0.4567	1.3680	79.28
5	7.61	99.26	100	0.4561	1.8241	143.27
6	7.59	99.06	100	0.4551	2.2793	62.94
					Average	**92.87**

APPENDIX I

MOLECULAR WEIGHT DISTRIBUTION

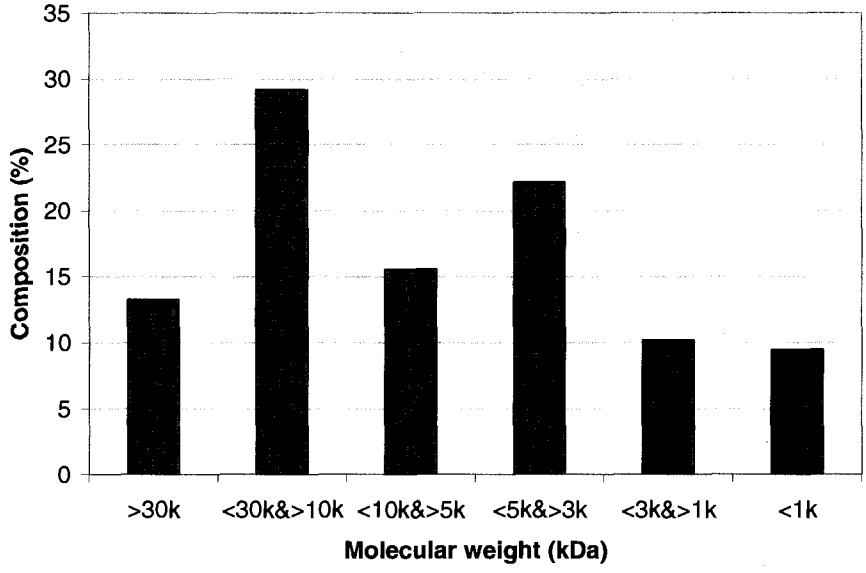

Figure I.1a. Molecular weight distribution for chemically pretreated ORW (BWF = 1 h; BWT = 1 min)

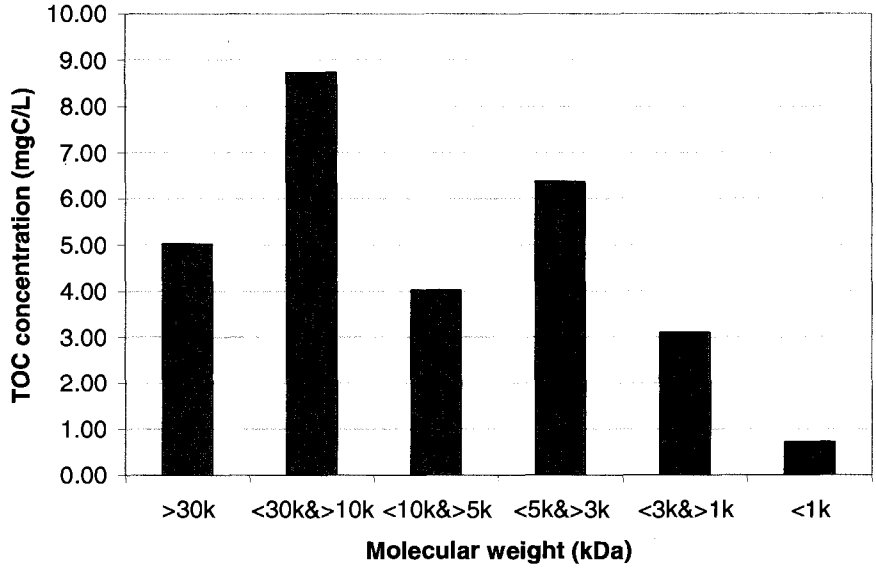

Figure I.1b. Molecular weight distribution for chemically pretreated ORW (BWF = 1 h; BWT = 1 min)

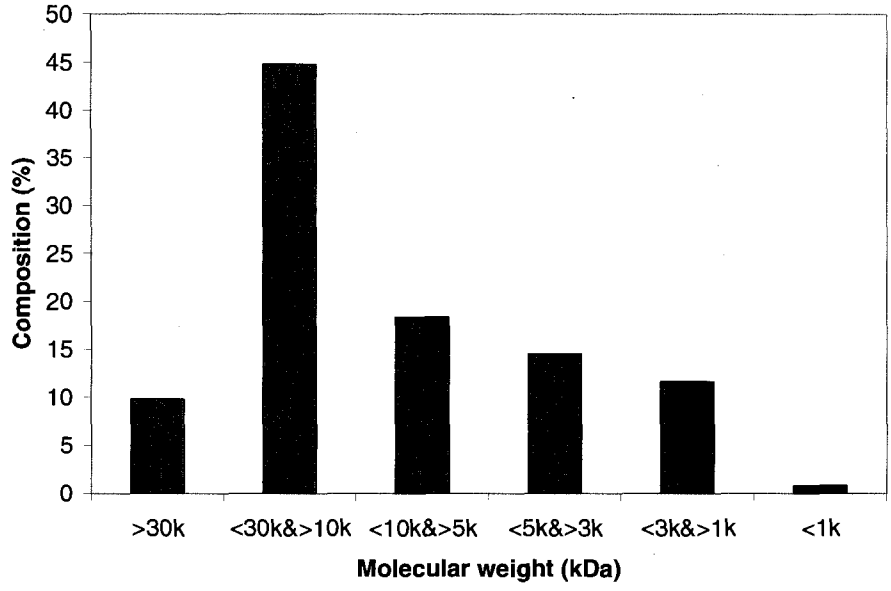

Figure I.2a. Molecular weight distribution for permeated ORW (BWF = 1 h; BWT = 1 min)

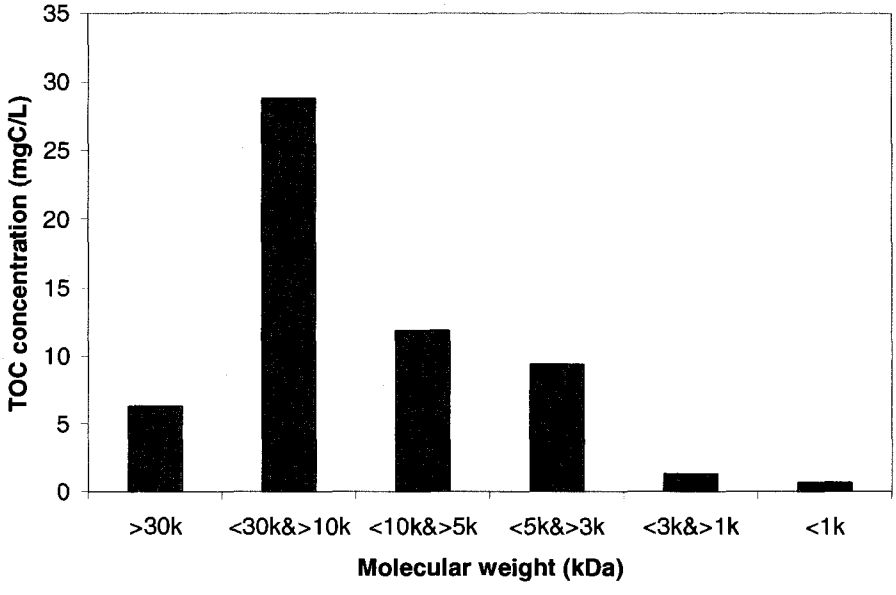

Figure I.2b. Molecular weight distribution for permeated ORW (BWF = 1 h; BWT = 1 min)

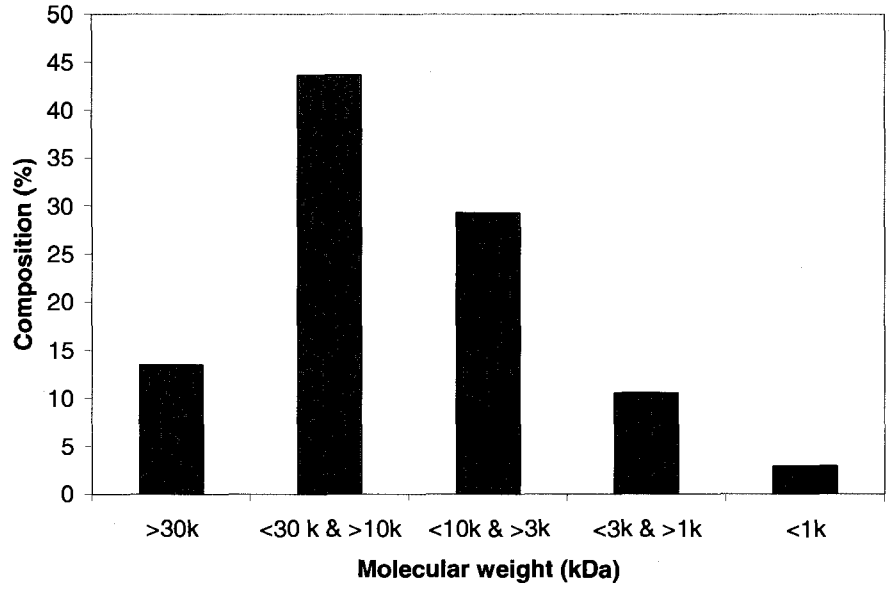

Figure I.3a. Molecular weight distribution for ORW

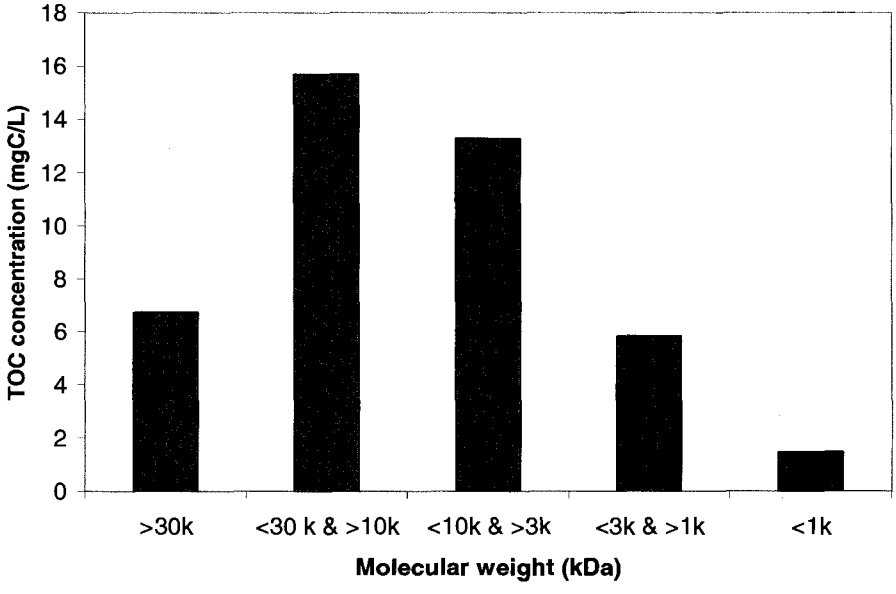

Figure I.3b. Molecular weight distribution for ORW

APPENDIX J

EFFECTS OF MEMBRANE COMPACTION

The linearity of the pressure—flux profile from clean water ultrafiltration testing illustrated by Figure J.1 and Figure J.2 indicates that the effects of membrane compaction were negligible in the range of conditions tested for two membrane modules.

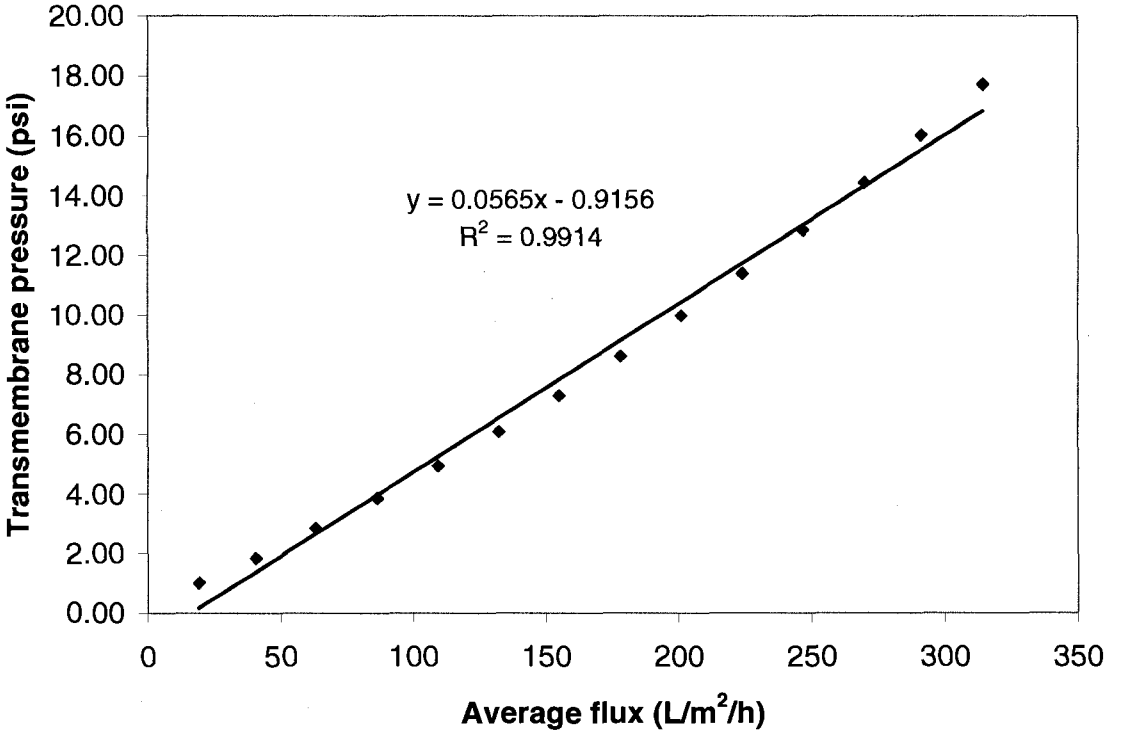

Figure J.1. Pressure flux profile from clean water UF testing

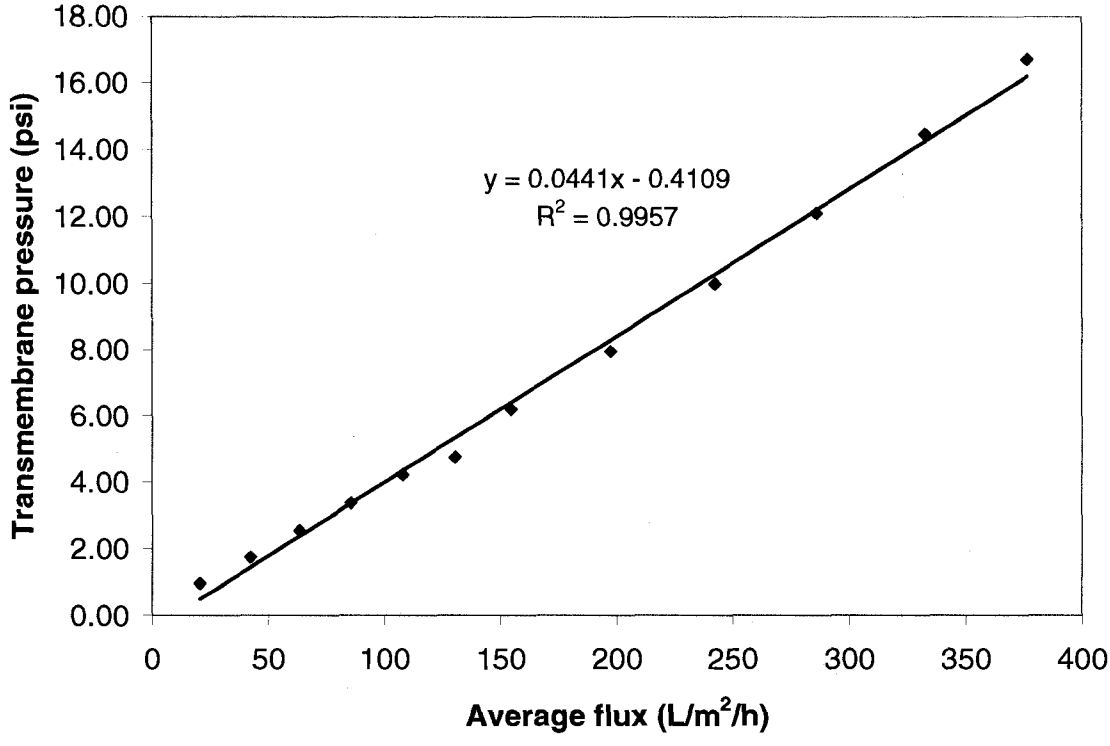

Figure J.2. Pressure flux profile from clean water UF testing

APPENDIX K

MANUAL ULTRAFILTRATION SYSTEM

Figure K.1 depicts the manual system used for feed pump testing. The system was upgraded to the system shown in Chapter 3, Figure 3.3.

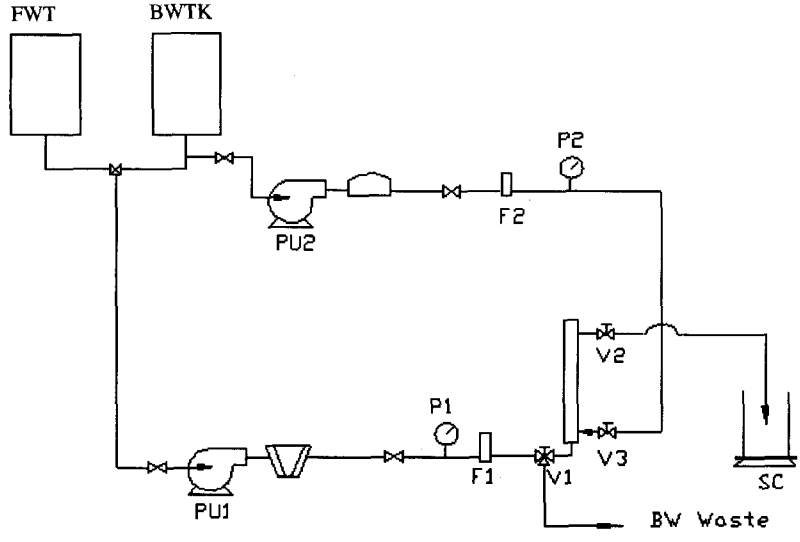

Figure K.1. Pressure flux profile from clean water UF testing

PU1 – Feed water pump
PU2 – Backwash pump
F1 – Filtration flowmeter
F2 – Backwash flowmeter
P1 – Filtration pressure gauge
P2 – Backwash pressure gauge
V1 – 3-way needle valve
V2 – 2-way needle valve
V3 – 2-way needle valve
SC – Scale
FWT – Feed water tank
BWTK – Backwash water tank

APPENDIX L

STATISTICAL ESTIMATION OF CRITICAL FLUX

Tables L.1 and L.2 depict T-test and F-test results of the rate of change of TMP versus permeate flux (Section 4.3). Both statistical approaches indicate that a sudden change in $\Delta TMP/\Delta t$ occurred between 0.124 kPa/min (0.018 psi/min) and 0.290 kPa/min (0.042 psi/min) which is equivalent to permeate flux vales of 59 $L/m^2/h$ and 77 $L/m^2/h$ respectively.

Table L.1. F-test results between successive values of dp/dt

Varible 1 (psi/min)	Varible 2 (psi/min)	F
0.000	0.006	1.2
0.006	0.011	0.625
0.011	0.018	0.872
0.018	0.025	0.19
0.025	0.042	0.516
0.042	0.065	0.845
0.065	0.090	0.225
0.090	0.144	-

Table L.2. T-test results between successive values of dp/dt

Varible 1 (psi/min)	Varible 2 (psi/min)	t
0.000	0.006	-1.41
0.006	0.011	-1.4
0.011	0.018	-1.41
0.018	0.025	-1.32
0.025	0.042	-1.39
0.042	0.065	-1.41
0.065	0.090	-1.33
0.090	0.144	-

APPENDIX M

CONFIDENCE INTERVAL FOR TOC REJECTION

Tables M.1 to M.7 depict the lower 95% confidence limits for TOC rejection for different BWF and BWT and constant flux of 100 L/m^2/h. Tables M.8 to M.10 depict the lower 95% confidence limit for TOC rejection for different operating flux values and constant BWF and BWT of 30 minutes and one minute respectively. The confidence limits were calculated from the average TOC rejection from duplicate runs under the same operating conditions. The results support the findings in Subsections 4.4.3 and 4.5.3 respectively.

M.1. Confidence limits for TOC rejection for different BWF and BWT and constant flux

Sample ID	Average TOC Rejection		Mean	STDEV	Lower 95%
	(BWT-15 min, BWT-1 min)	(BWT-15 min, BWT-2 min)			Confidence Limit
Composits 2	0.132	0.123	0.128	0.0065	0.115
Composits 3	0.127	0.118	0.123	0.0058	0.111
Composits 4	0.128	0.117	0.123	0.0077	0.108
Composits 5	0.126	0.118	0.122	0.0052	0.112
Composits 6	0.124	0.115	0.119	0.0065	0.107
Composits 7	0.128	0.118	0.123	0.0071	0.109
				Ave	**0.110**

M.2. Confidence limits for TOC rejection for different BWF and BWT and constant flux

Sample ID	Average TOC Rejection		Mean	STDEV	Lower 95%
	(BWT-30 min, BWT-1 min)	(BWT-30 min, BWT-2 min)			Confidence Limit
Composits 2	0.099	0.103	0.101	0.0022	0.097
Composits 3	0.079	0.098	0.089	0.0134	0.063
Composits 4	0.077	0.097	0.087	0.0147	0.058
Composits 5	0.080	0.094	0.087	0.0097	0.068
Composits 6	0.086	0.095	0.090	0.0065	0.077
Composits 7	0.087	0.092	0.090	0.0034	0.083
				Ave	**0.074**

M.3. Confidence limits for TOC rejection for different BWF and BWT and constant flux

Sample ID	Average TOC Rejection		Mean	STDEV	Lower 95% Confidence Limit
	(BWT-1 h, BWT-1 min)	(BWT-1 h, BWT-2 min)			
Composits 2	0.082	0.080	0.081	0.0017	0.078
Composits 3	0.077	0.076	0.076	0.0011	0.074
Composits 4	0.076	0.075	0.076	0.0012	0.073
Composits 5	0.078	0.071	0.075	0.0049	0.065
Composits 6	0.082	0.072	0.077	0.0073	0.063
				Ave	**0.071**

M.4. Confidence limits for TOC rejection for different BWF and BWT and constant flux

Sample ID	Average TOC Rejection		Mean	STDEV	Lower 95% Confidence Limit
	(BWT-15 min, BWT-1 min)	(BWT-30 min, BWT-1 min)			
Composits 2	0.132	0.099	0.116	0.0231	0.070
Composits 3	0.127	0.079	0.103	0.0335	0.037
Composits 4	0.128	0.077	0.102	0.0367	0.031
Composits 5	0.126	0.080	0.103	0.0322	0.040
Composits 6	0.124	0.086	0.105	0.0271	0.052
Composits 7	0.128	0.087	0.108	0.0291	0.051
				Ave	**0.047**

M.5. Confidence limits for TOC rejection for different BWF and BWT and constant flux

Sample ID	Average TOC Rejection		Mean	STDEV	Lower 95% Confidence Limit
	(BWT-30 min, BWT-1 min)	(BWT-60 min, BWT-1 min)			
Composits 2	0.099	0.082	0.091	0.0120	0.068
Composits 3	0.095	0.077	0.086	0.0125	0.062
Composits 4	0.092	0.076	0.084	0.0113	0.062
Composits 5	0.096	0.078	0.087	0.0125	0.062
Composits 6	0.101	0.082	0.092	0.0132	0.066
				Ave	**0.064**

M.6. Confidence limits for TOC rejection for different BWF and BWT and constant flux

Sample ID	Average TOC Rejection		Mean	STDEV	Lower 95% Confidence Limit
	(BWT-15 min, BWT- 2 min)	(BWT-30 min, BWT-2 min)			
Composits 2	0.123	0.103	0.113	0.0144	0.084
Composits 3	0.118	0.098	0.108	0.0143	0.080
Composits 4	0.117	0.097	0.107	0.0143	0.079
Composits 5	0.118	0.094	0.106	0.0174	0.072
Composits 6	0.115	0.095	0.105	0.0142	0.077
Composits 7	0.118	0.092	0.105	0.0186	0.069
				Ave	**0.077**

M.7. Confidence limits for TOC rejection for different BWF and BWT and constant flux

Sample ID	Average TOC Rejection		Mean	STDEV	Lower 95% Confidence Limit
	(BWT-30 min, BWT- 2 min)	(BWT-1 h, BWT-2 min)			
Composits 2	0.103	0.080	0.091	0.0158	0.060
Composits 3	0.098	0.076	0.087	0.0159	0.056
Composits 4	0.097	0.075	0.086	0.0159	0.055
Composits 5	0.094	0.071	0.083	0.0160	0.051
Composits 6	0.095	0.072	0.083	0.0160	0.052
				Ave	**0.055**

M.8. Confidence limits for TOC rejection for different operating flux values and constant BWF and BWT

Sample ID	Average TOC Rejection		Mean	STDEV	Lower 95% Confidence Limit
	50 $L/m^2/h$	70 $L/m^2/h$			
Composits 2	0.159	0.130	0.144	0.0206	0.104
Composits 3	0.159	0.125	0.142	0.0236	0.096
Composits 4	0.157	0.124	0.141	0.0229	0.096
Composits 5	0.156	0.121	0.138	0.0246	0.090
Composits 6	0.153	0.122	0.138	0.0221	0.094
Composits 7	0.155	0.119	0.137	0.0251	0.088
				Ave	**0.095**

M.9. Confidence limits for TOC rejection for different operating flux values and constant BWF and BWT

Sample ID	Average TOC Rejection		Mean	STDEV	Lower 95% Confidence Limit
	70 L/m^2/h	100 L/m^2/h			
Composits 2	0.130	0.099	0.114	0.0213	0.073
Composits 3	0.125	0.095	0.110	0.0214	0.068
Composits 4	0.124	0.092	0.108	0.0227	0.064
Composits 5	0.121	0.096	0.108	0.0178	0.074
Composits 6	0.122	0.101	0.112	0.0147	0.083
Composits 7	0.119	0.103	0.111	0.0117	0.088
				Ave	**0.075**

M.10. Confidence limits for TOC rejection for different operating flux values and constant BWF and BWT

Sample ID	Average TOC Rejection		Mean	STDEV	Lower 95% Confidence Limit
	100 L/m^2/h	120 L/m^2/h			
Composits 2	0.099	0.074	0.087	0.0179	0.052
Composits 3	0.079	0.073	0.076	0.0043	0.068
Composits 4	0.077	0.073	0.075	0.0024	0.070
				Ave	**0.063**